EFFECT OF THE VARIATION OF EXHAUST AND FUEL INJECTION TIMING ON THE GENERAL MOTORS DIESEL ENGINE MODEL 1-53X3

HERBERT D. TRENHAM

EFFECT OF THE VARIATION OF EXHAUST AND FUEL INJECTION TIMING ON THE GENERAL MOTORS DIESEL ENGINE MODEL 1-53X3

* * * * *

Herbert D. Trenham

EFFECT OF THE VARIATION OF EXHAUST AND FUEL INJECTION TIMING ON THE GENERAL MOTORS DIESEL ENGINE MODEL 1-53X3

by

Herbert D. Trenham
Lieutenant, United States Navy

Submitted in partial fulfillment of
the requirements for the degree of

MASTER OF SCIENCE
IN
MECHANICAL ENGINEERING

United States Naval Postgraduate School
Monterey, California

1 9 6 3

EFFECT OF THE VARIATION OF EXHAUST AND FUEL INJECTION TIMING ON THE GENERAL MOTORS DIESEL ENGINE MODEL 1-53X3

by

Herbert D. Trenham

This work is accepted as fulfilling
the thesis requirements for the degree of
MASTER OF SCIENCE
IN
MECHANICAL ENGINEERING

from the
United States Naval Postgraduate School

ABSTRACT

The GM Diesel Model 1-53X3 is a single cylinder two stroke cycle engine rated at 30 hp at 3000 rpm. It was developed with both two and four exhaust valve cylinder heads. Variable exhaust and injector cam shaft gears have been added to facilitate changes in timing. The purpose of this investigation was to determine the effects of the variation of exhaust and fuel injection timing on engine performance. A piezoelectric pressure pickup was used to obtain oscilloscope displays of pressure versus crank angle which were photographed. Injection from 20 °BTC to 5 °BTC for three exhaust timing configurations have been investigated for each head. Engine performance under these conditions are presented and discussed. The engine as instrumented lends itself to a variety of student exercises and demonstrations.

ACKNOWLEDGMENTS

The writer wishes to express his appreciation to Professor Gregg King for his assistance and encouragement during this project, and to Professor Paul F. Pucci for his suggestion of the topic. He wishes also to thank Mr. Kenneth Mothersell for his performance of machine work. A special thanks goes to Mr. Joseph Beck for his many hours of capable assistance cheerfully given to all phases of the instrumentation and testing.

TABLE OF CONTENTS

Section	Title	Page
1.	Introduction	1
2.	Description of Equipment	2
3.	Procedure	16
4.	Results	27
5.	Discussion	65
6.	Conclusions	69
7.	Bibliography	70
Appendix		
A.	Fixed Parameters	71
B.	Equipment	72
	1. Cylinder heads	72
	2. Characteristics of the pressure sensing equipment	74
	3. Pressure transducer calibration	75
	4. Special tools	78
	5. Miscellaneous notes on equipment operation	79
C.	Sample Data Sheet	81
D.	Sample Calculations	82
E.	Effect of the Pressure Transducer on Compression Ratio	90
F.	Uncertainity Analysis	91

LIST OF TABLES

Table		Page
1.	Tabulated Results of Test A-1	29
2.	Tabulated Results of Test B-1	30
3.	Tabulated Results of Test A-2	31
4.	Tabulated Results of Test B-2	32
5.	Tabulated Results of Tests A-3 and B-3	33
6.	Tabulated Results of Two Valve Tests-Exhaust Normal	34
7.	Tabulated Results of Two Valve Tests-Exhaust Advanced 12°	35
8.	Tabulated Results of Two Valve Tests-Exhaust Retarded 12°	36
9.	Tabulated Results of Four Valve Tests-Exhaust Normal	37
10.	Tabulated Results of Four Valve Tests-Exhaust Advanced 12°	38
11.	Tabulated Results of Four Valve Tests-Exhaust Retarded 12°	39
12.	Tabulated Results of Four Valve Tests-Exhaust Retarded, Injection Constant and Speed Varied	40

LIST OF ILLUSTRATIONS

Figure		Page
1.	General view of engine and supporting units	5
2.	Two exhaust valve cylinder head installed	6
3.	Four exhaust valve cylinder head installed	7
4.	Water manifold	8
5.	Bottom view of four exhaust valve cylinder head	9
6.	Adaptor, pickup and cables	10
7.	Pressure measurement instrumentation connected	11
8.	Close-up of piezo-calibrator, oscilloscope and camera	12
9.	Magnetic pickups	13
10.	Variable timing gears	14
11.	Special tools	15
12.	Timing diagrams for two valve head	19
13.	Timing diagrams for four valve head	20
14.	Timing diagrams for A-3 and B-3	21
15.	Exhaust valve lift and cam profile, two valve head	22
16.	Exhaust valve lift and cam profile, four valve head	23
17.	Injector cam profile and plunger travel	24
18.	Model 71 Injector pumping characteristics	25
19.	Injector timing using fixed length timing gauges	26
20.	Pressure-crank angle photographs - two valve, exhaust normal	41
21.	Pressure-crank angle photographs - two valve, exhaust advanced	42
22.	Pressure-crank angle photographs - two valve, exhaust retarded	43

LIST OF ILLUSTRATIONS

Figure		Page
23.	Pressure-crank angle photographs - four valve, exhaust normal	44
24.	Pressure-crank angle photographs - four valve, exhaust advanced	45
25.	Pressure-crank angle photographs - four valve, exhaust retarded	46
26.	Pressure-crank angle photographs - exhaust retarded, injection constant, speed varied	47
27.	Typical pressure-crank angle photographs of motoring	48
28.	Selected pressure-crank angle photographs of the exhaust and inlet process	49
29.	Performance curves of A-1 and B-1; full load	50
30.	Performance curves of A-2 and B-2; full load	51
31.	Performance curves of A-3 and B-3; full load	52
32.	Indicated and friction horsepower versus fuel injection point	53
33.	Brake horsepower versus injection point for various exhaust timings	54
34.	Air flow rate versus injection point for various exhaust timings	55
35.	Peak firing pressures versus fuel injection point for various exhaust timings	56
36.	Brake specific fuel consumption versus fuel injection point for various exhaust timings	57
37.	Brake thermal efficiency versus fuel injection point for various exhaust timings	58
38.	Exhaust temperatures versus fuel injection point for various exhaust timings	59
39.	Pressure-volume diagram, injection at 5 °BTC	60
40.	Pressure-volume diagram, injection at 10.8 °BTC	61

LIST OF ILLUSTRATIONS

Figure		Page
41.	Pressure-volume diagram, injection at 15.8 °BTC	62
42.	Pressure-volume diagram, injection at 20 °BTC	63
43.	Effect of injection timing on pressure-crank angle diagram	64

LIST OF SYMBOLS

Symbol	
A	piston area, sq. in.; designates test using four valve head
ABC	after bottom center
API	specific gravity, American Petroleum Institute units
ATC	after top center
B	designates test using two valve head
BBC	before bottom center
BDC	bottom dead center
bhp	brake horsepower, hp.
bmep	brake mean effective pressure, psi
bsac	brake specific air consumption, lb_m air/bhp-hr
bsfc	brake specific fuel consumption, lb_m fuel/bhp-hr
BTC	before top center
BTU	British Thermal Unit
C_D	coefficient of discharge
C_p	specific heat, BTU / lb_m - °F
$\overline{C}_p$	specific heat, BTU / lb mole- °F
cm	centimeter
cu. in.	cubic inches
cu. ft.	cubic feet
d	diameter, feet
°F	degrees Fahrenheit
fhp	friction horsepower, hp.
fps	feet per second
ft.	foot or feet

LIST OF SYMBOLS

Symbol	
h	fuel column height, inches
hg.	mercury
hp.	horsepower
hr.	hour
ihp	indicated horsepower, hp.
imep	indicated mean effective pressure, psi
in.	inch
isac	indicated specific air consumption, lb_{in} air/ihp-hr
isfc	indicated specific fuel consumption, lb_m fuel/ihp-hr
lb	pound
L	stroke, ft.
LHV	lower heating valve of fuel, BTU / lb_m fuel
$\dot{m}$	mass rate, lb_m / hr.
M_p	molecular weight of products of combustion
min.	minute
mm	millimeter
msec	milliseconds
mv	millivolts
N	engine revolutions per minute
p	pressure, psia or in.-hg.
psi	pounds per square inch
psia	pounds per square inch absolute
r_k	compression ratio
rpm	revolutions per minute

LIST OF SYMBOLS

Symbol	
°R	degrees Rankine
R	pressure drop across air inlet nozzles, inches of water
Re	Reynold's number
R_s	scavenging ratio
sec	seconds
sp. gr.	specific gravity
sq. in.	square inches
sq. ft.	square feet
t	duration of run, sec.; temperature, °F
T	torque, ft-lb_f ; temperature, °R
TDC	top dead center
V	velocity, fps
V_c	clearance volume, cu. in.
V_d	displacement volume, cu. in.
η	efficiency, percent
ν	kinematic viscosity, sq. ft. / sec.
ρ	density, lb_m / cu. ft.

Subscripts	Meaning
a	air
b	brake
c	clearance
d	displacement
D	discharge
e	exhaust

LIST OF SYMBOLS

Subscripts	Meaning
f	fuel or force
i	inlet or indicated
k	compression
m	mass or mechanical
o	ambient state
p	pressure or products
s	scavenging
t	temperature or thermal
w	water

Superscript	Meaning
o	degrees of temperature or degrees of crank angle

1. Introduction.

The General Motors 1-53X3 Diesel engine has been installed and used as a laboratory unit since 1960. The installation and initial tests are described in LCDR McCord's thesis /1/. The purpose of this project was to determine the effect of varying exhaust and injection timing on engine performance using both the two and four exhaust valve cylinder heads.

In previous tests indicated horsepower has been determined from measured brake horsepower plus friction horsepower obtained from motoring tests. In this investigation a piezoelectric pressure transducer was also used to obtain this information, as well as ignition delay, compression pressures and peak pressures. The use of an electric pressure transducer in high speed engines is mentioned briefly in many text books on mechanical measurements and internal combustion engines /2,3/, but few give other than general information. Its use in this project is described and results displayed and discussed.

Since the two valve head had not been installed previously, data was taken to compare its performance with that of the four valve head.

The equipment and its use is described. The test procedure is given and results are presented in several forms and discussed.

Appendices are included which provide information that will assist future users.

2. Description of equipment.

The General Motors 1-53X3 is a single cylinder two stroke cycle Diesel engine rated at 30 hp. at 3000 rpm. The engine and its supporting systems are detailed in McCord's thesis. Appendix A contains engine parameters required for this report. Fig. 1 is an overall view of the engine and auxiliary units. Fig. 2 and 3 show the physical differences in external connections to the two cylinder heads. Appendix B, Part 1, describes these differences and the modifications necessary to adapt the heads for receiving the pressure transducer. Fig. 4 is a view of the water manifold not visible in Fig. 1.

The pressure transducer is a Kistler Corporation Model 601 miniature quartz pickup. It can be used in high temperature and pressure applications and has good low frequency response. The pickup is protected from the cylinder temperatures by a water cooled adaptor. The adaptor is mounted flush in the cylinder cavity. See Fig. 5 for a view of the pressure cavity and its relation to the injector and exhaust valves in the four valve head. The location in the two valve head is similiar. The pressure within the engine cylinder develops an electromotive force in the crystal which is transmitted to a Kistler Model 651 Piezo-calibrator via cables supplied by the manufacturer. This device permits reading the pressure signal in psi, calibration of the pickup, the producing of a calibration test signal and checking of oscilloscope sensitivity. Characteristics and operating instructions for this equipment are contained in the manufacturer's instruction book /4/. Certain of these are presented in Appendix B, Part 2.

Fig. 6 shows the necessary cables, the pickup and the water cooled adaptor. This equipment assembled and connected for pressure measurement

is given in Fig. 7.

Prior to using the pickup for cylinder pressure measurements it was calibrated statically in a dead weight tester. The procedure for calibration is given by the manufacturer /4/, but certain additional information, and the procedure employed are given in Appendix B, Part 3. As previously mentioned, the piezo-calibrator provides a calibration signal. This permits checking of the oscilloscope during testing and provides a reference signal from which the magnitude of engine pressures are determined. These calibrated signals are based upon data from the static test. The pickup was rechecked about half-way through the test program. No change was detected.

The pressure signal after passing through the piezo-calibrator was displayed on the vertical plates of a Hewlett Packard Model 130 oscilloscope. The horizontal signal was derived from a time sweep triggered externally by a magnetic pickup. This sweep was set to start at BDC. Sweep time was adjusted to give full scope travel for one engine revolution. The result is a pressure-crank angle diagram. Another magnetic pickup was used to provide a check on the sweep rate and to indicate TDC as a reference on the pressure-crank angle diagram. The display was photographed with a Hewlett-Packard Model 196A oscilloscope camera. Fig. 8 is a close-up of the piezo-calibrator, oscilloscope and camera.

A total of three magnetic pickups were used. The use of two has been described. The third provided a measurement of engine rpm. These pickups generate a voltage when their magnetic field is cut by rotating gears with ferrous teeth. The voltage generated is a function of the clearance between the teeth and the pickup, the size of the teeth and the speed of rotation. There are 60 teeth on the rpm gear and one tooth on the others. This equipment is mounted on the dynamometer shaft end and is shown in Fig. 9.

Variable timing gears were manufactured by General Motors after the initial installation was completed. They had not been used prior to this project. They permit making changes of up to $\pm$ 15° in exhaust and injection timing. Previously it was necessary to remove a cam gear, shift it, and accept changes of an integer times the number of degrees per tooth. This was a tedious task. With the variable gears timing changes in both injection and exhaust can be accomplished in about 20 minutes, and there is no need to wait for the engine to cool. The performance of the gears was found to be satisfactory. Fig. 10 is a photograph of the gears installed and set on zero.

Various temperatures obtained from iron-constantan thermocouples are displayed on a Speedomax recorder which has an upper limit of 800°F. A potentiometer was installed to measure the exhaust gas temperature, thus providing information previously obtained by extrapolation.

Special tools produced for this project are described in Appendix B, Part 4, and shown in Fig. 11.

Some of the equipment problems which arose, and suggestions for future users are given in Appendix B, Part 5.

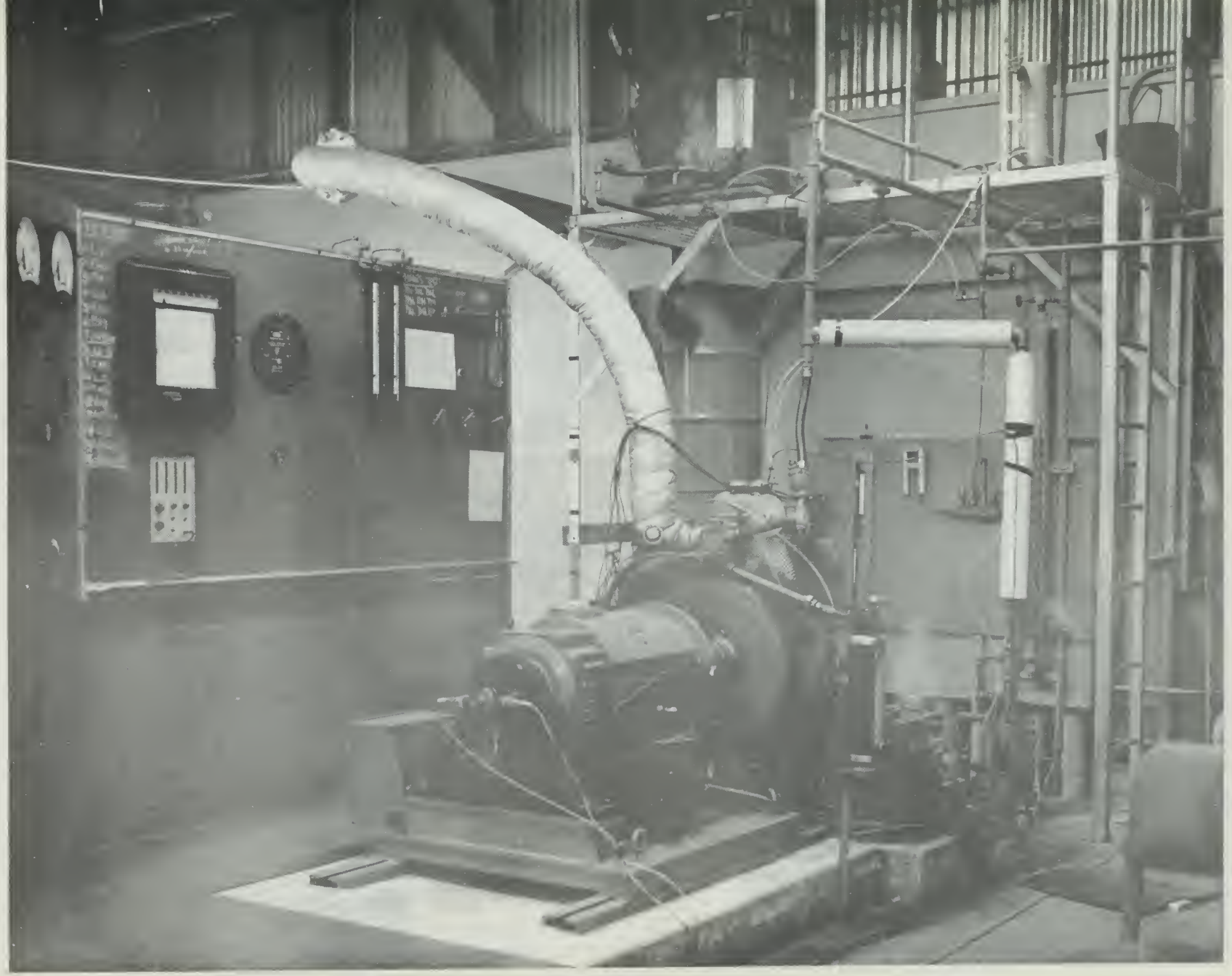

Fig. 1. General view of engine and supporting units.

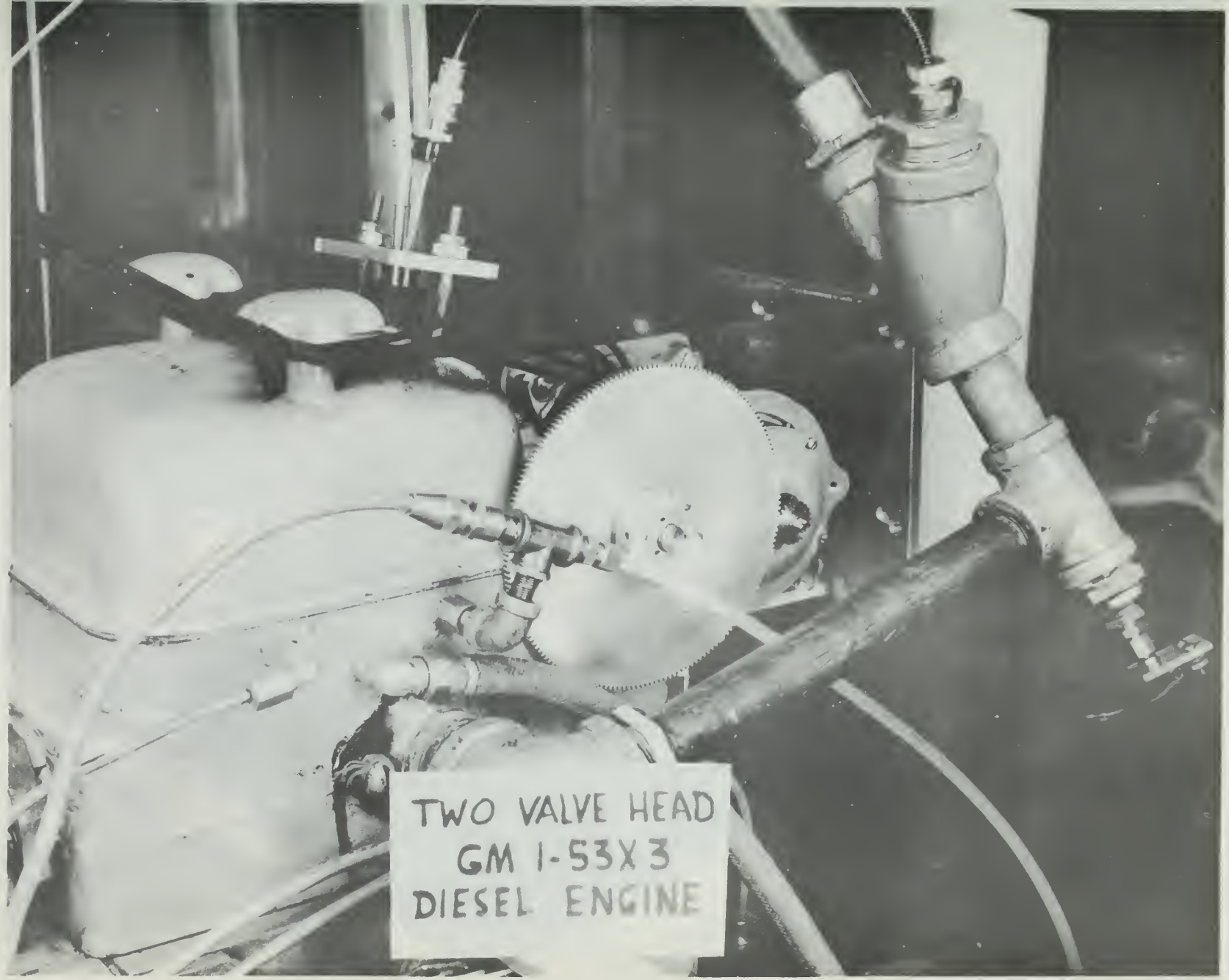

Fig. 2. Two exhaust valve cylinder head installed.

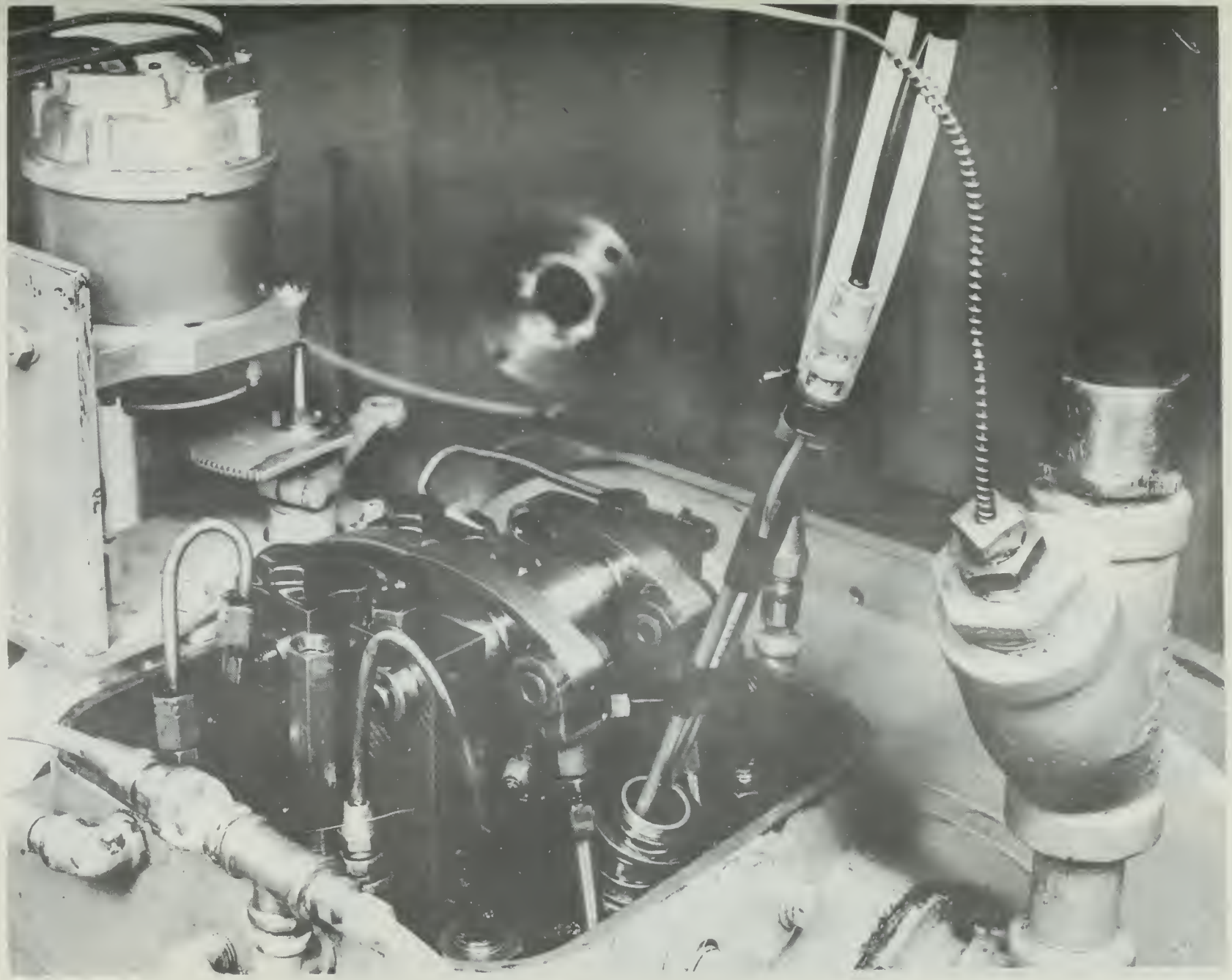

Fig. 3. Four exhaust valve cylinder head installed.

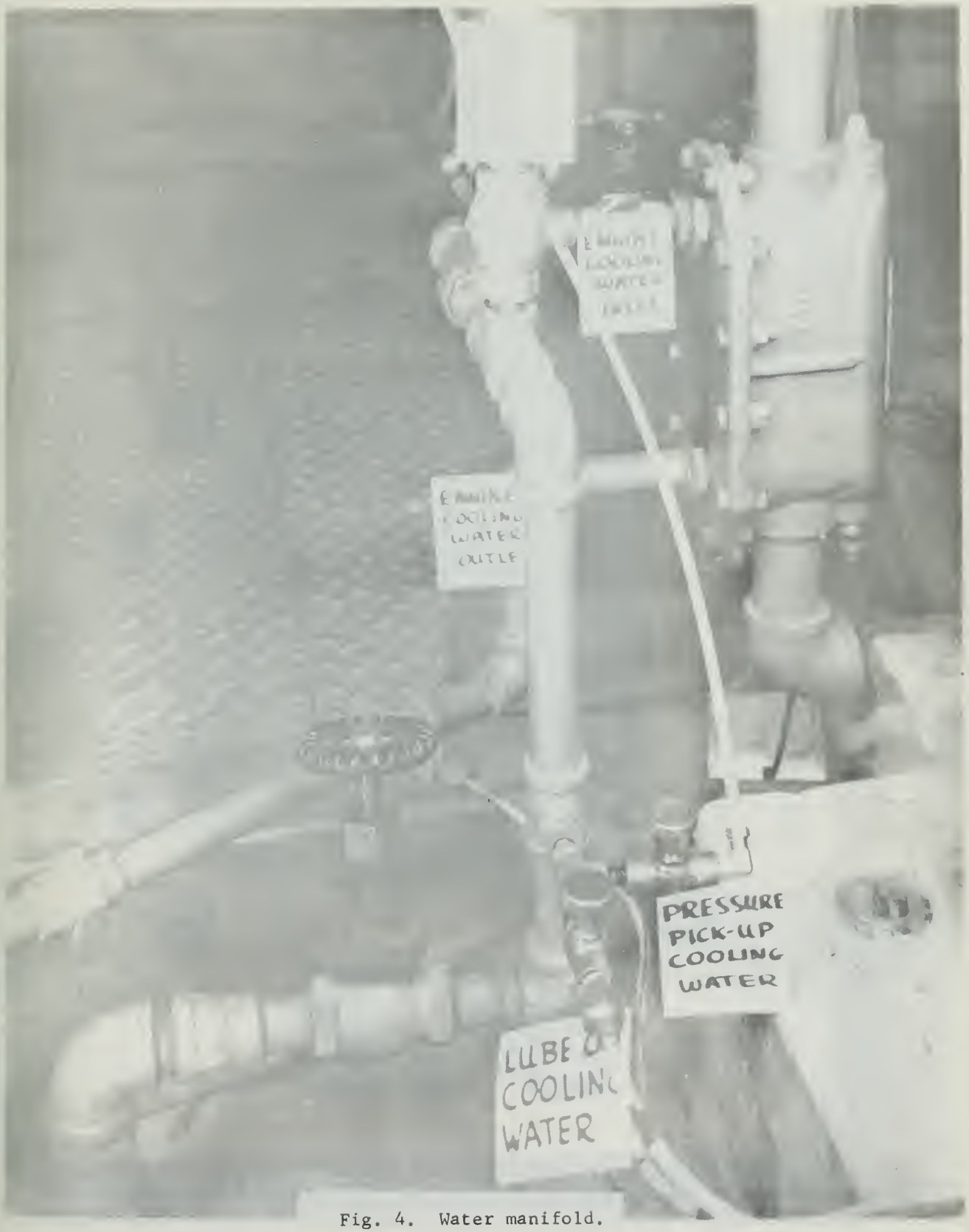

Fig. 4. Water manifold.

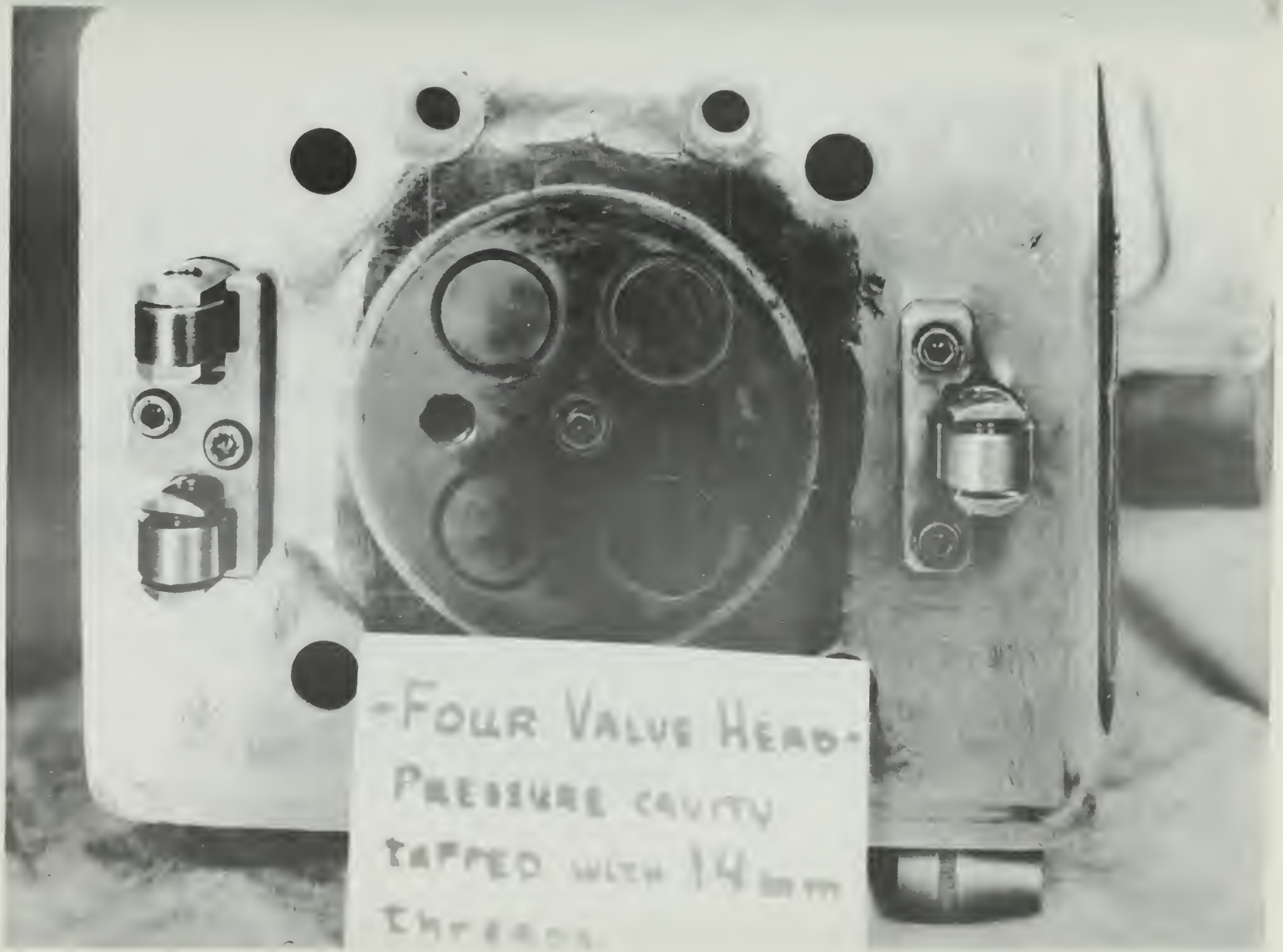

Fig. 5. Bottom view of four exhaust valve cylinder head.

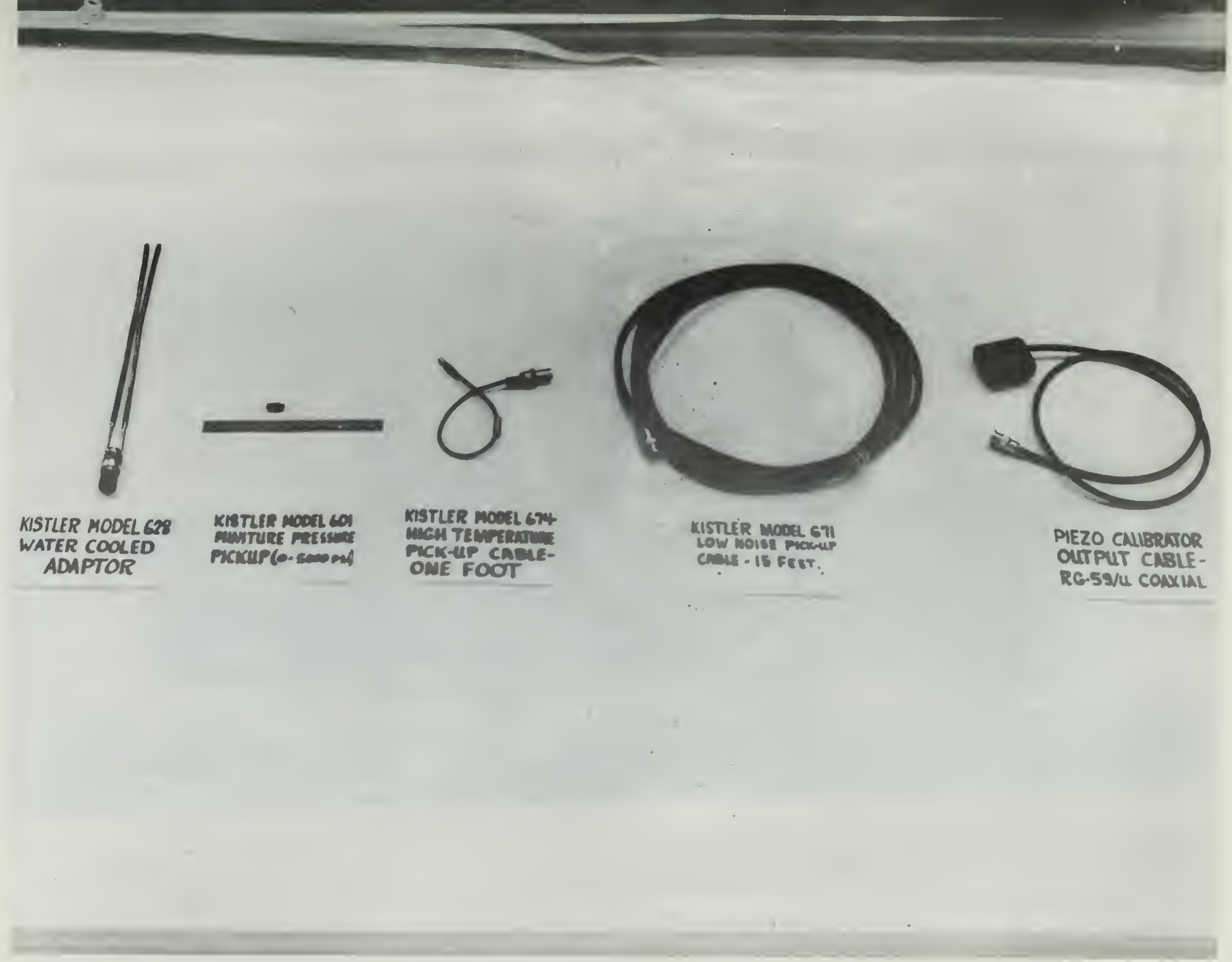

Fig. 6. Adaptor, pickup and cables.

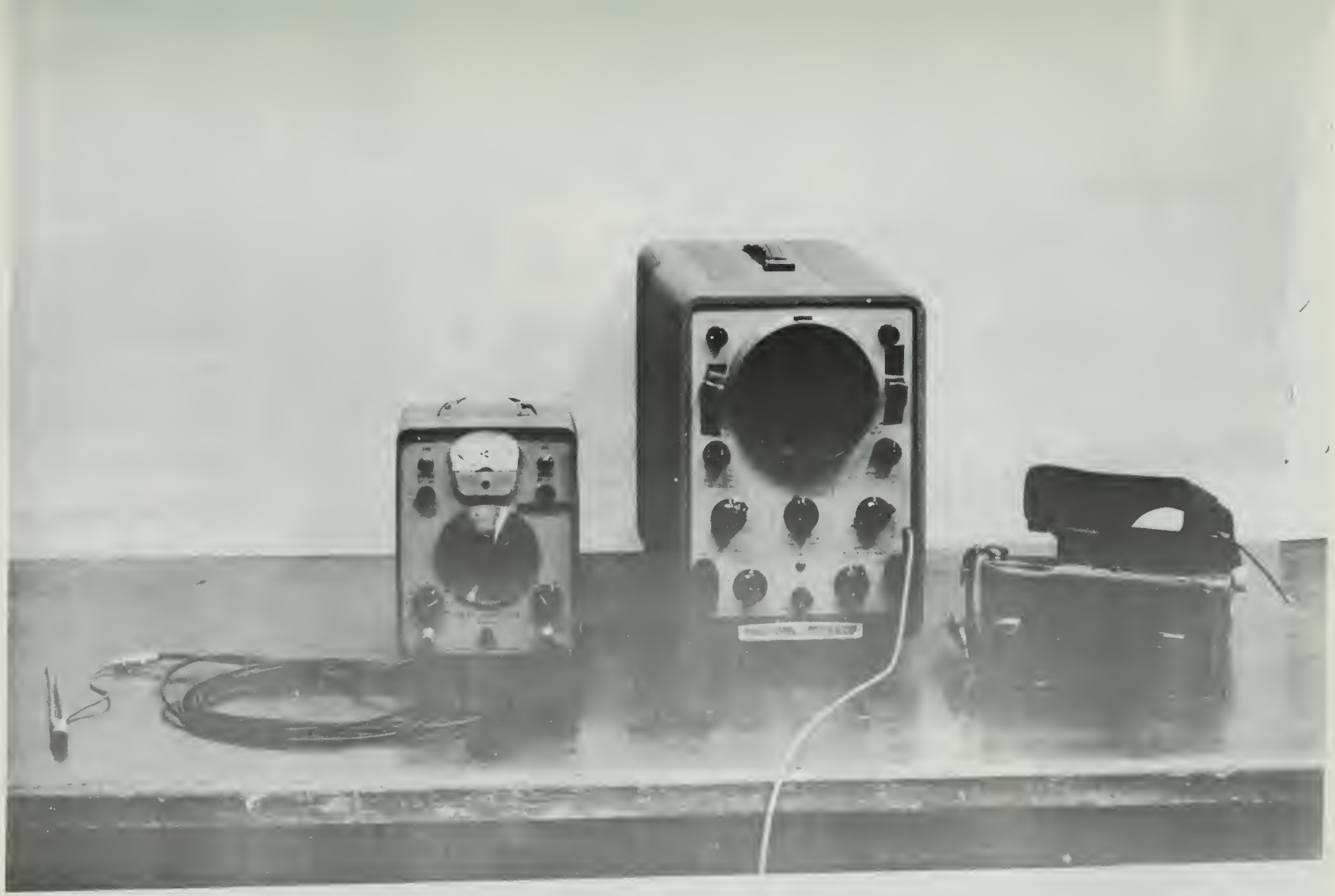

Fig. 7. Pressure measurement instrumentation connected.

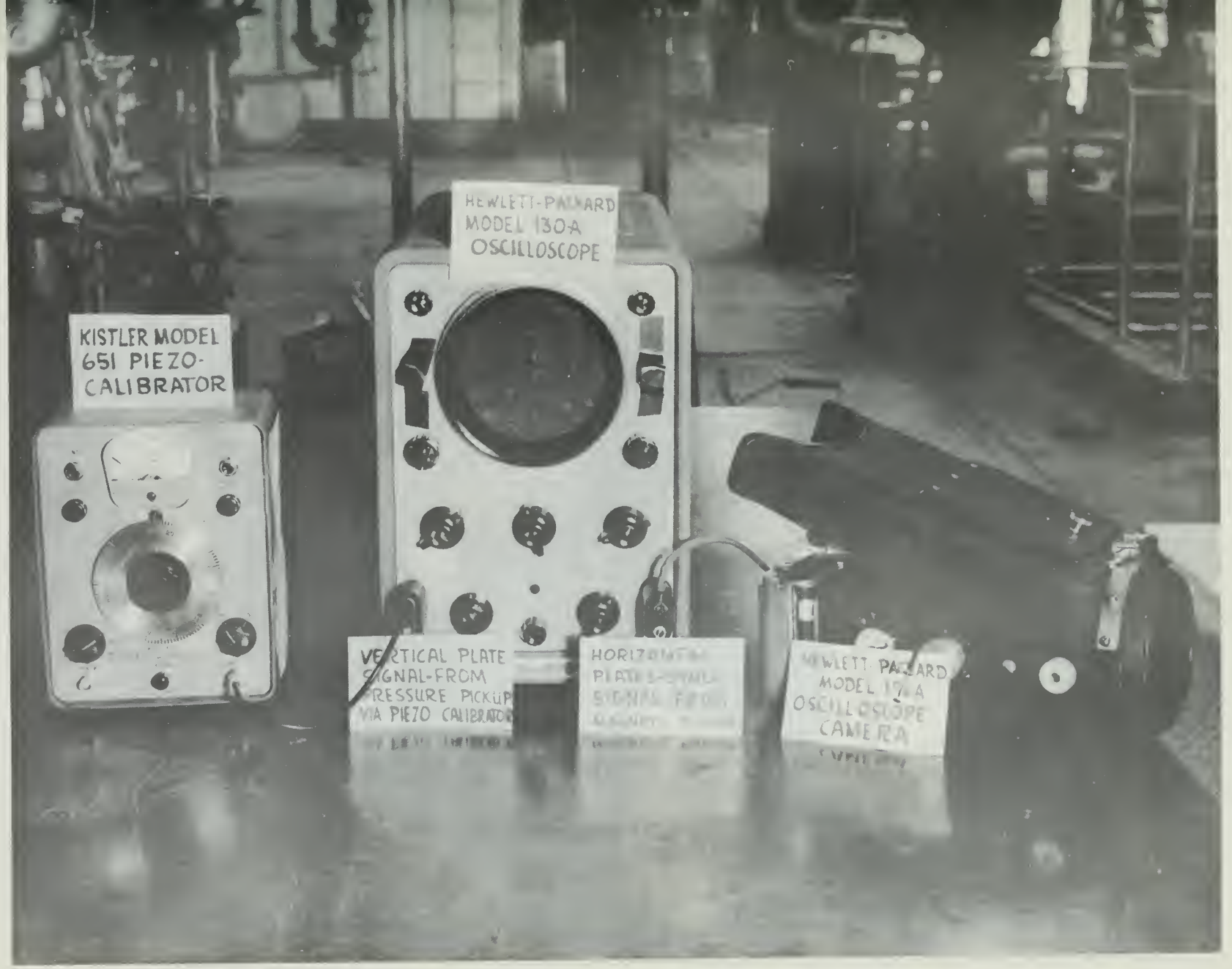

Fig. 8. Close-up of piezo-calibrator, oscilloscope and camera.

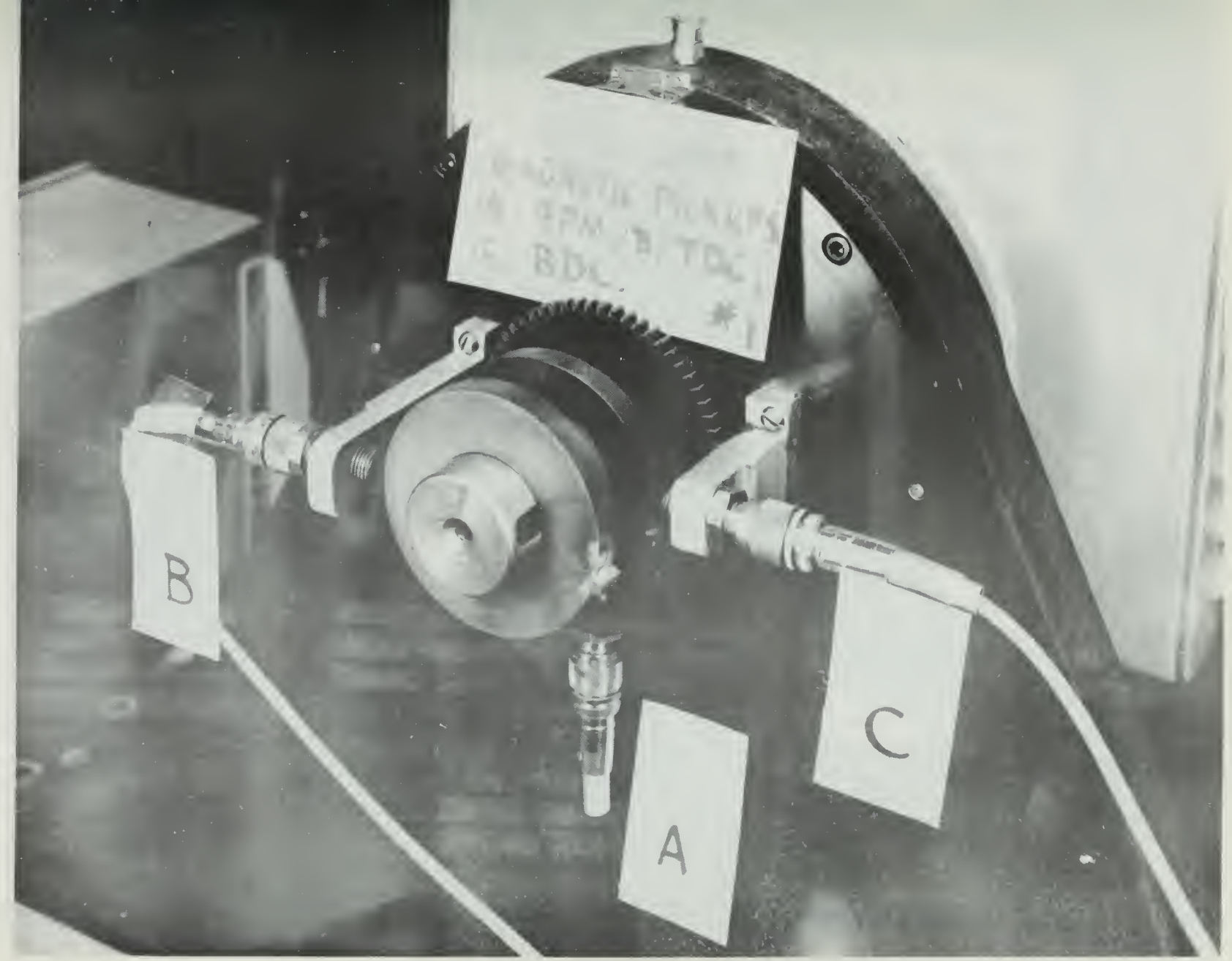

Fig. 9. Magnetic pickups.

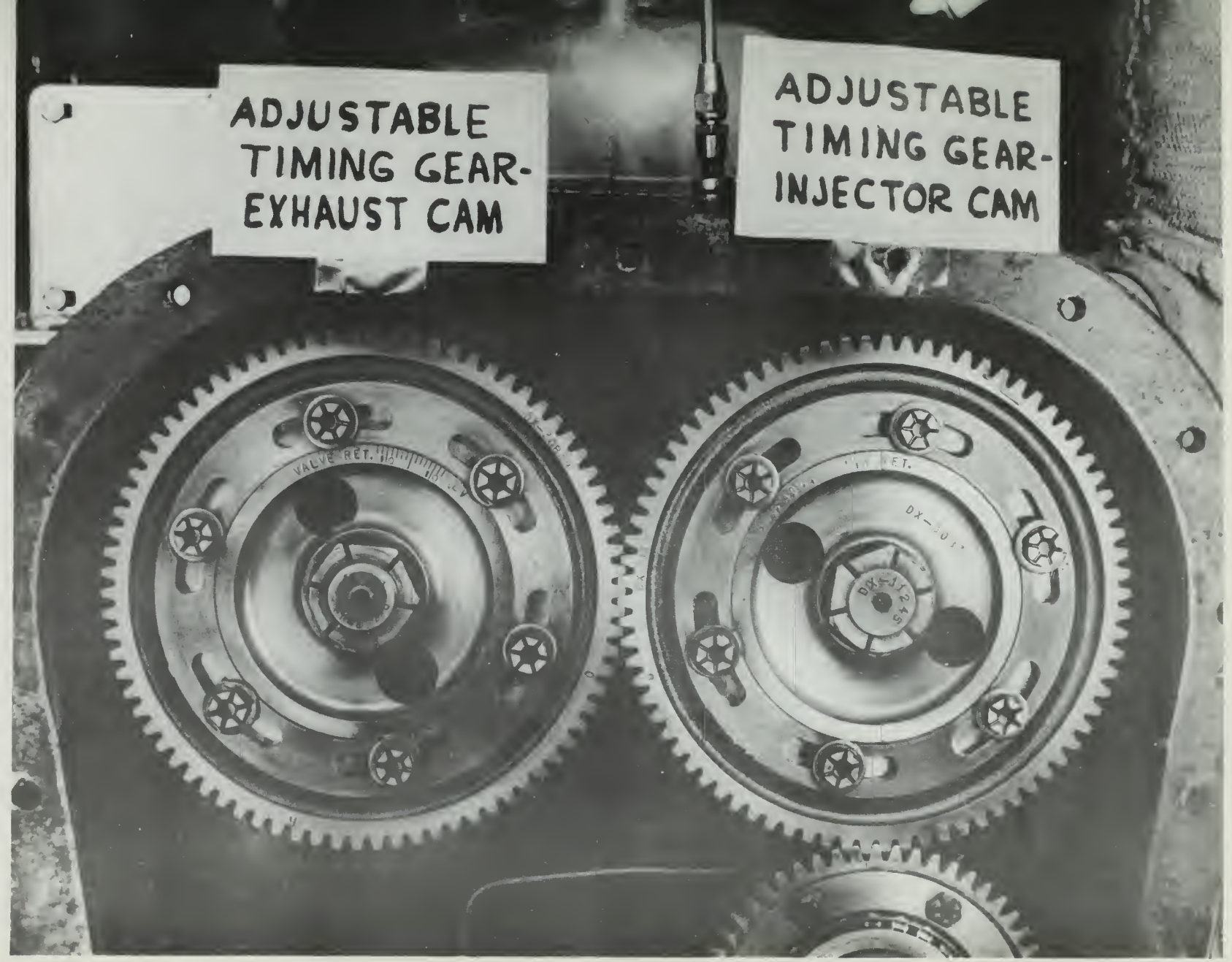

Fig. 10. Variable timing gears.

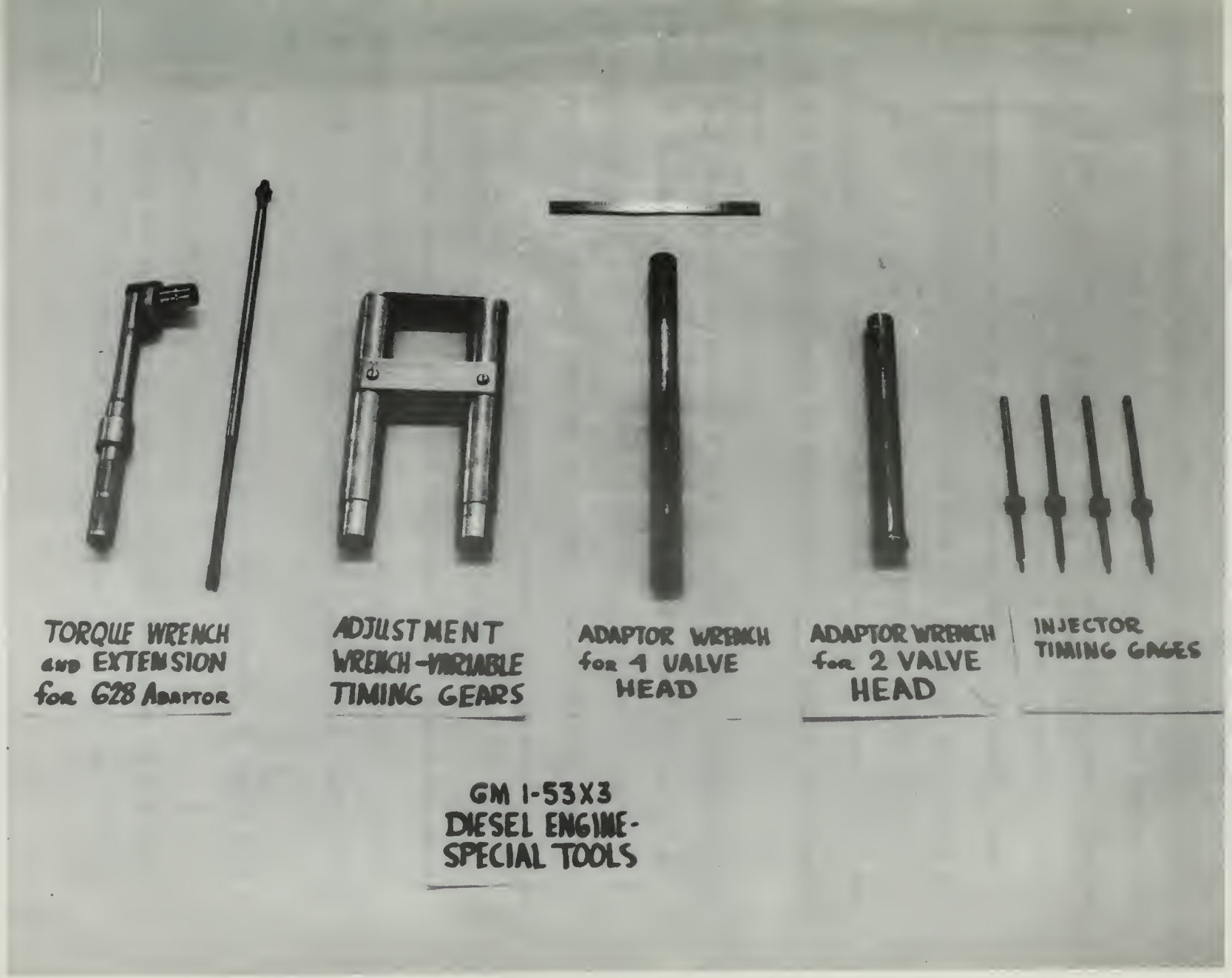

Fig. 11. Special tools.

3. Procedure.

In order to observe the effects of timing changes on engine performance it was necessary to maintain other variables as constant as possible. To accomplish this end equilibrium was established before data was recorded. Water and lube oil, engine speed and load were closely controlled. The exhaust temperature provided a good indication of a steady condition. Ambient temperatures and pressures did not vary appreciably during the test period, but nonetheless all horsepowers have been corrected to a basis of 60 °F and one atmosphere. Engine speed was maintained within $\pm$ one percent during controlled runs. Inlet water temperatures of about 170 °F were used, and the lube oil temperature was at least 160 °F before fully loading the engine.

Full load is defined herein to be full throttle and that load applied, via the dynamometer, which will maintain the speed at the desired value. Lesser loads are a percentage of the torque obtained at full load.

Prior to any runs for data all instruments were inspected, cleaned as necessary and calibrated. Test runs were performed and the results checked against those previously reported for the four valve head.

During the engine warm up period instruments were checked for proper response. The oscilloscope was monitored to detect unwanted signals, signal drift or fluctuation and as a visual check on the timing configuration set.

When equilibrium was established data were recorded. A sample data sheet is given in Appendix C.

Following the recording of data, photographs were made of the oscilloscope presentation. Various scales were observed on each test so as to

detect any unusual or interesting events.

The test program can be subdivided into several catagories. The first of these consisted of runs made at 1500 rpm and full load with exhaust timing set for one of three configurations and injection starting at one of four points. This results in a total of 12 different timing modes. These tests were conducted using each of the heads. A second set of runs was made at full load over a range of rpm for one timing condition. The third set of runs was made for variable speed and loads for the two valve head using the timing configurations equivalent to those reported by McCord /1/ for the four valve head.

Figs. 12 - 14 depict the various timing configurations. It is seen that injection was varied from 20 °BTC to 5 °BTC for each of the three exhaust timings. The A-3 and B-3 timing do not fall into these basic patterns. The letter A refers to the four valve head and B to the two valve head. The number suffix refers to a particular timing mode for that head. The A-3 mode was tested by McCord /1/ and B-3 was done for comparison. The angular location at which events occur for the A-1,2,3, modes are not as reported by McCord /1/ and have been corrected here.

The normal configuration is that in which the gear train is aligned in accordance with the manufacturer's blueprint, the injector plunger height set at 1.484 in. and exhaust valve clearances set in accordance with the maintenance manual. The injector plunger height is measured from the upper surface of the injector plunger follower to the upper surface of the injector body when cam lift is zero, and therefore provides the zero, or base, from which plunger stroke is measured.

Figs. 15 and 16 are exhaust cam and valve lift profiles for the two heads. This data was obtained with a dial indicator at both the push rod

and valve bridge/valve stem position. The reason for the difference in readings on the forward and after valves in the four valve head could not be determined. In order to have the four valves open and close at the same angular location valve clearances were set to compensate for the difference. In addition, the exhaust rocker arms differ in length on the two heads so that the same exhaust period could not be duplicated. Therefore, the normal for each head was established as defined here. A-1 and B-1 modes are the normal timing configurations.

The injector cam and plunger travel diagram reported by McCord /1/ was found to be in error, since he had shown only the cam profile and given plunger travel as a constant times cam lift. The constant was true only for the point of maximum lift. Therefore Fig. 17 is given. Using this and Fig. 18, which shows the pumping characteristics of the injector used, the injection angle for full throttle is accurately determined.

Fig. 19 provides information on the range of injection timing possible using the injector timing gauges. This supercedes one given by McCord /1/ since the injector plunger travel on which it was predicated was in error. However, timing changes are more readily made at the cam gear, and this method was used.

In order to obtain friction horsepower data the dynamometer was used to drive the engine with fuel secured. These runs were made upon securing from engine tests and conducted as swiftly as possible to retain high oil and water temperatures. Motoring was conducted over a range of speeds up to 1600 rpm in 100 rpm increments. For data above this speed it was necessary to extrapolate. Motoring tests were conducted for each exhaust timing since these changes had a measurable effect upon friction horsepower.

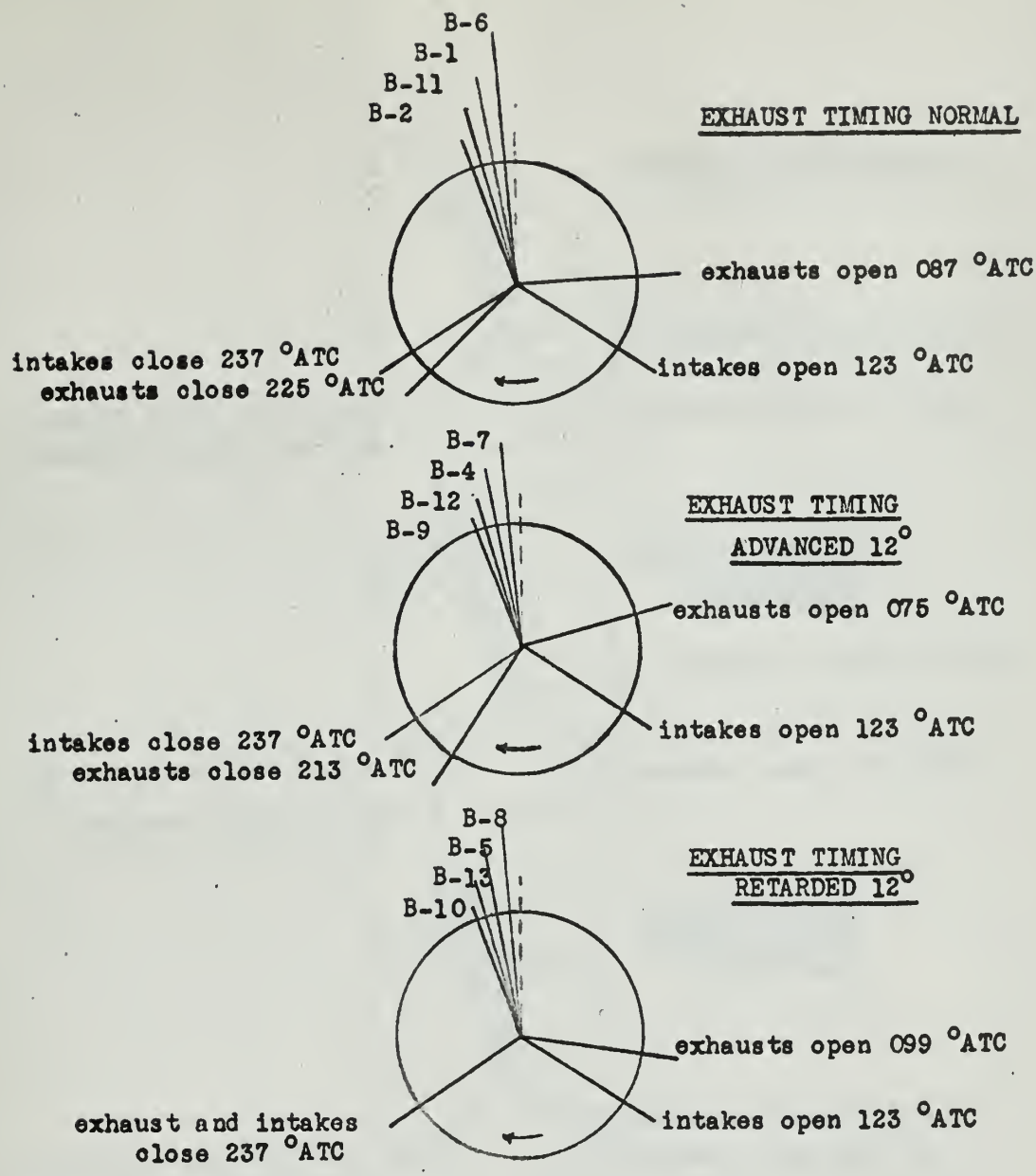

Timing mode	Injection starts	Injection stops
B-2,9,10	20.0 °BTC	7.1 °BTC
B-11,12,13	15.8 °BTC	2.9 °BTC
B-1,4,5	10.8 °BTC	2.1 °ATC
B-6,7,8	5.0 °BTC	7.9 °ATC

Fig. 12. Timing diagrams for two valve head.

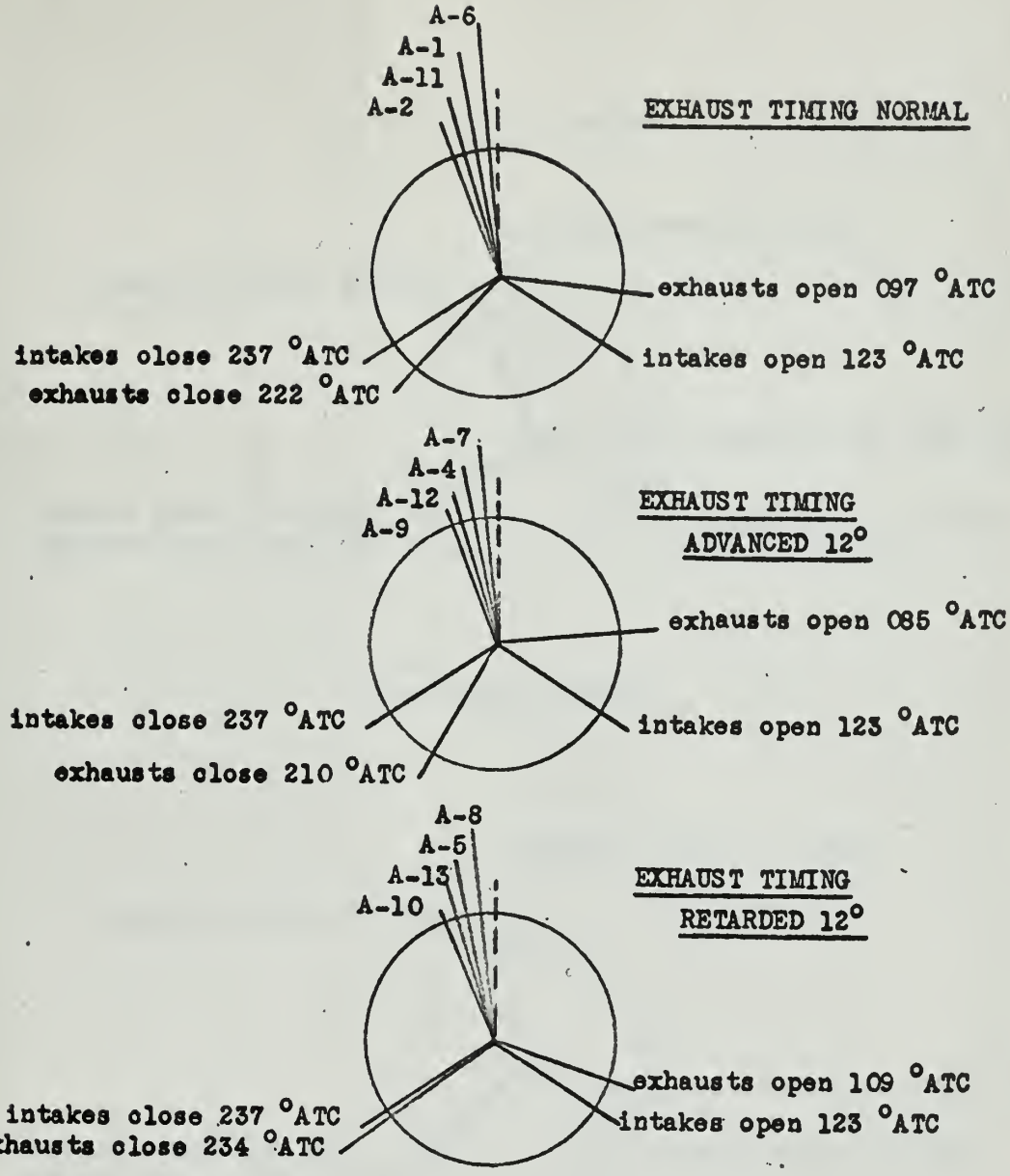

Timing mode	Injection starts	Injection stops
A-2,9,10	20.0 °BTC	7.1 °BTC
A-11,12,13	15.8 °BTC	2.9 °BTC
A-1,4,5	10.8 °BTC	2.1 °ATC
A-6,7,8	5.0 °BTC	7.9 °ATC

Fig. 13. Timing diagrams for four valve head.

B-3 timing diagram

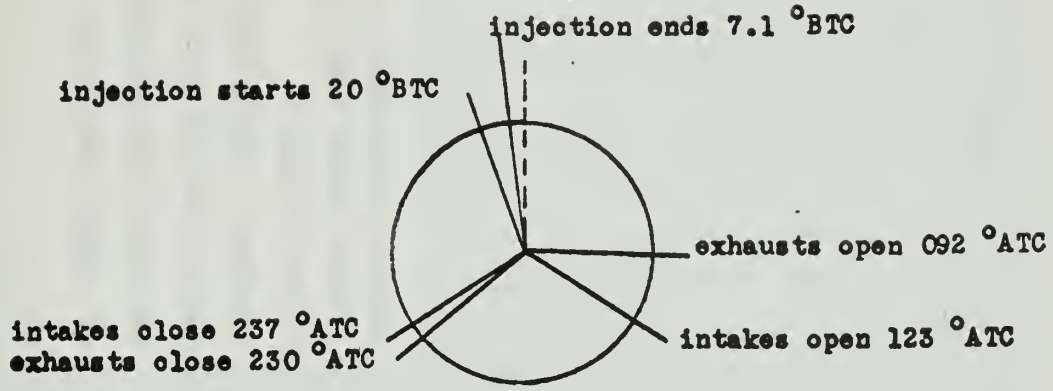

A-3 timing diagram

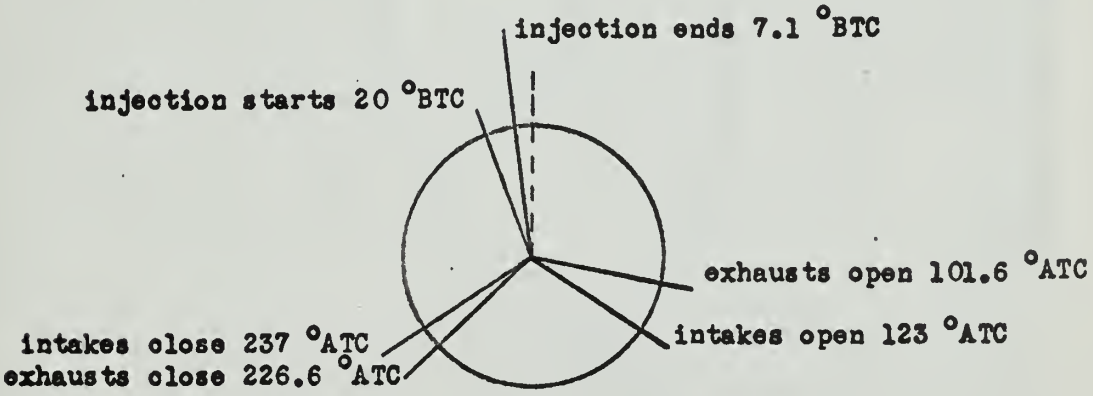

Fig. 14. Timing diagrams for A-3 and B-3.

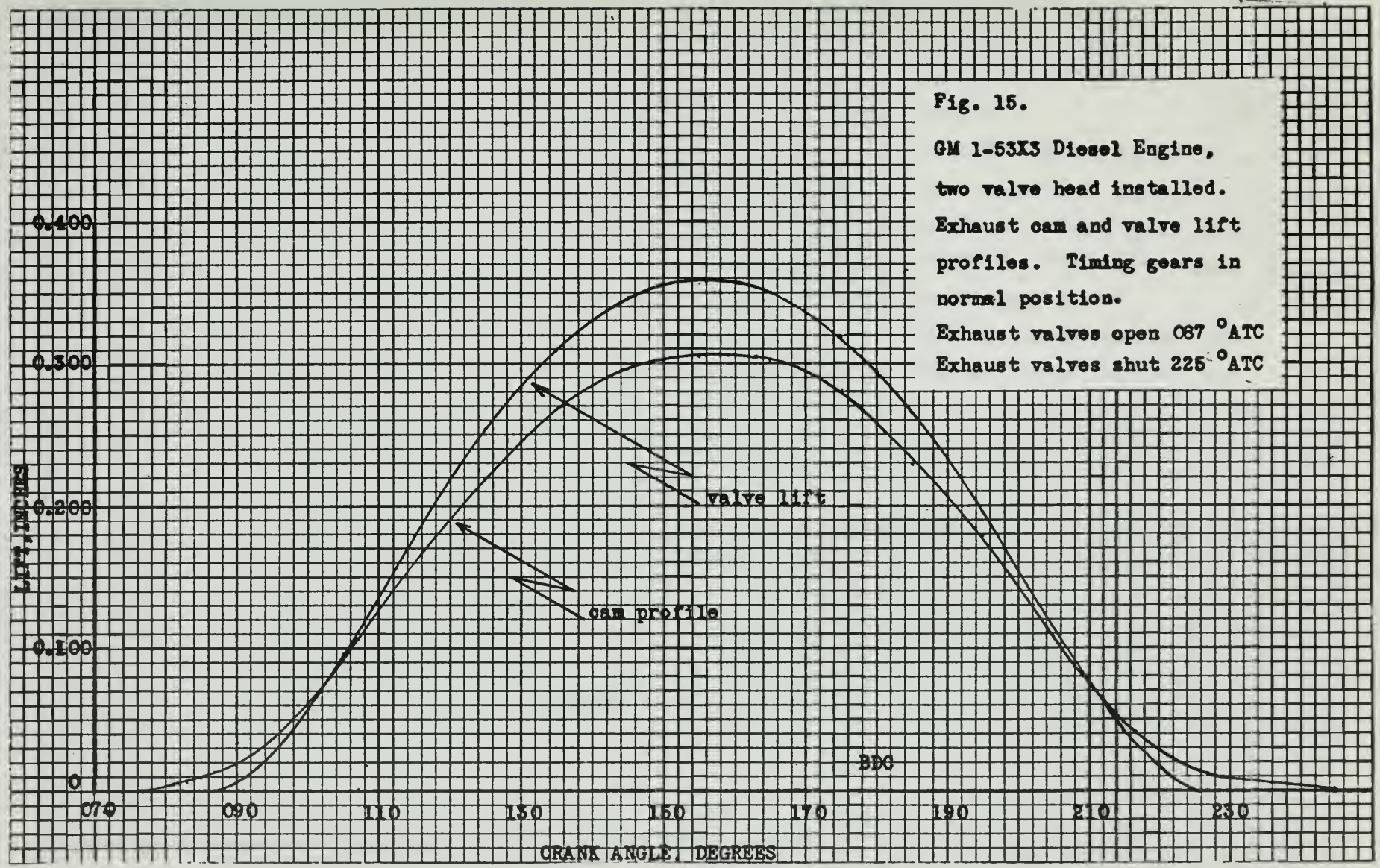
Fig. 15.
GM 1-53X3 Diesel Engine,
two valve head installed.
Exhaust cam and valve lift
profiles. Timing gears in
normal position.
Exhaust valves open 087 °ATC
Exhaust valves shut 225 °ATC
0.400
0.300
0.200
0.100
0
valve lift
cam profile
BDC
070
090
110
130
150
170
190
210
230
CRANK ANGLE, DEGREES

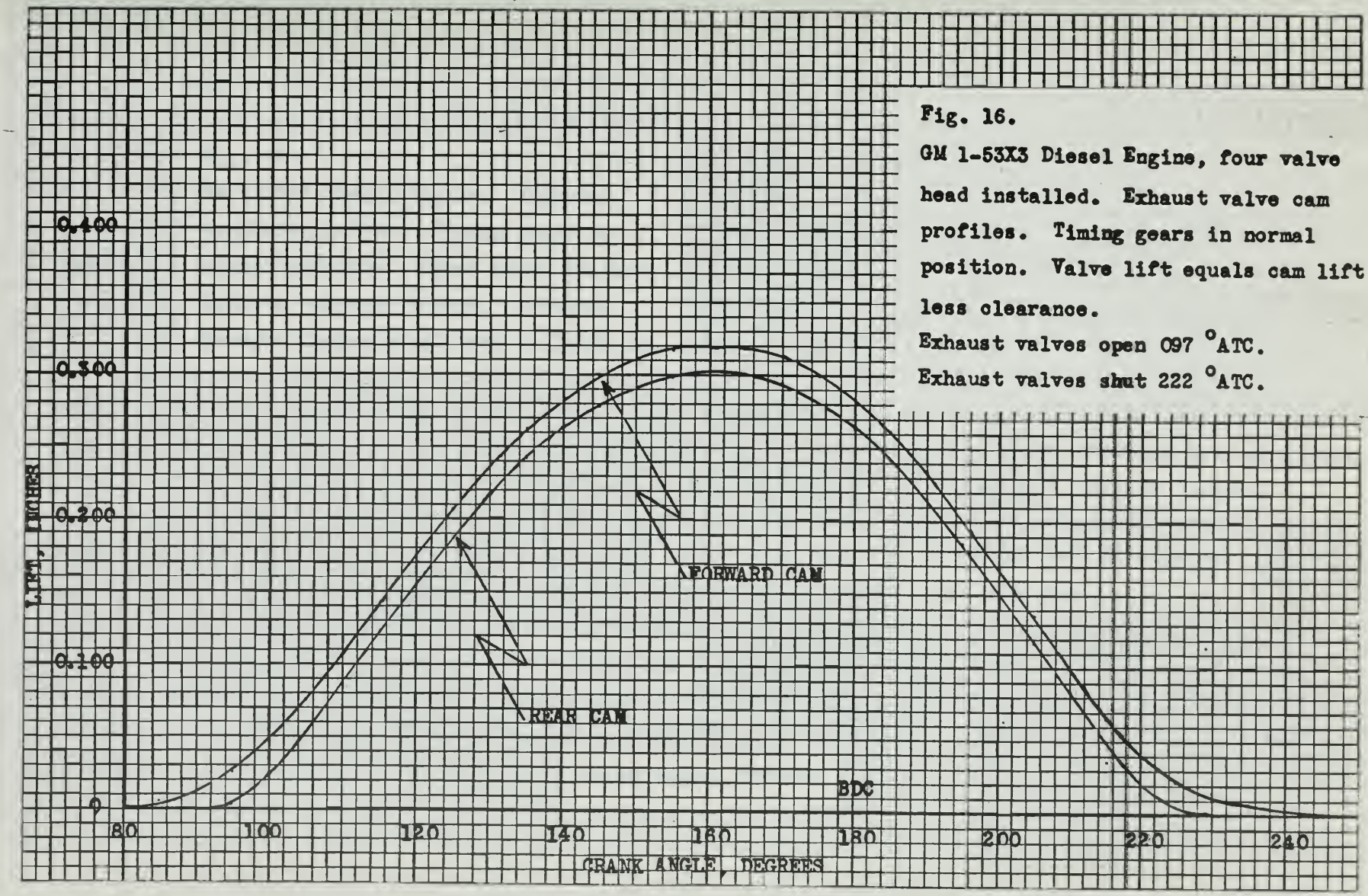

Fig. 16.

GM 1-53X3 Diesel Engine, four valve head installed. Exhaust valve cam profiles. Timing gears in normal position. Valve lift equals cam lift less clearance.

Exhaust valves open 097 °ATC.

Exhaust valves shut 222 °ATC.

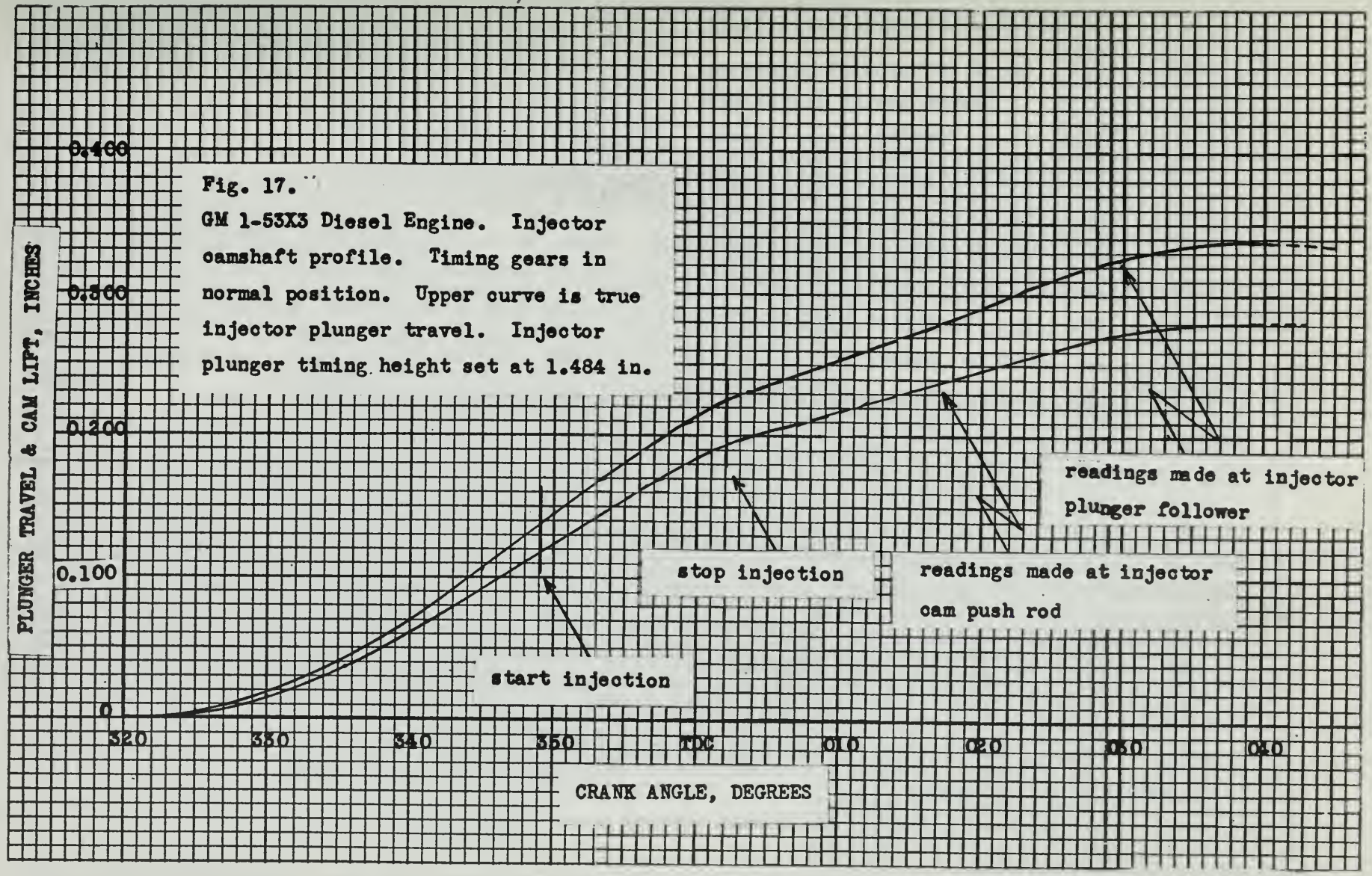
Fig. 17.
GM 1-53X3 Diesel Engine. Injector camshaft profile. Timing gears in normal position. Upper curve is true injector plunger travel. Injector plunger timing height set at 1.484 in.
PLUNGER TRAVEL & CAM LIFT, INCHES
0.400
0.300
0.200
0.100
0
320
330
340
350
TDC
010
020
030
040
CRANK ANGLE, DEGREES
start injection
stop injection
readings made at injector plunger follower
readings made at injector cam push rod

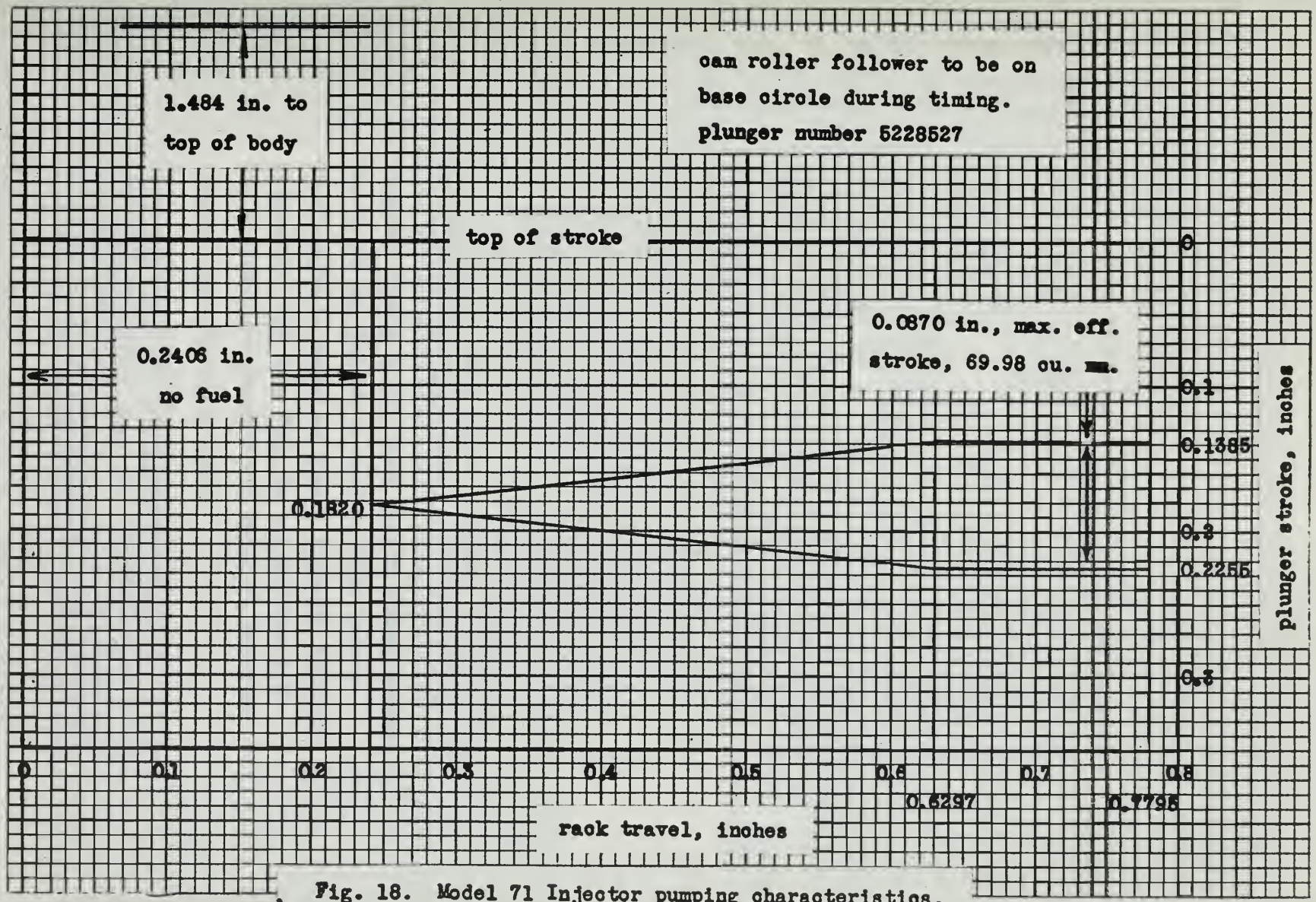

Fig. 18. Model 71 Injector pumping characteristics.

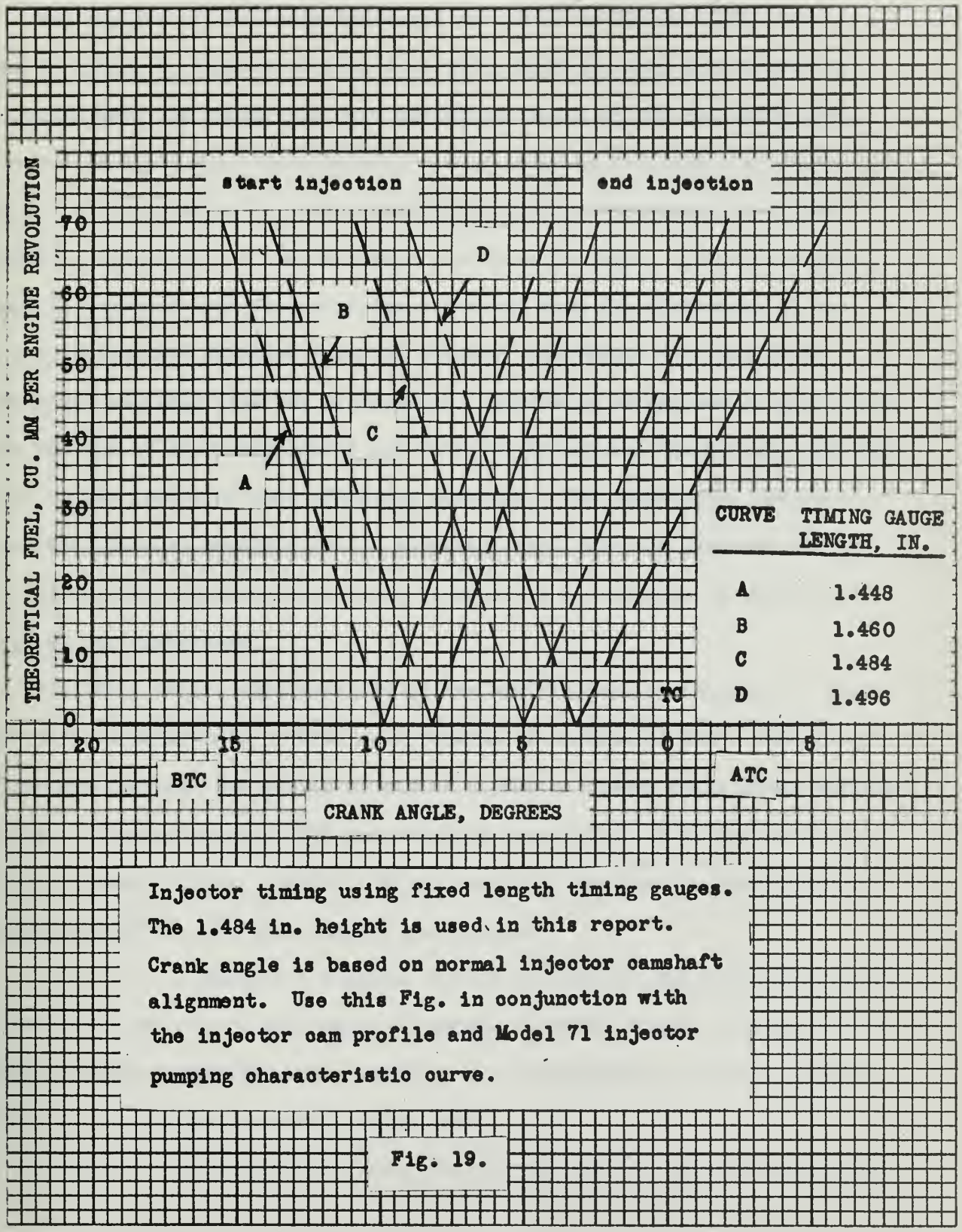

Injector timing using fixed length timing gauges. The 1.484 in. height is used in this report. Crank angle is based on normal injector camshaft alignment. Use this Fig. in conjunction with the injector cam profile and Model 71 injector pumping characteristic curve.

Fig. 19.

4. Results.

The results of the tests conducted are given in Tables 1-12. The data in Tables 1, 3 and 5 for the four valve head are from McCord /1/ and are given here for comparison with equivalent tests on the two valve head. Certain terms given in the tabulated results require definition at this point. Fuel horsepower is that power which would be produced if all the energy of combustion of the fuel were converted to power. Friction horsepower is computed both from motoring tests and from the difference of indicated horsepower obtained from the pressure transducer data and brake horsepower obtained from the dynamometer. Indicated horsepower is given both from the sum of brake horsepower and friction horsepower (motoring), and that based on the indicated mean effective pressure. The compression pressure is that peak pressure obtained during motoring tests from the pressure pickup. The theoretical compression pressure is based on an empirical equation and is given for comparison.

Fig. 20 - 28 are reproductions of the oscilloscope photographs of pressure versus crank angle. These are presented in groups of four. The first six groups indicate the effect of varied injection timing for a given exhaust timing. All were made at 1500 rpm and full load. Fig. 26 is for injection, exhaust timing and load constant and rpm varied. The last two figures are selected motoring and inlet-exhaust photographs.

Figs. 29 - 31 compare the engine operation with two and four valve heads at full load and over a wide range of speeds for three timing configurations. Torque, brake horsepower, brake specific fuel consumption and brake thermal efficiency are plotted against engine speed.

Figs. 32 - 38 are various performance curves for the two and four valve

heads operating at 1500 rpm and full load with changes in injection and exhaust timing.

Figs. 39 - 42 are pressure versus volume diagrams transcribed from pressure-crank angle photographs for the four valve head with normal exhaust timing, 1500 rpm, full load, but varied fuel injection timing.

Fig. 43 shows the effect of fuel injection on the pressure-crank angle diagram. It is for the same timings as depicted in Fig. 23 and Figs. 39 - 42.

Table 1. Tabulated Results of Test A-1.

rpm	torque	bhp	fuel hp	η_{tb}	bsfc	R_s	air-fuel ratio
526	50.7	4.94	27.6	17.8	0.738	1.3	25/1
524	37.1	3.72	13.75	27.0	0.505		50.4/1
526	25.1	2.46	10.00	24.6	0.540		69/1
526	12.5	1.22	6.84	17.9	0.745		101/1
987	62.4	11.41	47.1	24.4	0.547	1.395	28.2/1
987	46.6	8.59	30.8	27.9	0.478		43.2/1
987	31.4	5.77	22.95	25.2	0.529		58/1
987	15.6	2.86	15.00	19.1	0.695		89/1
1495	61.5	17.1	67.6	25.2	0.526	1.63	34/1
1495	46.1	12.8	45.1	28.4	0.467		51.2/1
1495	31.0	8.60	33.9	25.4	0.523		68.4/1
1495	15.6	4.34	25.1	17.3	0.770		92/1
1998	53.4	20.6	86.0	22.8	0.576	1.47	31.8/1
1998	40.0	15.41	61.6	25.0	0.553		44.3/1
1998	26.4	10.2	44.6	22.8	0.605		61.4/1
1998	13.6	5.25	33.8	15.5	0.890		81/1
2496	47.1	22.8	105.4	21.6	0.640	1.56	34.5/1
2496	36.7	17.7	77.0	23.0	0.600		47.4/1
2496	23.8	11.5	60.4	19.06	0.726		60.2/1
2496	12.1	5.84	44.4	13.0	1.051		82/1
2955	39.8	22.8	124.8	18.22	0.759	1.56	34/1
2955	30.1	17.2	94.5	18.15	0.761		44.8/1
2955	19.8	11.3	78.5	14.36	0.960		54/1
2955	10.0	5.71	59.7	9.55	1.441		71/1

(these data are from McCord /1/ and given for comparison with B-1).

Table 2. Tabulated Results of Test B-1.

rpm	torque	bhp	fuel hp	η_{tb}	bsfc	R_s	air-fuel ratio
665	51.5	6.47	32.2	20.1	0.67	1.09	24.4/1
670	39.0	4.97	20.2	24.6	0.55	1.11	40.7/1
670	25.7	3.29	15.6	21.1	0.64	1.14	53.8/1
671	13.0	1.67	11.2	14.9	0.905	1.14	73.5/1
1000	57.5	10.95	42.8	25.6	0.528	1.13	29.2/1
1000	43.0	8.21	30.4	27.0	0.500	1.16	42.1/1
1000	28.8	5.50	23.7	23.2	0.582	1.17	54.4/1
1000	14.5	2.76	17.7	15.6	0.866	1.19	74.1/1
1525	62.0	18.1	57.9	28.4	0.432	1.25	36.3/1
1503	46.0	13.2	44.7	29.6	0.458	1.25	46.7/1
1495	31.0	8.85	34.8	25.4	0.530	1.25	59.5/1
1500	15.5	4.44	28.8	15.4	0.874	1.23	71.7/1
2010	54.7	21.0	75.1	28.0	0.484	1.26	37.4/1
2006	41.0	15.7	61.0	25.8	0.525	1.26	46.2/1
1998	27.0	10.28	47.9	21.5	0.629	1.28	59.1/1
2002	13.8	5.26	37.3	14.1	0.959	1.28	75.8/1
2520	49.5	23.8	92.0	25.9	0.523	1.22	37.4/1
2500	36.7	17.52	73.0	24.0	0.563	1.22	47.2/1
2505	24.7	11.8	61.2	19.3	0.701	1.22	56.3/1
2503	12.6	6.02	49.4	12.2	1.108	1.22	69.9/1
2650	46.0	23.25	104.0	22.35	0.605	1.23	35.4/1
2650	34.5	17.45	78.7	22.2	0.609	1.23	46.8/1
2650	23.0	11.62	66.6	17.5	0.774	1.23	54.4/1
2653	11.5	5.84	53.9	10.8	1.248	1.23	68.4/1

Table 3. Tabulated Results of Test A-2.

rpm	torque	bhp	fuel hp	η_{tb}	bsfc	R_s	air-fuel ratio
608	52.0	5.95	29.4	20.6	0.664		25.1/1
605	38.9	4.50	17.9	25.1	0.545	1.24	41.1/1
607	26.0	3.01	13.0	23.2	0.590		56.6/1
604	13.0	1.50	9.45	15.9	0.862		77.9/1
1015	55.6	10.8	48.4	22.4	0.614		26.7/1
1005	41.5	8.00	29.7	26.9	0.510	1.37	43.5/1
1004	27.4	5.27	22.6	23.4	0.586		51.1/1
1002	14.1	2.69	15.85	17.0	0.806		81.5/1
1506	62.5	18.0	63.0	28.8	0.478		33.0/1
1505	46.3	13.3	47.2	28.2	0.485	1.46	44.3/1
1504	30.8	8.85	36.2	24.4	0.558		57.5/1
1502	15.5	4.46	25.0	17.88	0.771		82.5/1
1990	55.2	21.0	85.9	24.4	0.560		32.9/1
1985	41.3	15.7	63.1	24.9	0.550	1.47	44.8/1
1989	26.7	10.25	47.0	21.8	0.638		60.2/1
1992	13.4	5.11	34.8	14.71	0.936		81.1/1
2493	51.0	24.3	102.9	23.9	0.578		35.6/1
2503	37.8	18.05	77.0	23.5	0.583	1.56	47.5/1
2503	25.4	12.17	60.4	20.1	0.680		60.5/1
2506	12.8	6.15	47.1	13.05	1.05		77.5/1
2952	45.0	25.4	121.9	20.9	0.656		34.8/1
2959	33.9	19.2	95.4	20.1	0.681	1.55	44.4/1
2954	22.3	12.6	77.0	16.4	0.837		55.0/1
2957	11.4	6.45	60.8	10.6	1.29		69.6/1

(these data are from McCord /1/ and given for comparison with B-2).

Table 4. Tabulated Results of Test B-2.

rpm	torque	bhp	fuel hp	η_{tb}	bsfc	R_s	air-fuel ratio
650	49.0	6.10	28.2	21.6	0.623	1.11	27.9/1
650	36.5	4.54	19.9	22.8	0.593	1.11	39.8/1
650	24.5	3.05	15.1	20.2	0.669	1.11	52.4/1
647	12.5	1.55	11.1	13.9	0.968	1.12	71.4/1
1008	55.0	10.63	41.1	25.9	0.522	1.20	31.8/1
998	40.75	7.80	30.8	25.4	0.534	1.19	42.1/1
997	27.25	5.22	24.3	21.5	0.629	1.19	53.4/1
995	14.8	2.82	18.5	15.3	0.887	1.19	70.0/1
1495	58.2	16.6	58.4	28.4	0.477	1.25	36.4/1
1506	43.5	12.5	47.1	26.5	0.509	1.21	43.9/1
1510	28.75	8.30	37.0	22.2	0.603	1.20	55.6/1
1503	14.5	4.18	28.4	14.7	0.915	1.21	72.4/1
2005	54.5	20.8	75.2	27.5	0.489	1.25	36.8/1
2000	41.0	15.6	63.0	24.8	0.545	1.25	44.0/1
2000	27.25	10.4	50.6	20.6	0.658	1.27	55.0/1
1998	13.5	5.12	35.6	14.4	0.938	1.27	78.3/1
2500	52.0	24.75	94.3	25.2	0.515	1.23	37.0/1
2500	39.0	18.5	80.0	23.2	0.584	1.23	43.5/1
2505	25.7	12.2	66.0	18.6	0.728	1.23	52.8/1
2500	12.7	6.03	51.4	11.8	1.15	1.23	67.7/1
2750	47.5	24.7	104.1	23.7	0.569	1.24	37.0/1
2750	35.0	18.3	87.0	21.1	0.642	1.24	44.3/1
2750	23.0	12.0	73.0	16.5	0.821	1.24	52.8/1
2750	12.0	6.26	60.0	10.4	1.29	1.24	64.2/1

Table 5. Tabulated Results of Tests A-3 and B-3.

A-3. (these data are from McCord /1/ and given for comparison with B-3)

rpm	torque	bhp	fuel hp	η_{tb}	bsfc	R_s	air-fuel ratio
608	54.8	6.35	28.8	22.0	0.617	1.271	26.3/1
1014	57.5	11.1	48.0	23.1	0.588	1.395	28.2/1
1502	63.6	18.22	64.0	28.5	0.478	1.465	33.4/1
2010	58.0	22.2	86.0	25.8	0.527	1.490	33.9/1
2514	53.2	25.2	101.2	25.0	0.544	1.520	36.2/1
2905	45.1	25.0	120.5	20.8	0.656	1.55	35.8/1

B-3.

rpm	torque	bhp	fuel hp	η_{tb}	bsfc	R_s	air-fuel ratio
660	52.5	6.65	30.1	22.1	0.611	1.16	27.6/1
1000	57.8	11.1	42.6	26.1	0.517	1.17	30.0/1
1505	58.0	16.7	61.7	27.1	0.501	1.25	33.4/1
2000	54.0	20.7	76.4	27.1	0.501	1.24	36.1/1
2505	53.1	25.5	96.7	26.4	0.511	1.24	36.0/1
2695	50.2	26.0	105.3	24.7	0.551	1.23	35.2/1

Table 6. Tabulated Results of Two Valve Tests, Exhaust Normal.

timing mode	B-2	B-11	B-1	B-6
load	full	full	full	full
rpm	1495	1500	1525	1503
sp. gr., burette	0.818	0.816	0.817	0.816
torque	58.2	61.5	62.0	60.5
bhp	16.55	17.58	18.0	17.4
bhp (corrected)	16.6	17.6	18.1	17.4
bmep	82.6	87.3	88.0	85.9
$\dot{m}_f$	7.88	8.09	7.82	7.91
$\dot{m}_a$	287	284	284	286
air-fuel ratio	36.4/1	35.1/1	36.3/1	36.2/1
hp loss to exhaust	20.0	20.6	22.3	23.1
hp loss to cooling water	8.4	7.4	7.9	7.4
fhp, motoring test	7.6	7.6	7.8	7.6
fuel hp	58.4	59.9	57.95	58.6
hp loss unaccounted	5.79	6.7	1.85	3.1
imep, from photograph	165	164	148	133
ihp, based on imep	33.2	33.0	29.8	26.8
fhp (ihp - bhp)	16.6	15.4	11.7	8.4
ihp (bhp + fhp)	24.2	25.2	25.9	25.0
bsfc	0.477	0.460	0.432	0.455
isfc	0.326	0.321	0.302	0.316
bsac	17.3	16.1	15.7	16.4
isac	11.88	11.27	10.96	11.44
η_{tb}	28.4	30.5	31.2	30.8
η_{ti}	41.4	43.6	44.7	44.2
η_m	68.6	69.8	69.9	69.6
exhaust temperature, ^{o}F	820	843	888	913
R_s	1.25	1.27	1.25	1.28
compression pressure, psia	580	580	580	580
theoretical comp. pressure, psia	569	565	565	567
exhaust starts, degrees ATC	087	087	087	087
exhaust stops, degrees ATC	225	225	225	225
injection starts, degrees BTC	20.0	15.8	10.8	5.0
combustion pressure rise starts	11 ^{o}BTC	7 ^{o}BTC	5 ^{o}BTC	5 ^{o}ATC
delay angle, degrees	9	8.8	5.8	10
delay period, ms.	1.0	0.98	0.645	1.1
peak pressure, psia	1335	1245	1085	875
peak pressure location	TDC	4 ^{o}ATC	9 ^{o}ATC	15 ^{o}ATC

Table 7. Tabulated Results of Two Valve Tests, Exhaust Advanced 12°.

timing mode	B-9	B-12	B-4	B-7
load	full	full	full	full
rpm	1501	1495	1500	1498
sp. gr., burette	0.817	0.817	0.818	0.816
torque	51.8	54.7	54.0	52.26
bhp	14.79	15.56	15.41	14.89
bhp (corrected)	14.7	15.5	15.3	14.8
bmep	73.6	77.7	76.7	74.2
$\dot{m}_f$	7.83	7.92	7.85	7.79
$\dot{m}_a$	270	267	268	268
air-fuel ratio	34.6/1	33.8/1	34.1/1	34.4/1
hp loss to exhaust	20.2	21.2	22.4	23.7
hp loss to cooling water	7.9	8.4	8.4	7.1
fhp, motoring test	8.55	8.55	8.55	8.55
fuel hp	58.05	58.71	58.17	57.72
hp loss unaccounted	6.7	5.06	3.52	3.27
imep, from photograph	166	154	141	134
ihp, based on imep	33.4	30.9	28.4	27.0
fhp (ihp - bhp)	18.7	15.4	13.1	12.2
ihp (bhp + fhp)	23.25	24.05	23.85	23.33
bsfc	0.533	0.509	0.513	0.526
isfc	0.337	0.329	0.329	0.334
bsac	18.4	17.2	17.5	18.1
isac	11.6	11.1	11.2	11.5
η_{tb}	25.3	26.4	26.3	25.8
η_{ti}	40.1	41.0	41.0	40.5
η_m	63.2	64.4	64.2	63.4
exhaust temperature, °F	870	905	945	990
R_s	1.20	1.19	1.19	1.20
compression pressure, psia	585	585	585	585
theoretical comp. pressure, psia	587	584	585	585
exhaust starts, degrees ATC	075	075	075	075
exhaust stops, degrees ATC	213	213	213	213
injection starts, degrees BTC	20.0	15.8	10.8	5.0
combustion pressure rise starts	9 °BTC	8 °BTC	4 °BTC	4 °ATC
delay angle, degrees	11	7.8	6.8	9
delay period, ms.	1.22	0.867	0.755	1.0
peak pressure, psia	1335	1215	1050	930
peak pressure location	2 °ATC	4 °ATC	8 °ATC	12 °ATC

Table 8. Tabulated Results of Two Valve Tests, Exhaust Retarded 12°.

timing mode	B-10	B-13	B-5	B-8
load	full	full	full	full
rpm	1495	1498	1505	1501
sp. gr., burette	0.818	0.817	0.817	0.816
torque	58.5	60.75	60.25	58.5
bhp	16.64	17.31	17.26	16.71
bhp (corrected)	16.4	17.1	17.1	16.5
bmep	83.1	86.3	85.6	83.1
$\dot{m}_f$	7.85	7.89	7.76	7.97
$\dot{m}_a$	288	288	291	290
air-fuel ratio	36.7/1	36.5/1	37.5/1	36.4/1
hp loss to exhaust	18.3	18.9	20.4	21.4
hp loss to cooling water	7.4	6.9	6.9	7.4
fhp, motoring test	7.6	7.6	7.6	7.6
fuel hp	58.17	58.49	57.53	59.09
hp loss unaccounted	8.47	8.0	5.53	6.2
imep, from photograph	162	147	132	124
ihp, based on imep	32.5	29.6	26.6	25.0
fhp (ihp - bhp)	16.1	12.5	9.5	8.5
ihp (bhp + fhp)	24.0	24.7	24.7	24.1
bsfc	0.479	0.461	0.454	0.483
isfc	0.321	0.319	0.314	0.331
bsac	17.6	16.8	17.0	17.6
isac	12.0	11.7	11.8	12.0
η_{tb}	28.2	29.2	29.7	27.9
η_{ti}	41.3	42.2	42.9	40.8
η_m	68.3	69.2	69.2	68.4
exhaust temperature, °F	765	790	827	872
R_s	1.28	1.28	1.29	1.30
compression pressure, psia	560	560	560	560
theoretical comp. pressure, psia	564	564	564	561
exhaust starts, degrees ATC	099	099	099	099
exhaust stops, degrees ATC	237	237	237	237
injection starts, degrees BTC	20.0	15.8	10.8	5.0
combustion pressure rise starts	8 °BTC	7 °BTC	3 °BTC	3 °ATC
delay angle, degrees	12	7.8	7.8	8
delay period, ms.	1.33	0.865	0.865	0.89
peak pressure, psia	1290	1155	1030	835
peak pressure location	5 °ATC	6 °ATC	8 °ATC	14 °ATC

Table 9. Tabulated Results of Four Valve Tests, Exhaust Normal.

timing mode	A-2	A-11	A-1	A-6
load	full	full	full	full
rpm	1500	1505	1508	1504
sp. gr., burette	0.820	0.817	0.817	0.817
torque	61	62	60.5	57.5
bhp	17.4	17.75	17.35	16.46
bhp (corrected)	17.4	17.81	17.32	16.5
bmep	86.6	88.0	85.8	81.6
$\dot{m}_f$	8.56	8.42	8.38	8.44
$\dot{m}_a$	296	288	298	294
air-fuel ratio	34.6/1	34.1/1	35.6/1	34.8/1
hp loss to exhaust	19.6	20.1	22.2	22.7
hp loss to cooling water	10.4	5.94	9.9	11.4
fhp, motoring test	7.9	7.9	7.9	7.9
fuel hp	63.5	62.4	62.1	62.6
hp loss unaccounted	8.2	10.65	4.78	4.1
imep, from photograph	145	143	133	126
ihp, based on imep	29.2	28.8	26.8	25.4
fhp (ihp - bhp)	11.8	11.0	9.48	8.9
ihp (bhp + fhp)	25.3	25.71	25.22	24.4
bsfc	0.492	0.472	0.484	0.511
isfc	0.338	0.327	0.332	0.346
bsac	17.0	16.1	17.2	17.8
isac	11.7	11.2	11.8	12.0
η_{tb}	27.4	28.5	27.9	26.4
η_{ti}	39.8	41.2	40.6	40.0
η_m	68.8	69.3	68.7	67.6
exhaust temperature, ^oF	775	809	848	923
R_s	1.31	1.29	1.31	1.30
compression pressure, psia	570	570	570	570
theoretical comp. pressure, psia	550	550	550	550
exhaust starts, degrees ATC	097	097	097	097
exhaust stops, degrees ATC	222	222	222	222
injection starts, degrees BTC	20.0	15.8	10.8	5.0
combustion pressure rise starts	10 ^{o}BTC	6 ^{o}BTC	3 ^{o}BTC	5 ^{o}ATC
delay angle, degrees	10	9.8	7.8	10
delay period, ms.	1.11	1.09	0.865	1.11
peak pressure, psia	1265	1105	950	765
peak pressure location	5.5 ^{o}ATC	7 ^{o}ATC	11 ^{o}ATC	18 ^{o}ATC

Table 10. Tabulated Results of Four Valve Tests, Exhaust Advanced 12°.

timing mode	A-9	A-12	A-4	A-7
load	full	full	full	full
rpm	1499	1500	1512	1497
sp. gr., burette	0.816	0.818	0.817	0.816
torque	56.7	57.5	57.2	53.5
bhp	16.2	16.4	16.4	15.25
bhp (corrected)	16.2	16.32	16.38	15.25
bmep	80.5	81.6	81.1	75.9
$\dot{m}_f$	8.45	8.39	8.43	8.32
$\dot{m}_a$	279	281	279	279
air-fuel ratio	33.0/1	33.5/1	33.1/1	33.6/1
hp loss to exhaust	19.4	20.6	23.4	24.1
hp loss to cooling water	10.9	10.4	10.4	10.4
fhp, motoring test	8.25	8.25	8.25	8.25
fuel hp	62.6	62.2	62.5	61.7
hp loss unaccounted	7.85	6.63	4.07	3.7
imep, from photograph	149	140	141	129
ihp, based on imep	30.0	28.1	28.3	26.0
fhp (ihp - bhp)	13.8	11.8	11.9	10.75
ihp (bhp + fhp)	24.45	24.57	24.63	23.5
bsfc	0.521	0.514	0.515	0.546
isfc	0.346	0.341	0.342	0.354
bsac	17.2	17.2	17.05	18.3
isac	11.4	11.4	11.3	11.9
η_{tb}	25.9	26.4	26.2	24.7
η_{ti}	39.1	39.5	39.4	38.0
η_m	66.3	66.4	66.5	64.9
exhaust temperature, °F	813	845	908	971
R_s	1.25	1.24	1.23	1.24
compression pressure, psia	550	550	550	550
theoretical comp. pressure, psia	564	564	564	564
exhaust starts, degrees ATC	085	085	085	085
exhaust stops, degrees ATC	210	210	210	210
injection starts, degrees BTC	20.0	15.8	10.8	5.0
combustion pressure rise starts	8 °BTC	6 °BTC	2 °BTC	5 °ATC
delay angle, degrees	12	9.8	8.8	10
delay period, ms.	1.33	1.09	0.97	1.11
peak pressure, psia	1215	1090	935	715
peak pressure location	5 °ATC	6 °ATC	11 °ATC	13 °ATC

Table 11. Tabulated Results of Four Valve Tests, Exhaust Retarded 12°.

timing mode	A-10	A-13	A-5	A-8
load	full	full	full	full
rpm	1509	1502	1505	1505
sp. gr., burette	0.817	0.816	0.818	0.817
torque	56.5	57.0	57.1	55.5
bhp	16.2	16.3	16.35	15.9
bhp (corrected)	16.2	16.33	16.3	15.88
bmep	80.2	80.9	81.0	78.8
$\dot{m}_f$	8.37	8.34	8.4	8.4
$\dot{m}_a$	294	291	298	293
air-fuel ratio	35.2/1	34.9/1	35.5/1	34.9/1
hp loss to exhaust	13.1	12.95	14.8	15.6
hp loss to cooling water	9.4	9.9	8.9	10.4
fhp, motoring test	7.7	7.7	7.7	7.7
fuel hp	62.1	61.8	62.3	62.3
hp loss unaccounted	15.7	14.92	14.6	12.72
imep, from photograph	141	139	133	120
ihp, based on imep	28.4	28.0	26.8	24.1
fhp (ihp - bhp)	12.2	11.7	10.5	9.2
ihp (bhp + fhp)	23.9	24.03	24.0	23.58
bsfc	0.516	0.511	0.515	0.528
isfc	0.350	0.347	0.350	0.356
bsac	18.15	17.8	18.3	18.45
isac	12.3	12.1	12.4	12.4
η_{tb}	26.1	26.4	26.2	25.5
η_{ti}	38.5	38.9	38.6	37.8
η_m	67.8	67.9	67.9	67.3
exhaust temperature, °F	662	672	728	764
R_s	1.31	1.30	1.32	1.30
compression pressure, psia	545	545	545	545
theoretical comp. pressure, psia	552	552	552	552
exhaust starts, degrees ATC	109	109	109	109
exhaust stops, degrees ATC	234	234	234	234
injection starts, degrees BTC	20.0	15.8	10.8	5.0
combustion pressure rise starts	8.5 °BTC	6 °BTC	2.5 °BTC	3.5 °ATC
delay angle, degrees	11.5	9.8	8.3	8.5
delay period, ms.	1.28	1.09	0.92	0.94
peak pressure, psia	1135	990	855	685
peak pressure location	4 °ATC	7 °ATC	12 °ATC	15 °ATC

Table 12. Tabulated Results of Four Valve Tests; Exhaust Retarded, Injection Constant and Speed Varied.

timing mode	A-13	A-13	A-13	A-13
load	full	full	full	full
rpm	1000	1502	2010	2506
sp. gr., burette	0.812	0.816	0.813	0.816
torque	54.0	57.0	52.5	47.0
bhp	10.28	16.3	20.05	22.4
bhp (corrected)	10.3	16.33	20.1	22.45
bmep	76.6	80.9	74.5	66.7
$\dot{m}_f$	6.31	8.34	10.79	12.61
$\dot{m}_a$	175	291	381	473
air-fuel ratio	27.7/1	34.9/1	35.3/1	37.5/1
hp loss to exhaust	8.5	12.95	17.8	22.6
hp loss to cooling water	9.9	9.9	12.9	13.4
fhp, motoring test	4.1	7.7	11.2	15.5
fuel hp	46.8	61.8	80.0	93.5
hp loss unaccounted	14.0	14.92	18.0	19.55
imep, from photograph	135	139	135	135
ihp, based on imep	18.1	28.0	36.2	45.2
fhp (ihp - bhp)	7.8	11.7	16.1	22.75
ihp (bhp + fhp)	14.4	24.03	31.3	37.95
bsfc	0.612	0.511	0.537	0.562
isfc	0.438	0.347	0.345	0.332
bsac	17.0	17.8	18.95	21.1
isac	12.2	12.1	12.2	12.5
η_{tb}	22.0	26.4	25.2	24.0
η_{ti}	30.8	38.9	39.1	40.6
η_m	71.5	67.9	64.2	59.2
exhaust temperature, ^oF	640	672	743	803
R_s	1.17	1.30	1.27	1.26
compression pressure, psia	---	545	---	---
theoretical comp. pressure, psia	527	552	595	654
exhaust starts, degrees ATC	109	109	109	109
exhaust stops, degrees ATC	234	234	234	234
injection starts, degrees BTC	15.8	15.8	15.8	15.8
combustion pressure rise starts	7 ^oBTC	6 ^oBTC	6 ^oBTC	6 ^oBTC
delay angle, degrees	8.8	9.8	9.8	9.8
delay period, ms.	1.47	1.09	0.814	0.655
peak pressure, psia	1020	990	920	900
peak pressure location	7 ^oATC	7 ^oATC	8.5 ^oATC	8.5 ^oATC

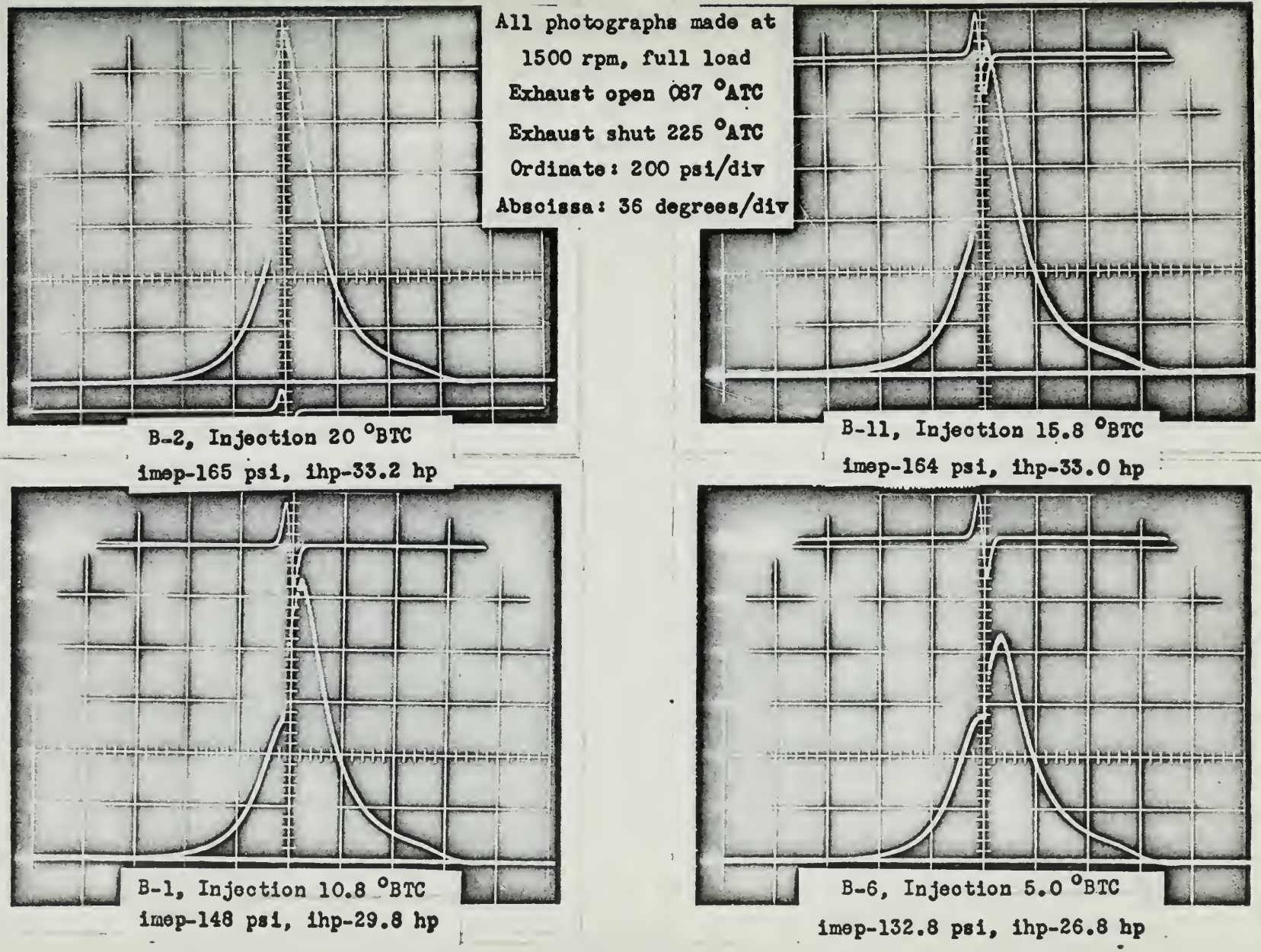

Fig. 20. Pressure-crank angle photographs - two valve, exhaust normal.

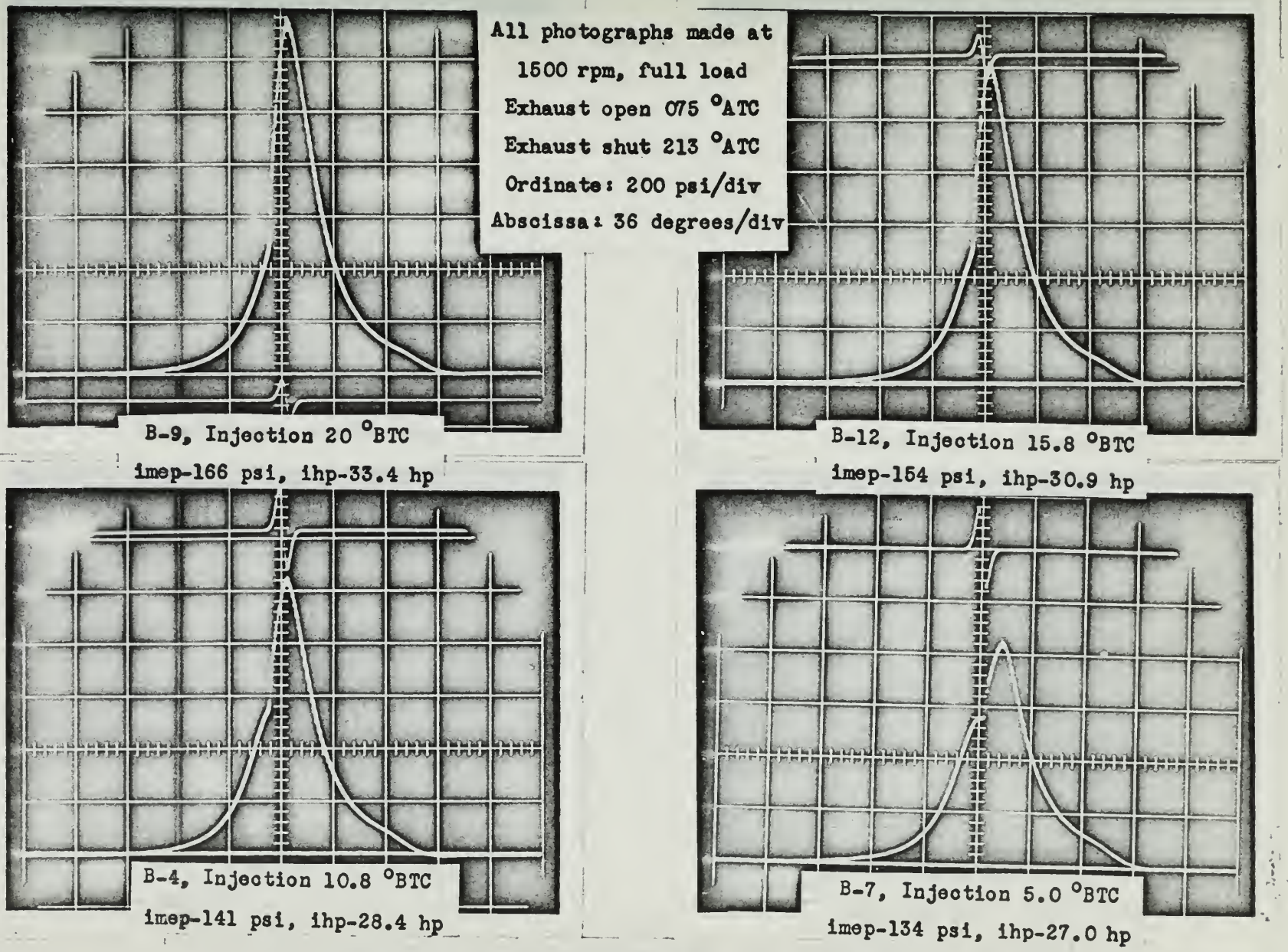

Fig. 21. Pressure-crank angle photographs, two valve, exhaust advanced.

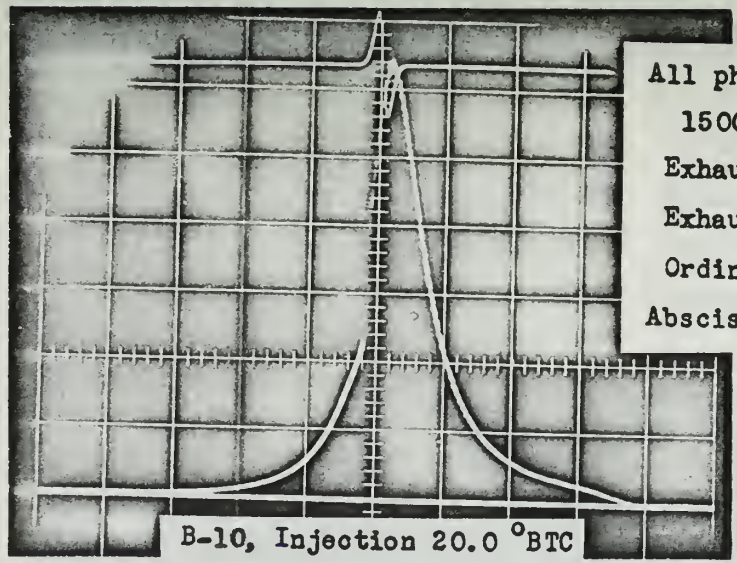

All photographs made at
1500 rpm, full load
Exhaust open 099 °ATC
Exhaust shut 237 °ATC
Ordinate: 200 psi/div
Abscissa: 36 degrees/div

B-10, Injection 20.0 °BTC
imep-162 psi, ihp-32.5 hp

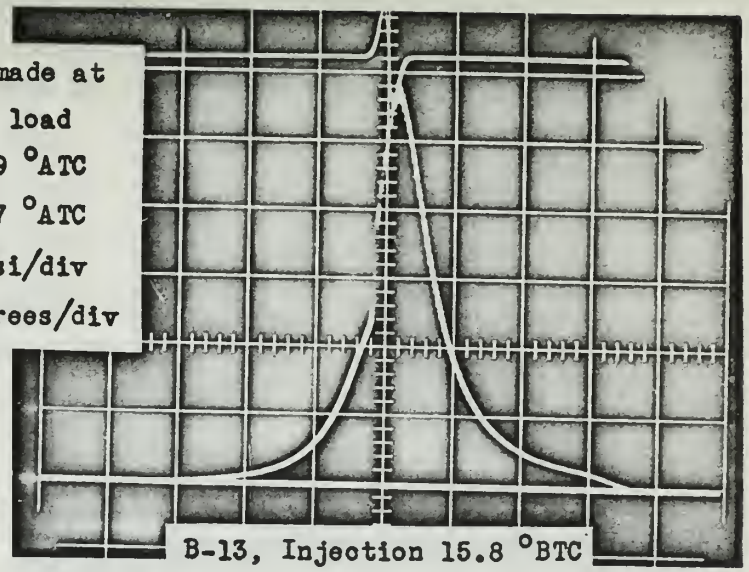

B-13, Injection 15.8 °BTC
imep-147 psi, ihp-29.6 hp

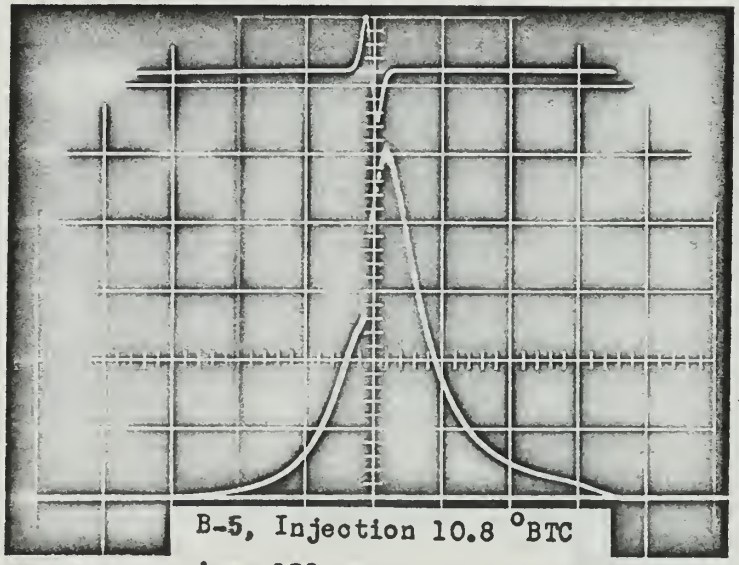

B-5, Injection 10.8 °BTC
imep-132 psi, ihp-26.6 hp

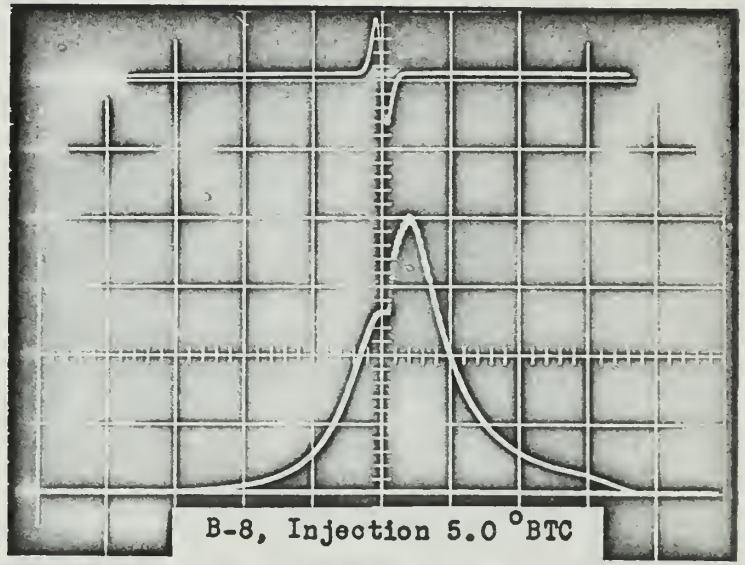

B-8, Injection 5.0 °BTC
imep-124 psi, ihp-25.0 hp

Fig. 22. Pressure-crank angle photographs, two valve, exhaust retarded.

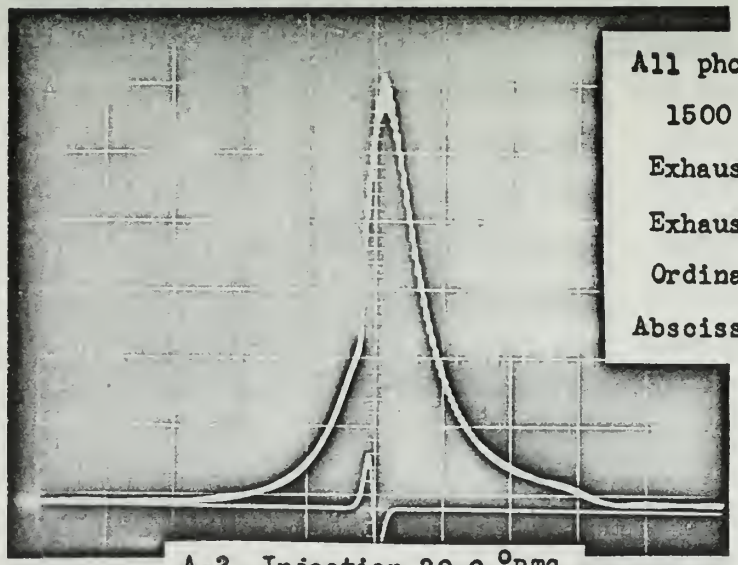

All photographs made at
1500 rpm, full load
Exhaust open 097 °ATC
Exhaust shut 222 °ATC
Ordinate: 200 psi/div
Abscissa: 36 degrees/div

A-2, Injection 20.0 °BTC
imep-145 psi, ihp-29.2 hp

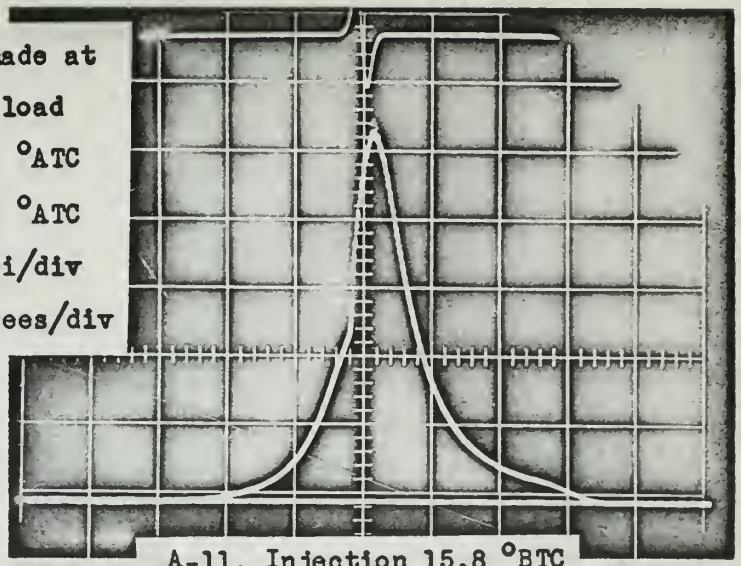

A-11, Injection 15.8 °BTC
imep-143 psi, ihp-28.8 hp

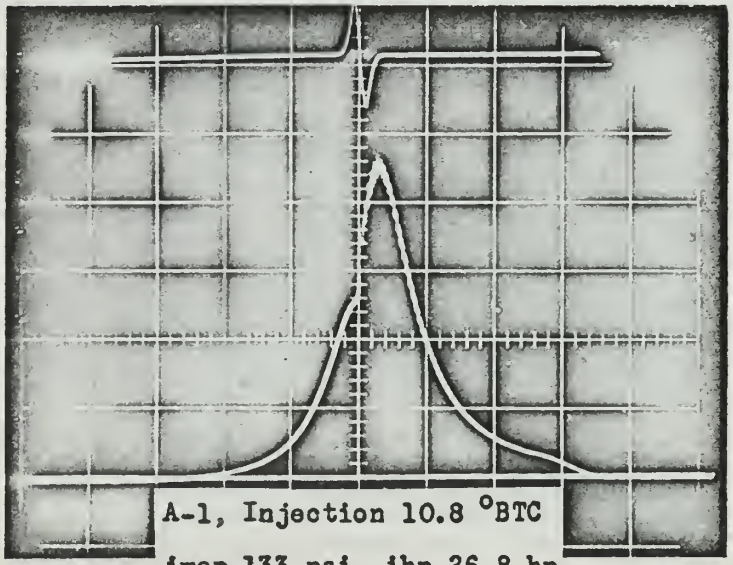

A-1, Injection 10.8 °BTC
imep-133 psi, ihp-26.8 hp

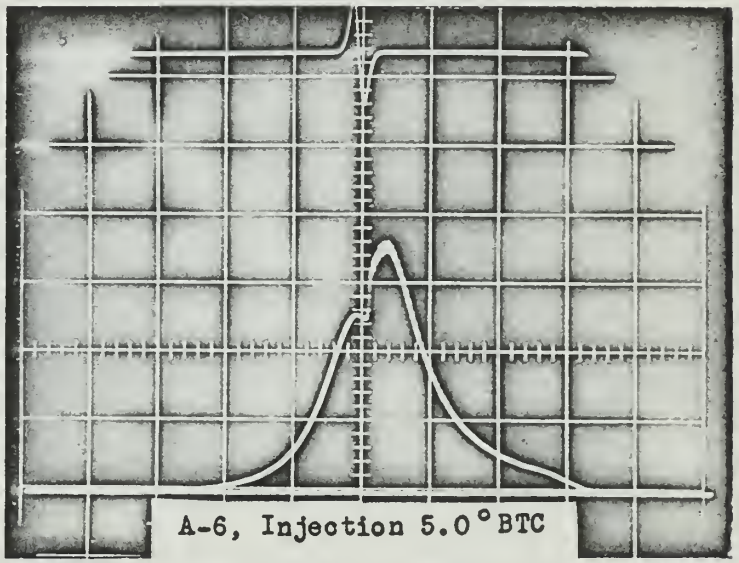

A-6, Injection 5.0 °BTC
imep-126 psi, ihp-25.4 hp

Fig. 23. Pressure-crank angle, four valve, exhaust normal.

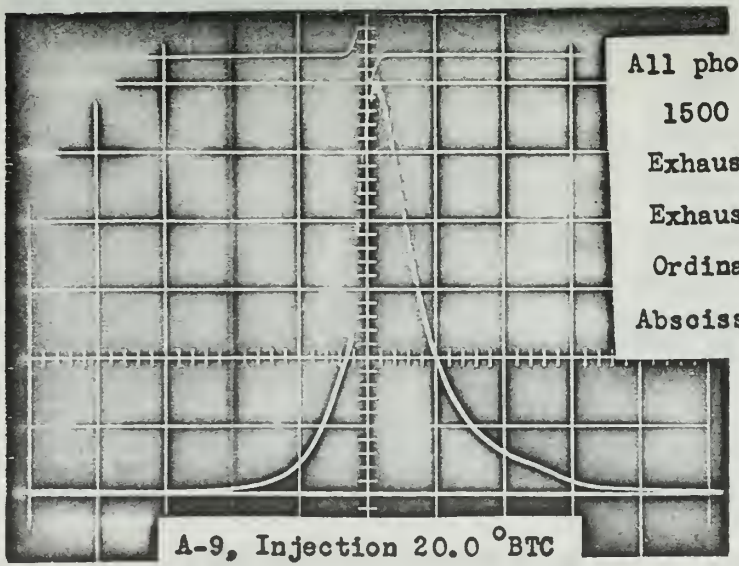

All photographs made at
1500 rpm, full load
Exhaust open 085 °ATC
Exhaust shut 210 °ATC
Ordinate: 200 psi/div
Abscissa: 36 degrees/div

A-9, Injection 20.0 °BTC
imep-149 psi, ihp-30.0 hp

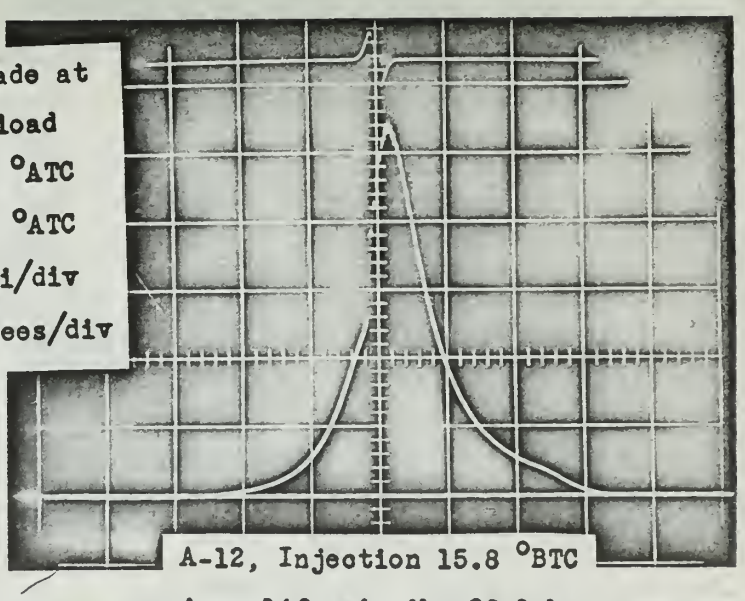

A-12, Injection 15.8 °BTC
imep-140 psi, ihp-28.1 hp

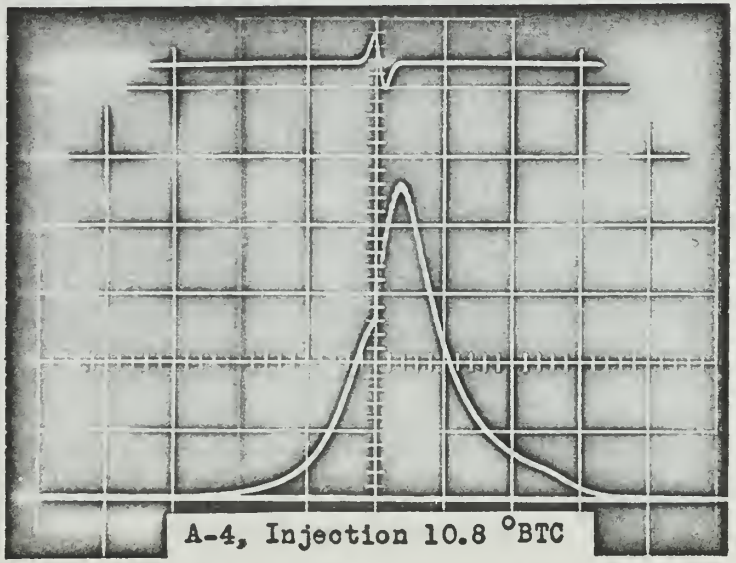

A-4, Injection 10.8 °BTC
imep-141 psi, ihp-28.3 hp

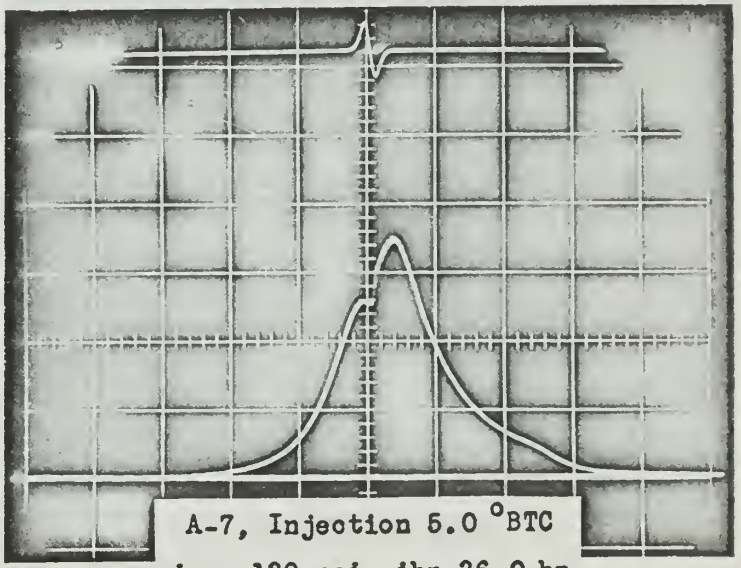

A-7, Injection 5.0 °BTC
imep-129 psi, ihp-26.0 hp

Fig. 24. Pressure-crank angle photographs, four valve, exhaust advanced.

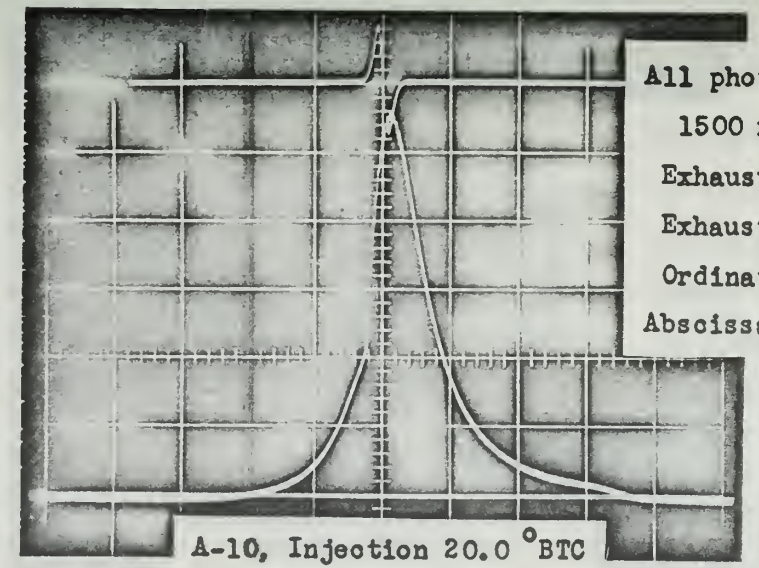

All photographs made at
1500 rpm, full load
Exhaust open 109 °ATC
Exhaust shut 234 °ATC
Ordinate: 200 psi/div
Abscissa: 36 degrees/div

A-10, Injection 20.0 °BTC
imep-141 psi, ihp-28.4 hp

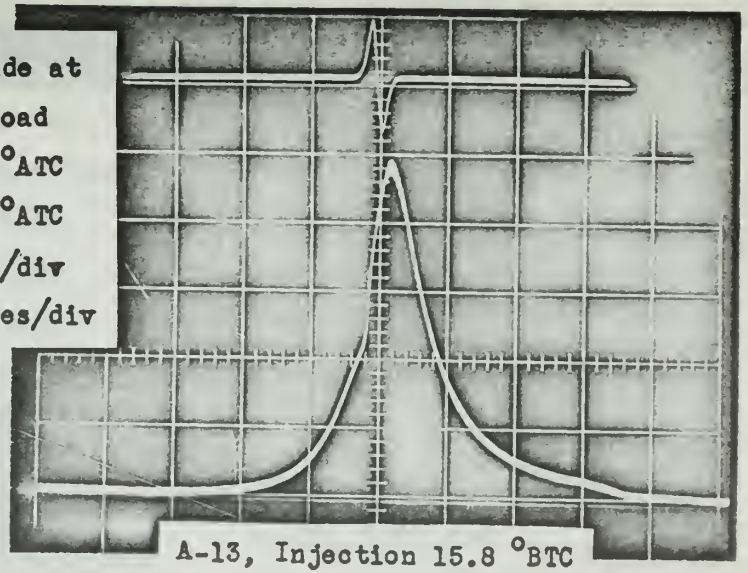

A-13, Injection 15.8 °BTC
imep-139 psi, ihp-28.0 hp

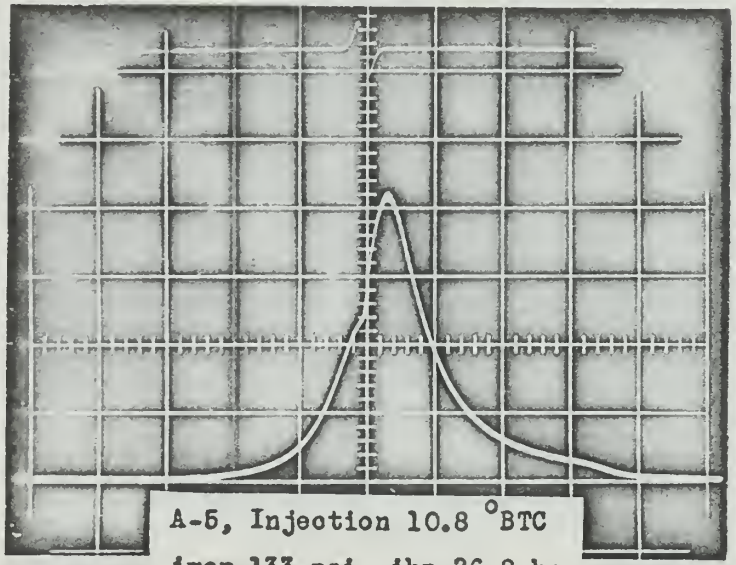

A-5, Injection 10.8 °BTC
imep-133 psi, ihp-26.8 hp

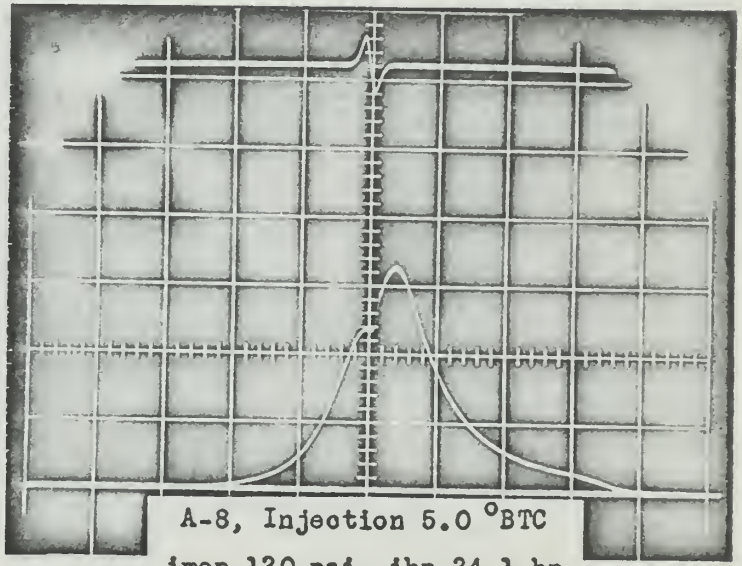

A-8, Injection 5.0 °BTC
imep-120 psi, ihp-24.1 hp

Fig. 25. Pressure-crank angle photographs, four valve, exhaust retarded.

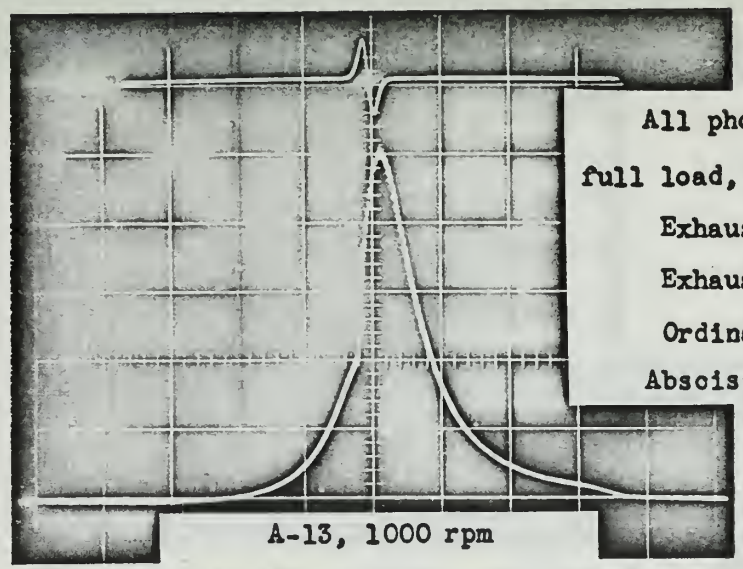

All photographs made at
full load, injection 20.0 °BTC
Exhaust open 109 °ATC
Exhaust shut 234 °ATC
Ordinate: 200 psi/div
Abscissa: 36 degrees/div

A-13, 1000 rpm
imep-135 psi, ihp-18.1 hp

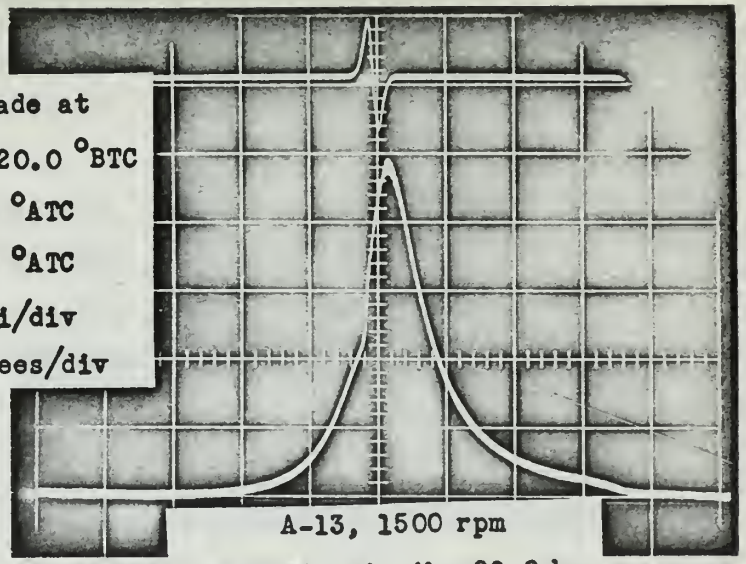

A-13, 1500 rpm
imep-139 psi, ihp-28.0 hp

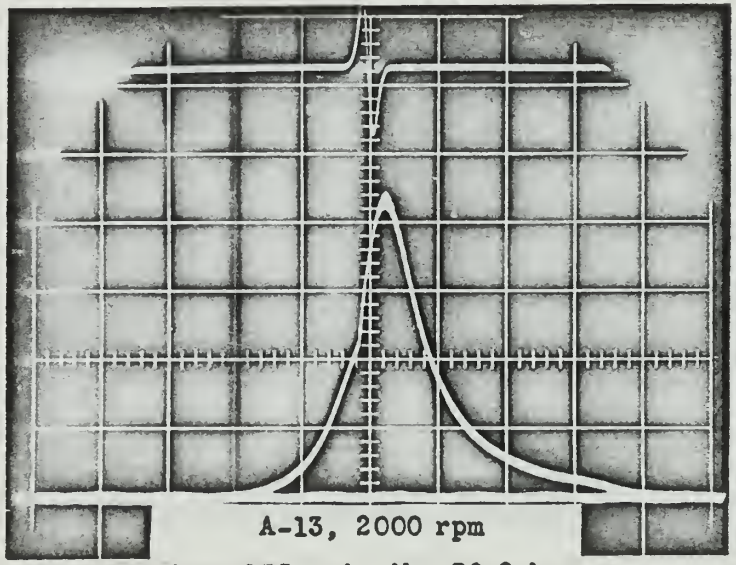

A-13, 2000 rpm
imep-135 psi, ihp-36.2 hp

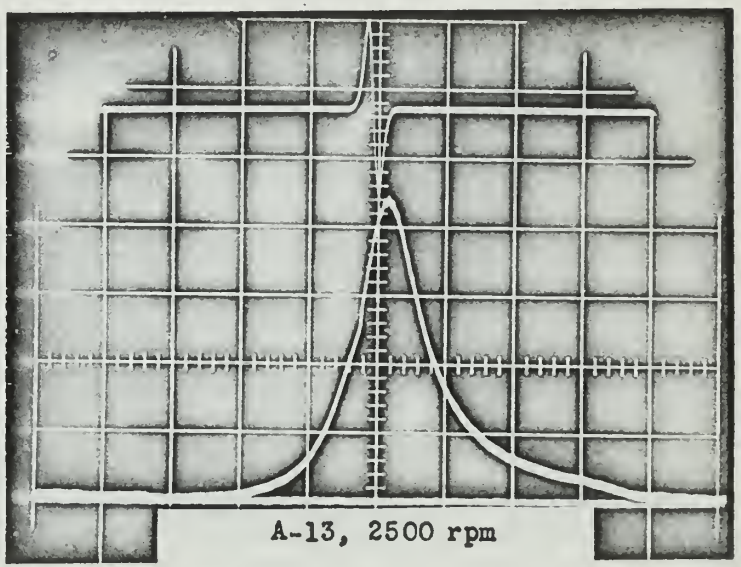

A-13, 2500 rpm
imep-135 psi, ihp-45.2 hp

Fig. 26. Pressure-crank angle photographs, four valve, exhaust retarded, injection constant, engine speed varied.

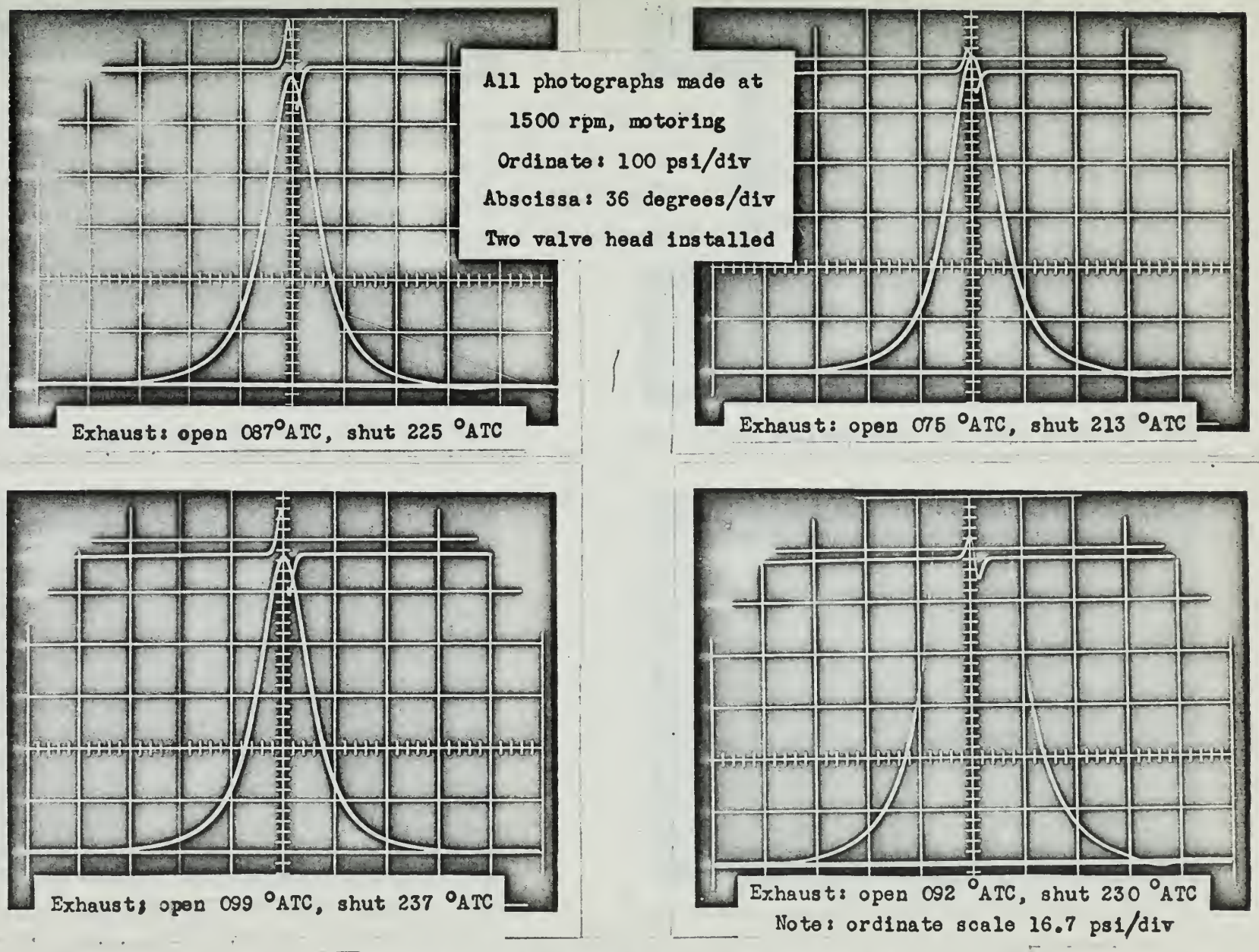

Fig. 27. Typical pressure-crank angle photographs of motoring.

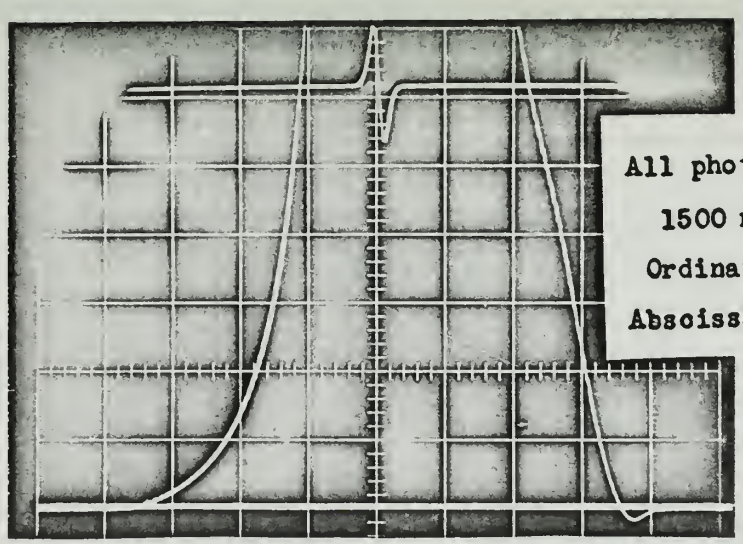

All photographs taken at
1500 rpm, full load
Ordinate: 16.7 psi/div
Abscissa: 36 degrees/div

Two valve; exhaust open 087 °ATC, shut 225 °ATC

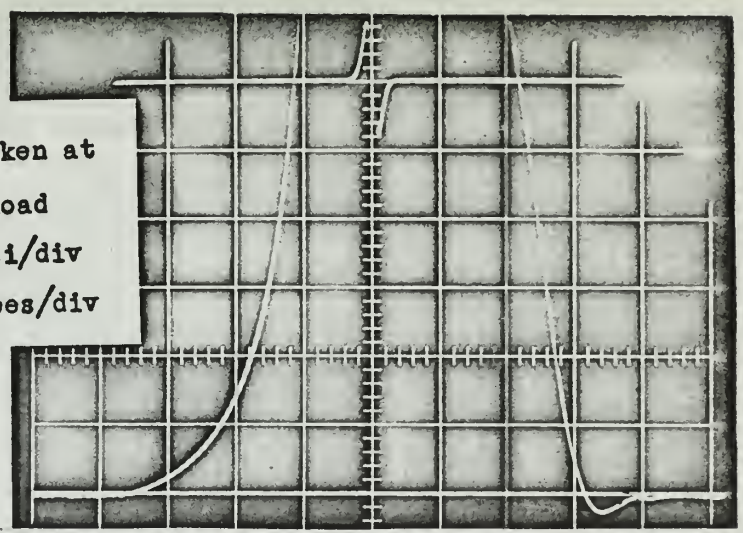

Two valve; exhaust open 075 °ATC, shut 213 °ATC

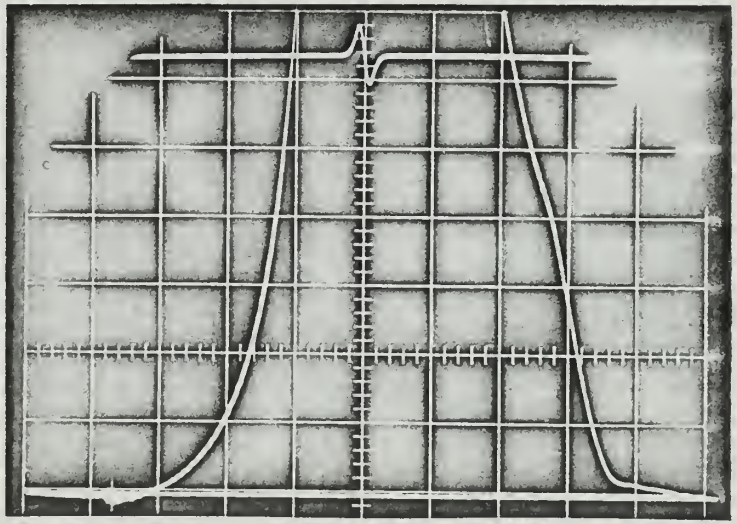

Four valve; exhaust open 097 °ATC, shut 222 °ATC

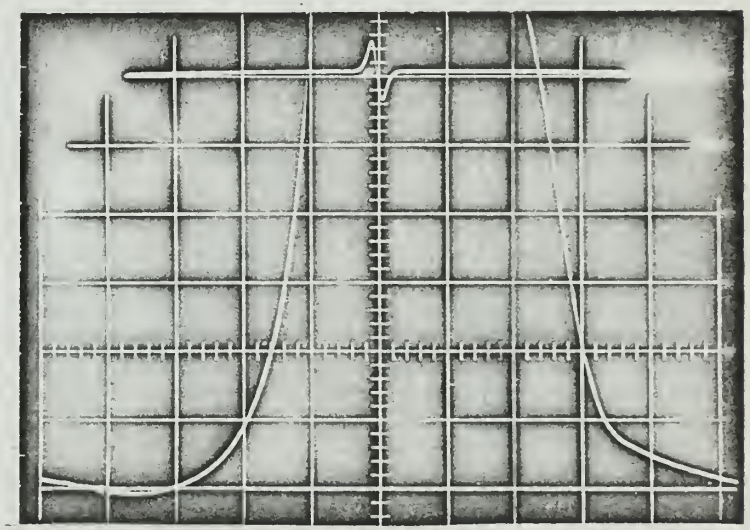

Four valve; exhaust open 085 °ATC, shut 210 °ATC

Fig. 28. Selected pressure-crank angle photographs of the exhaust and inlet process.

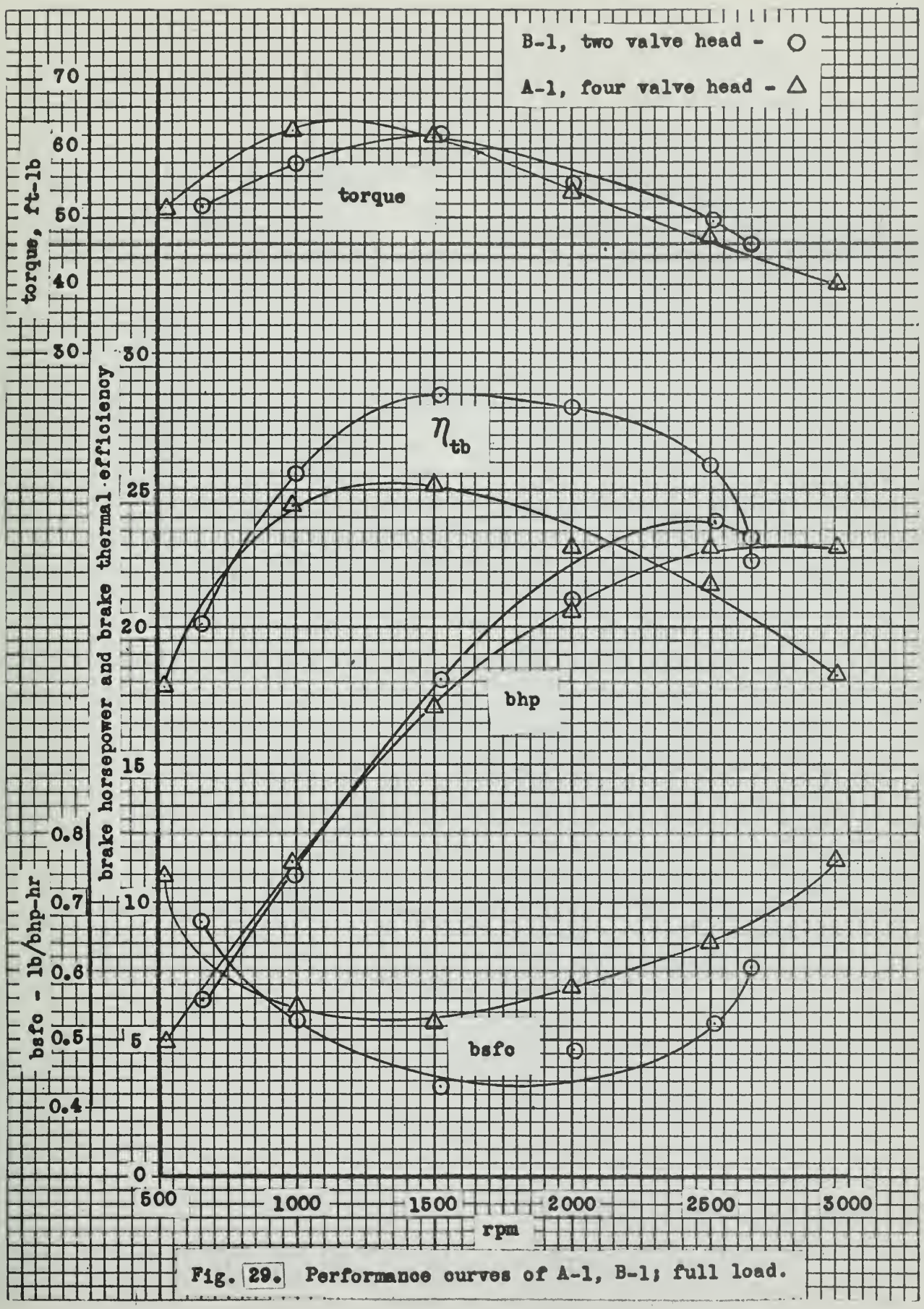

Fig. 29. Performance curves of A-1, B-1; full load.

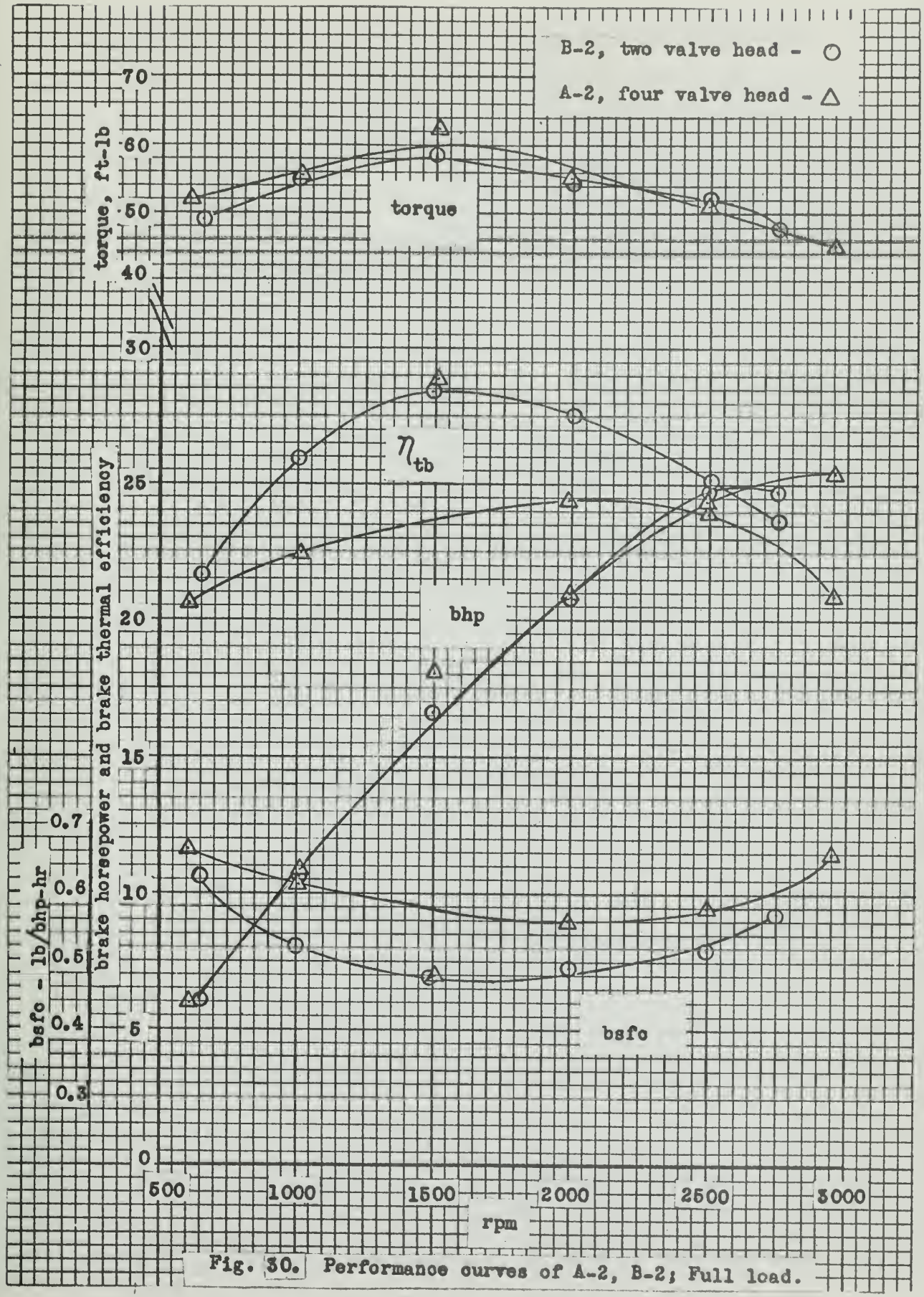

Fig. 30. Performance curves of A-2, B-2; Full load.

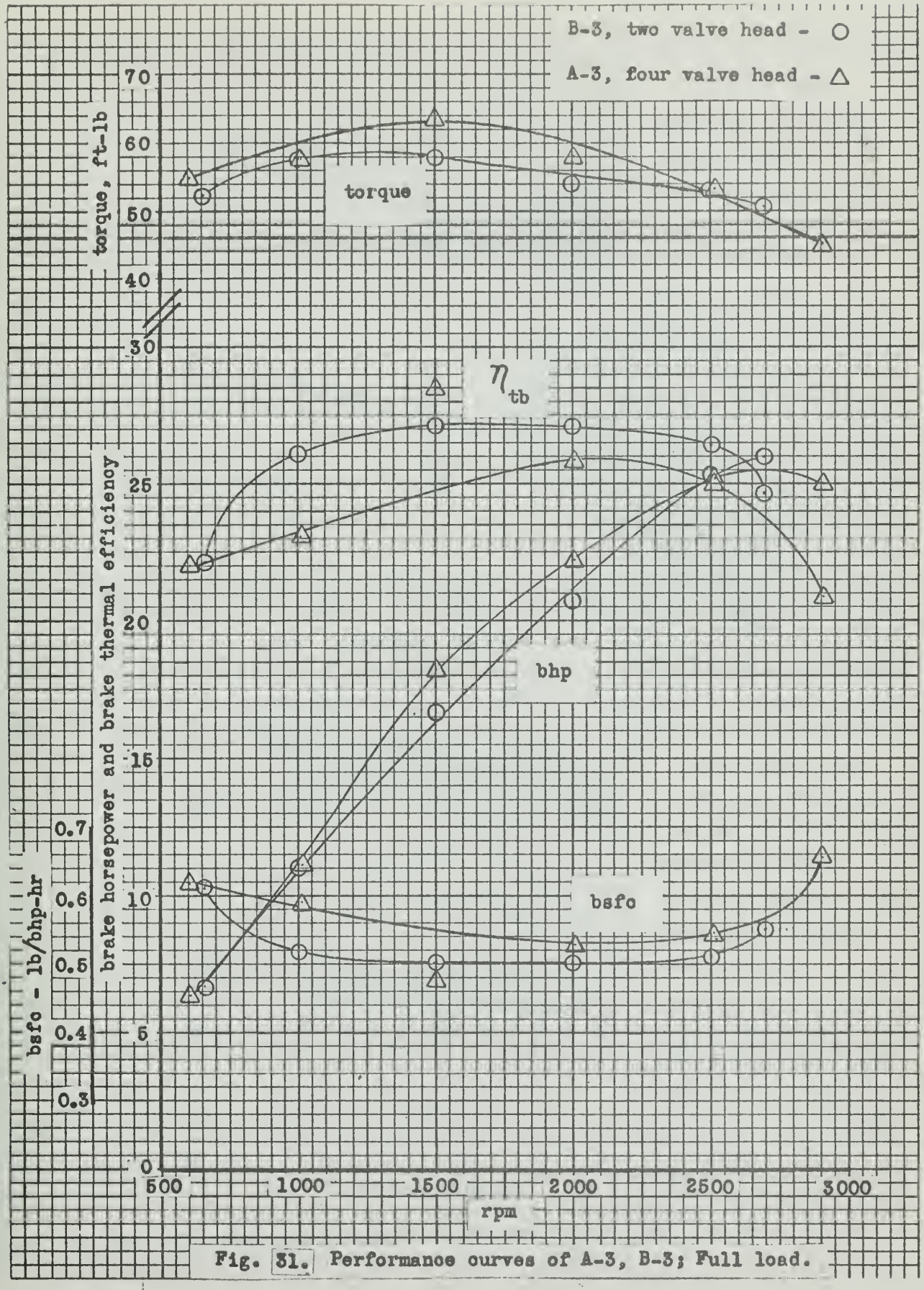

Fig. 31. Performance curves of A-3, B-3; Full load.

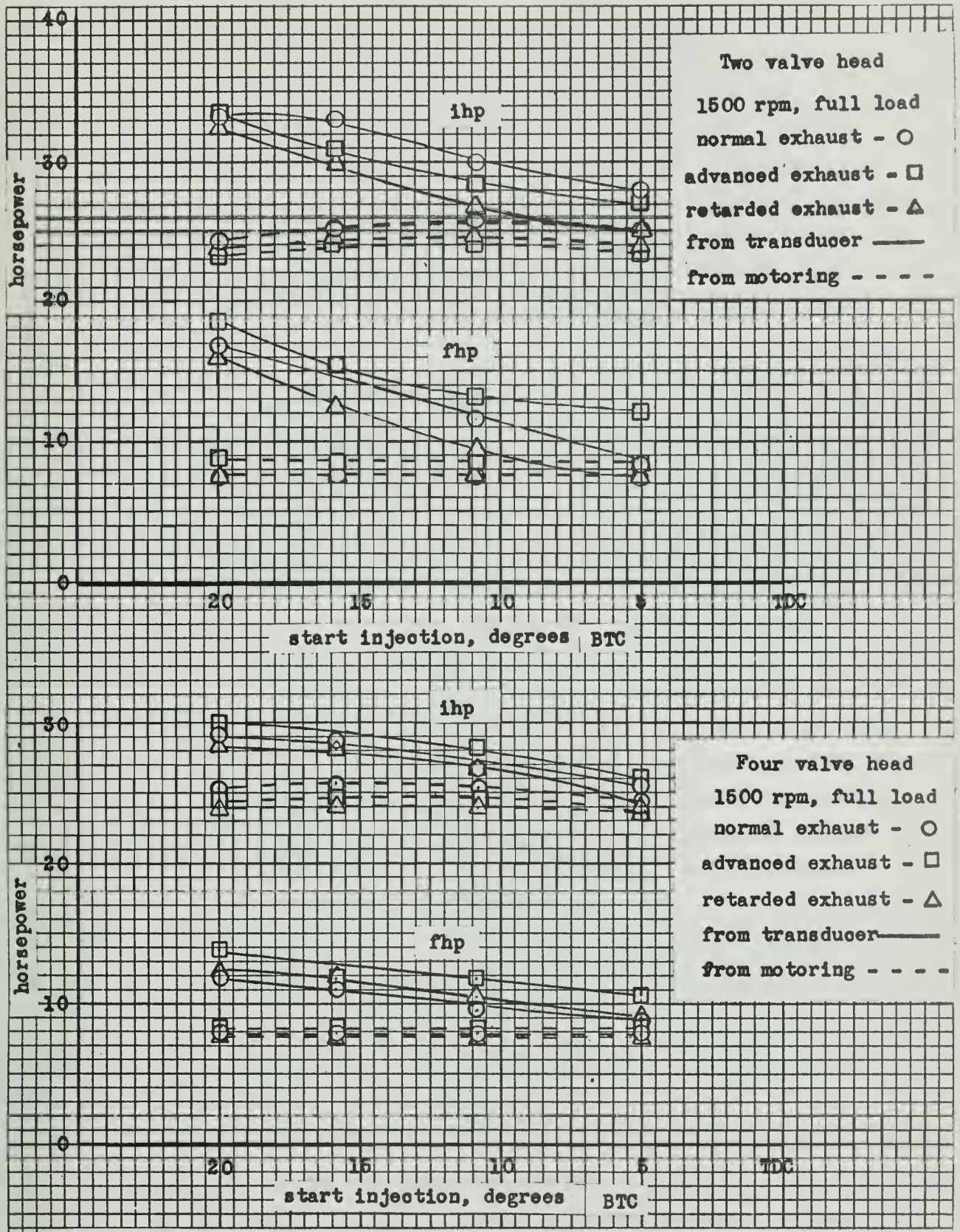

Fig. 32. Indicated and friction horsepower versus fuel injection point.

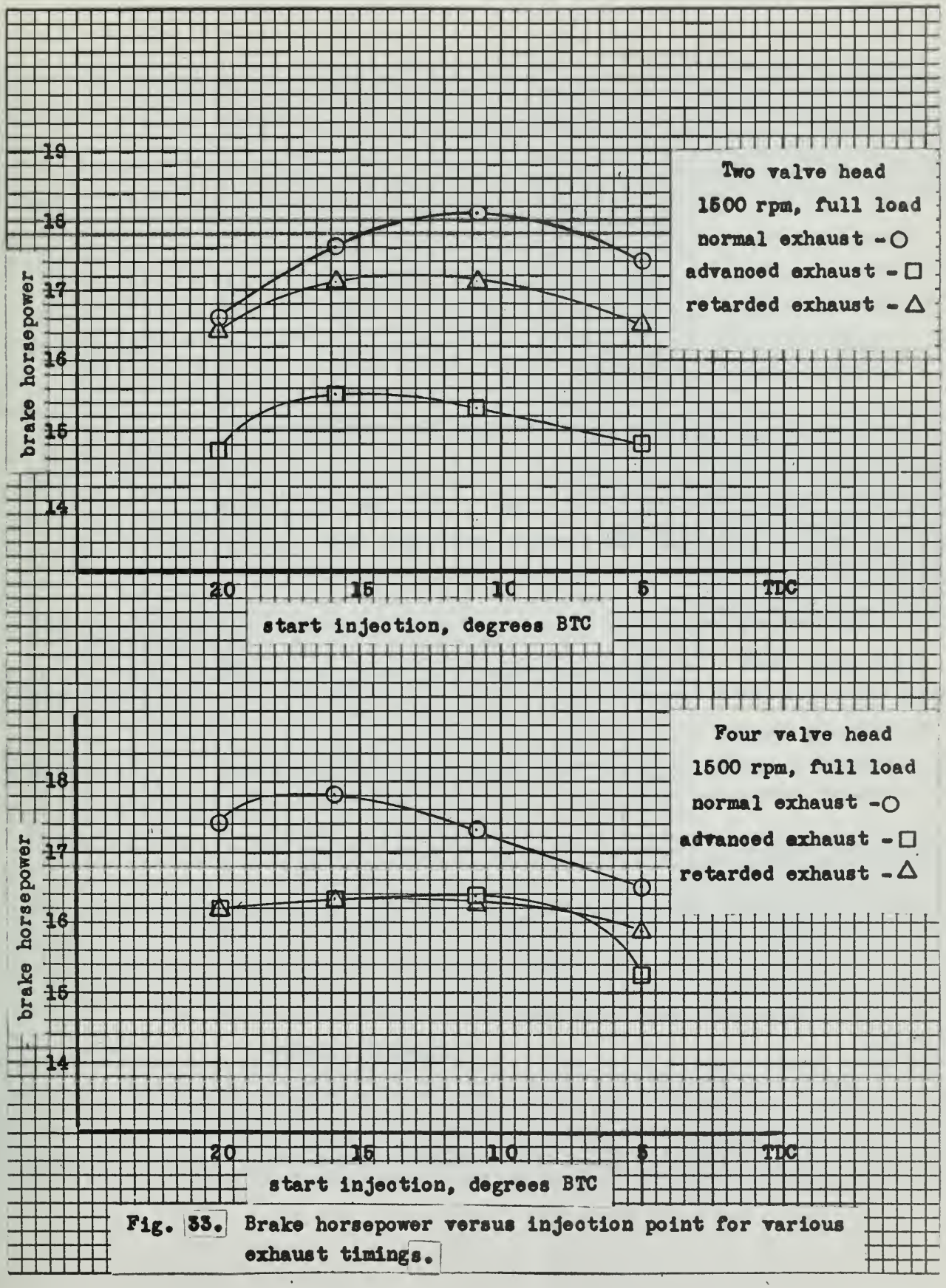

Fig. 33. Brake horsepower versus injection point for various exhaust timings.

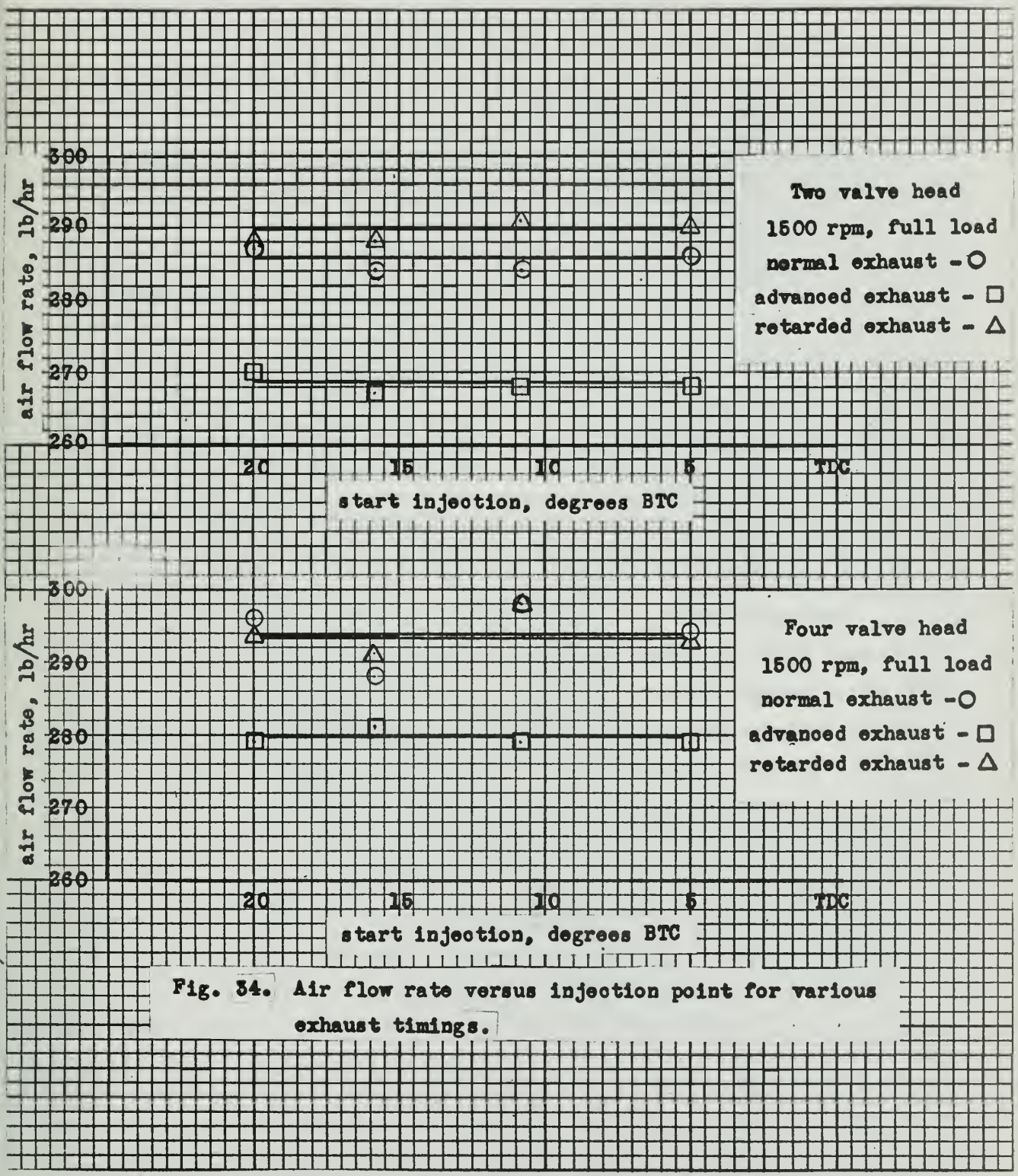

Fig. 34. Air flow rate versus injection point for various exhaust timings.

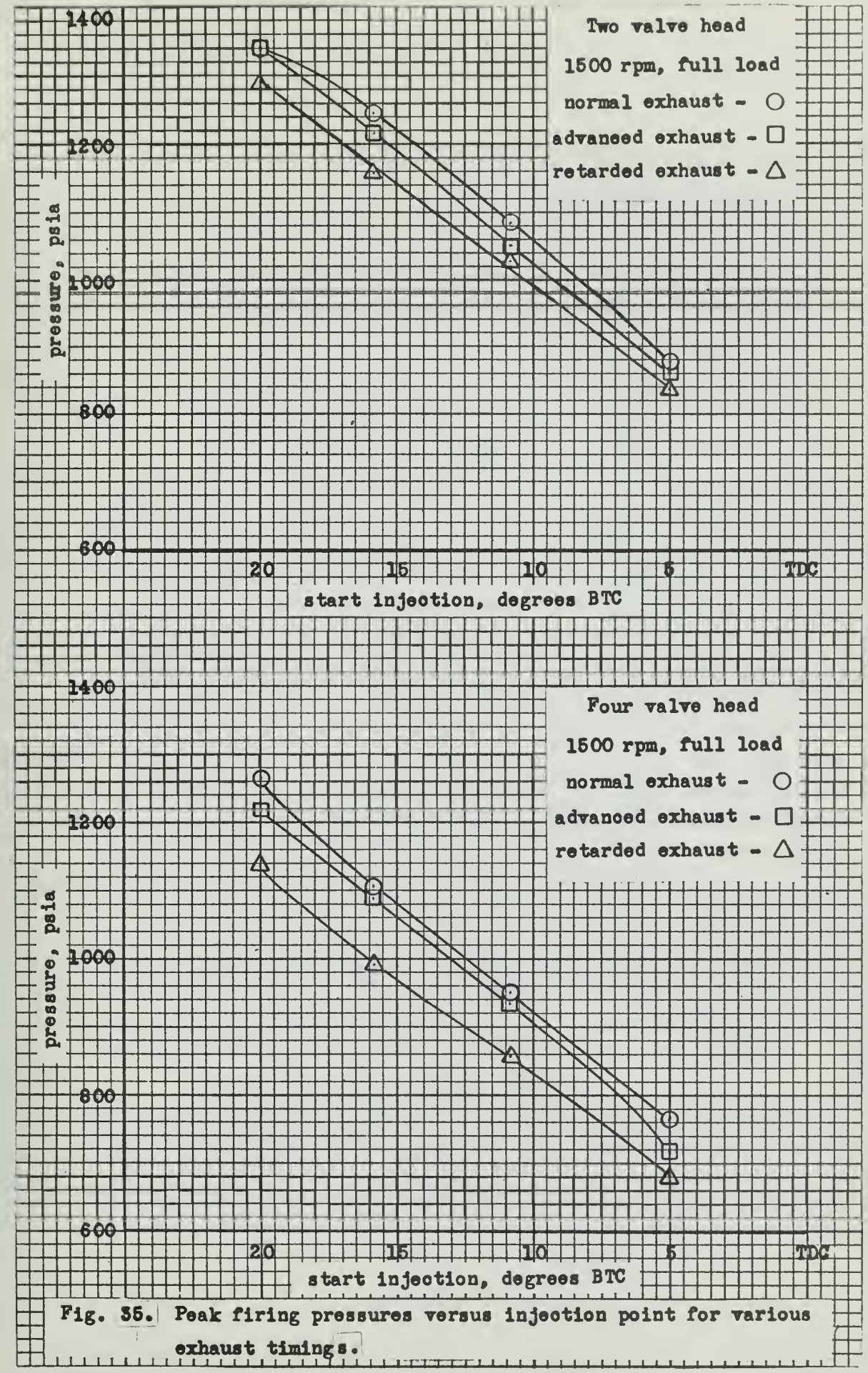

Fig. 35. Peak firing pressures versus injection point for various exhaust timings.

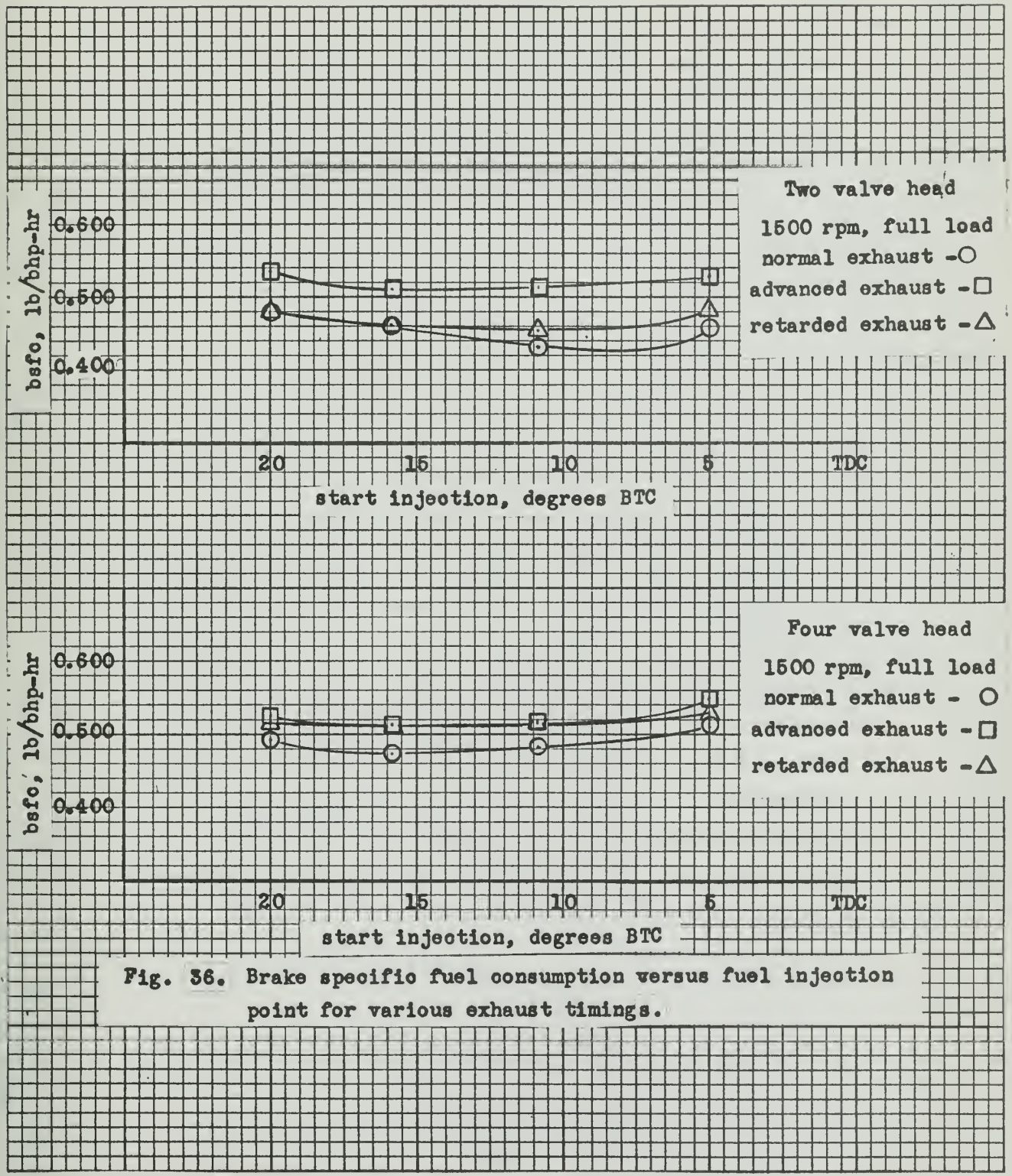

Fig. 36. Brake specific fuel consumption versus fuel injection point for various exhaust timings.

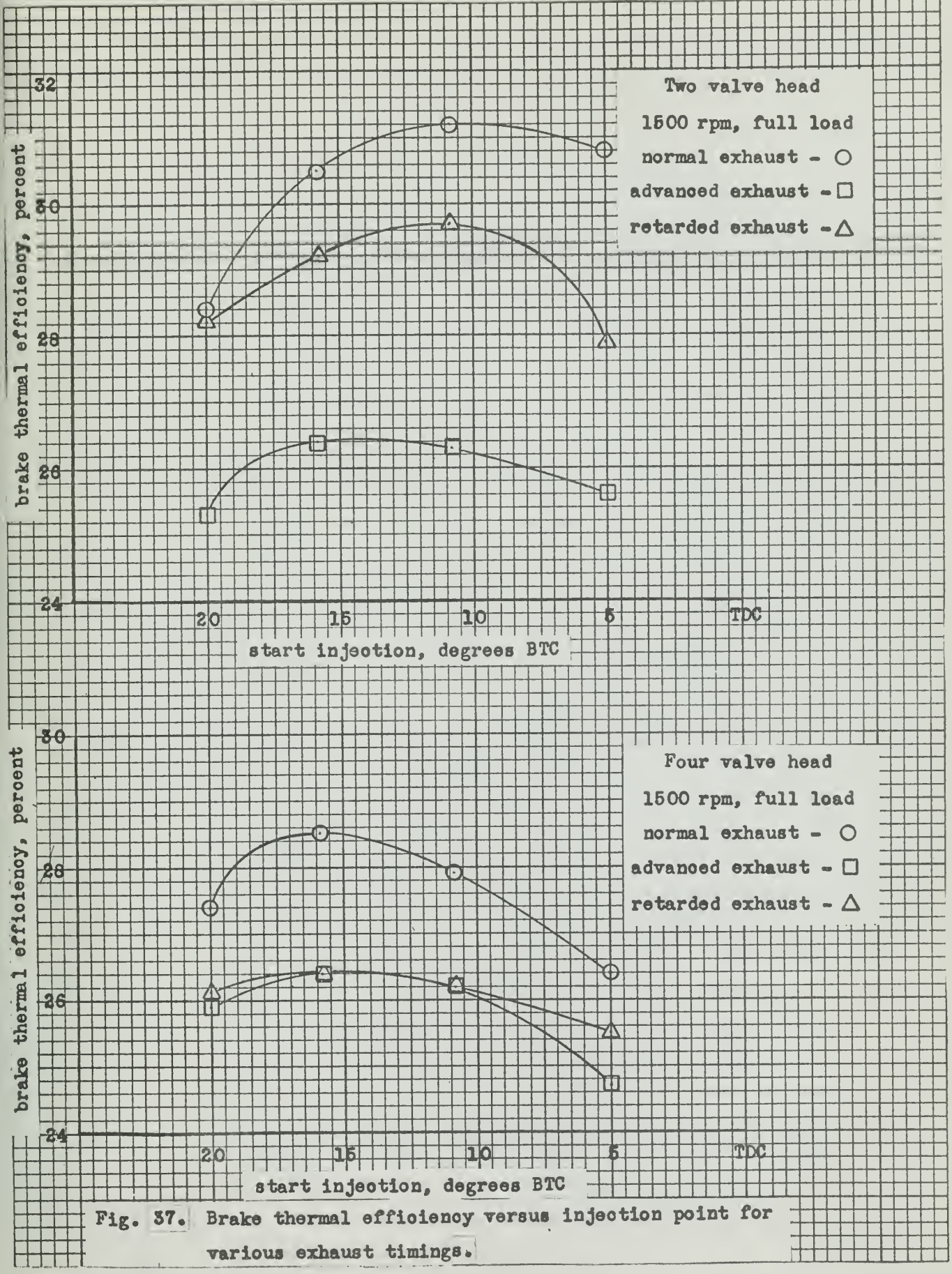

Fig. 37. Brake thermal efficiency versus injection point for various exhaust timings.

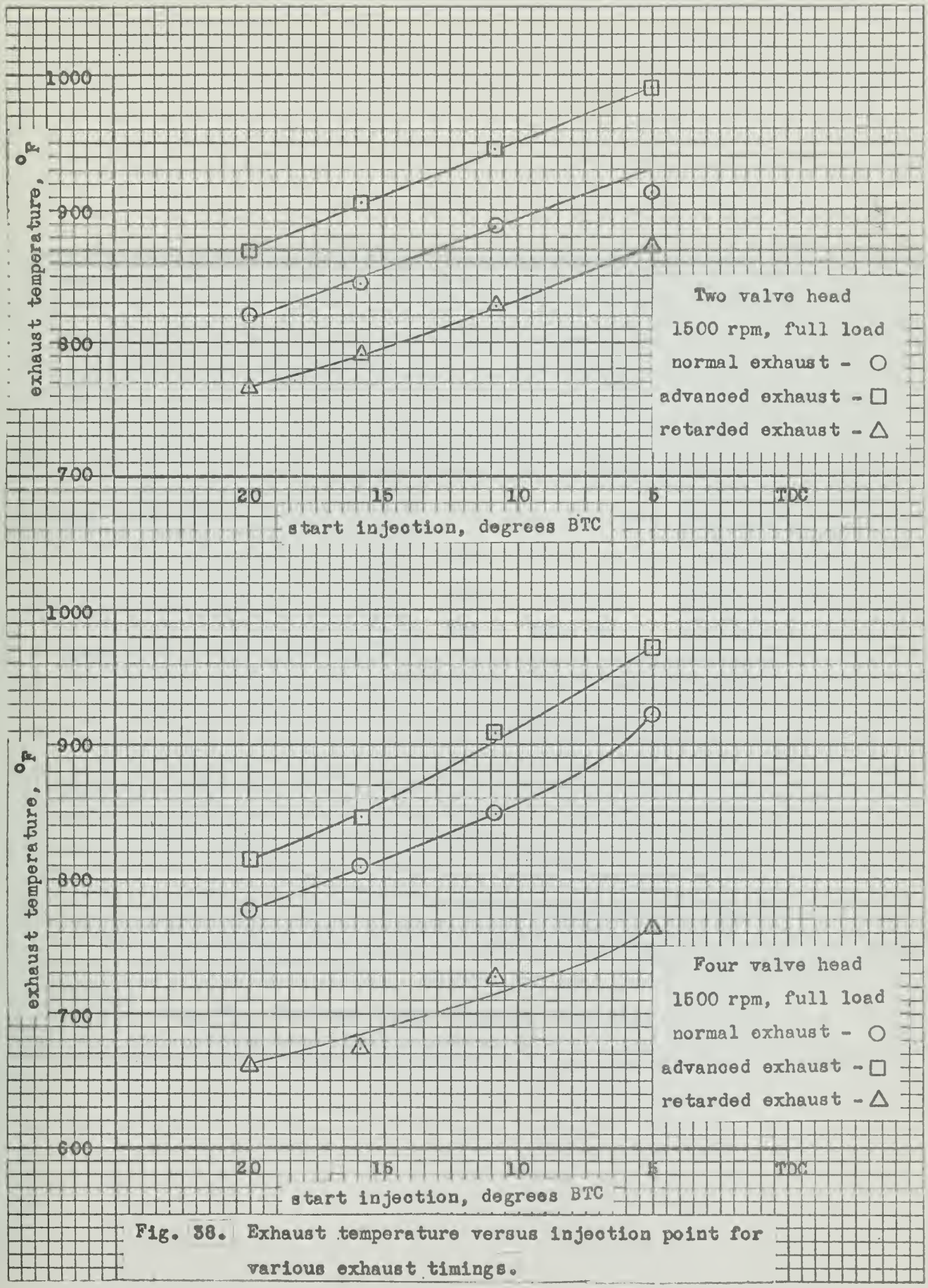

Fig. 38. Exhaust temperature versus injection point for various exhaust timings.

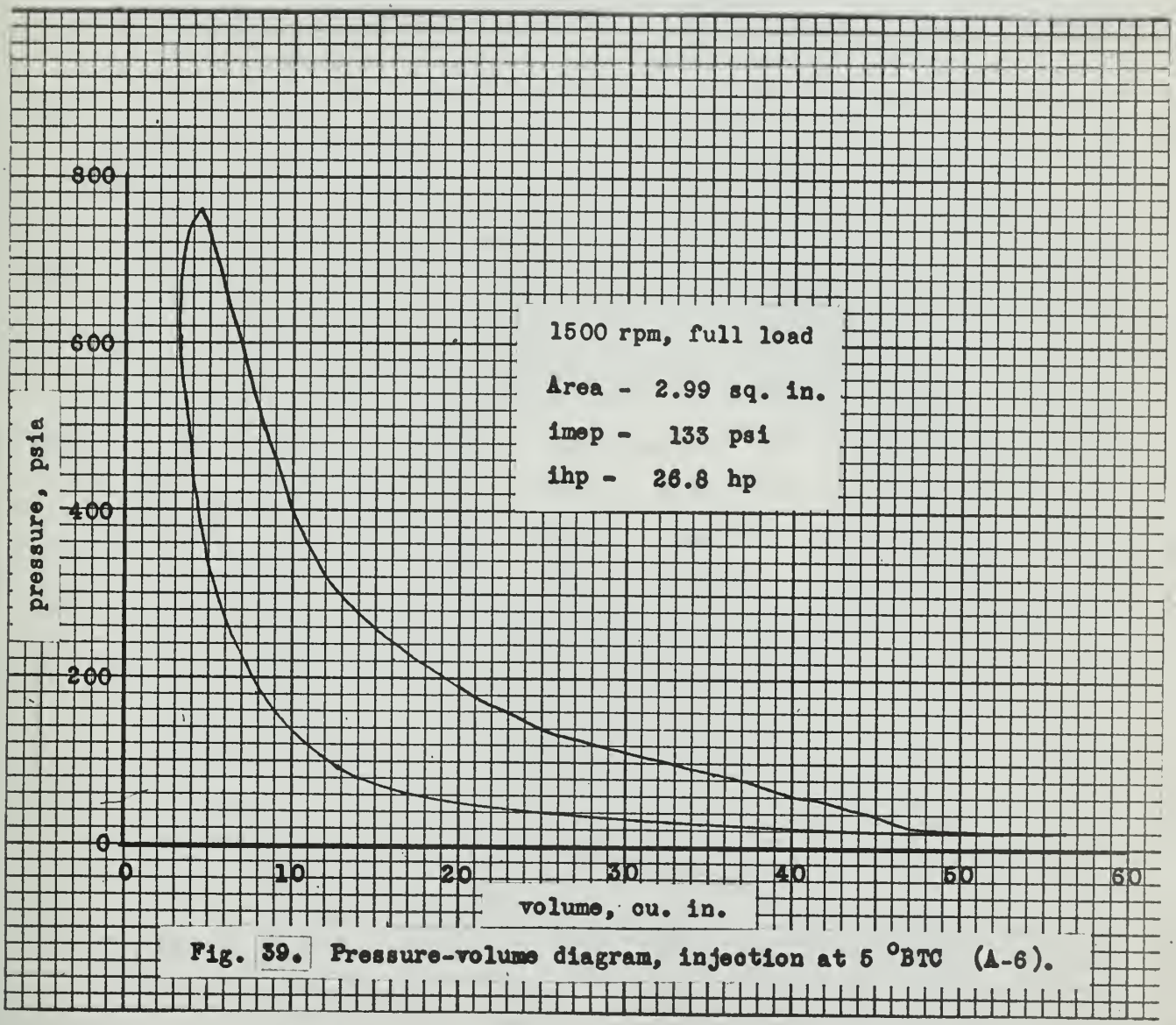

Fig. 39. Pressure-volume diagram, injection at 5 °BTC (A-6).

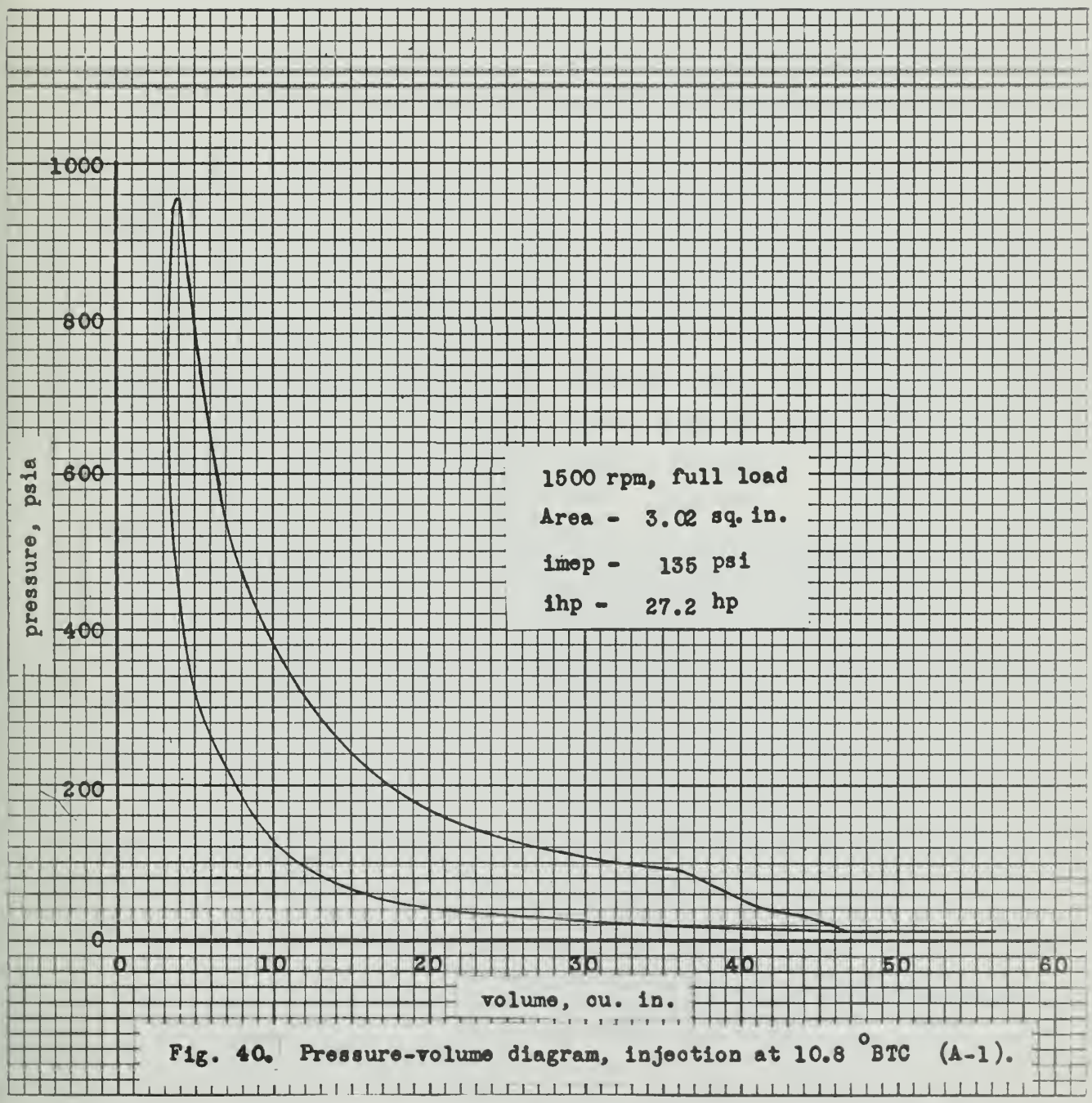

Fig. 40. Pressure-volume diagram, injection at 10.8 °BTC (A-1).

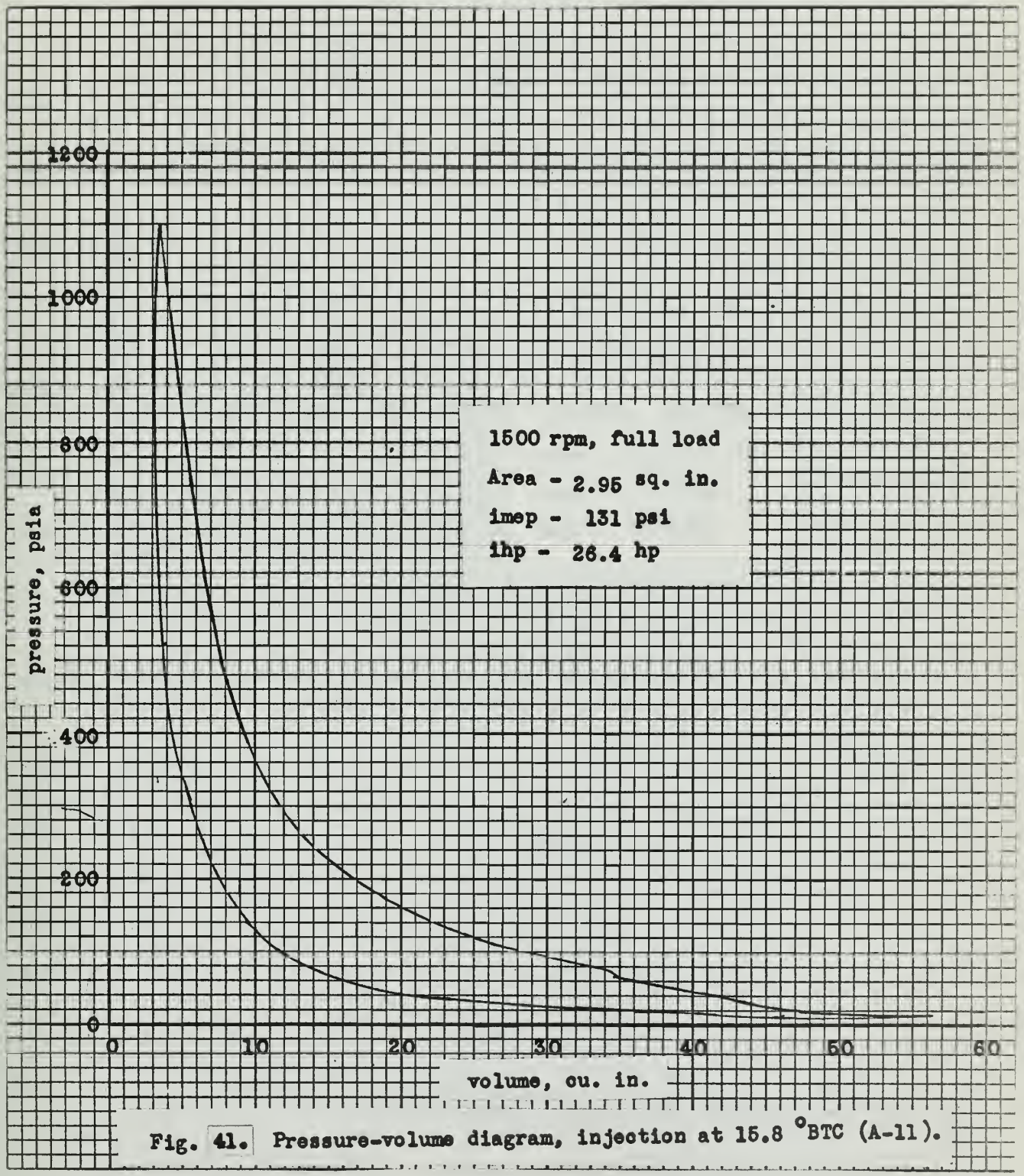

Fig. 41. Pressure-volume diagram, injection at 15.8 °BTC (A-11).

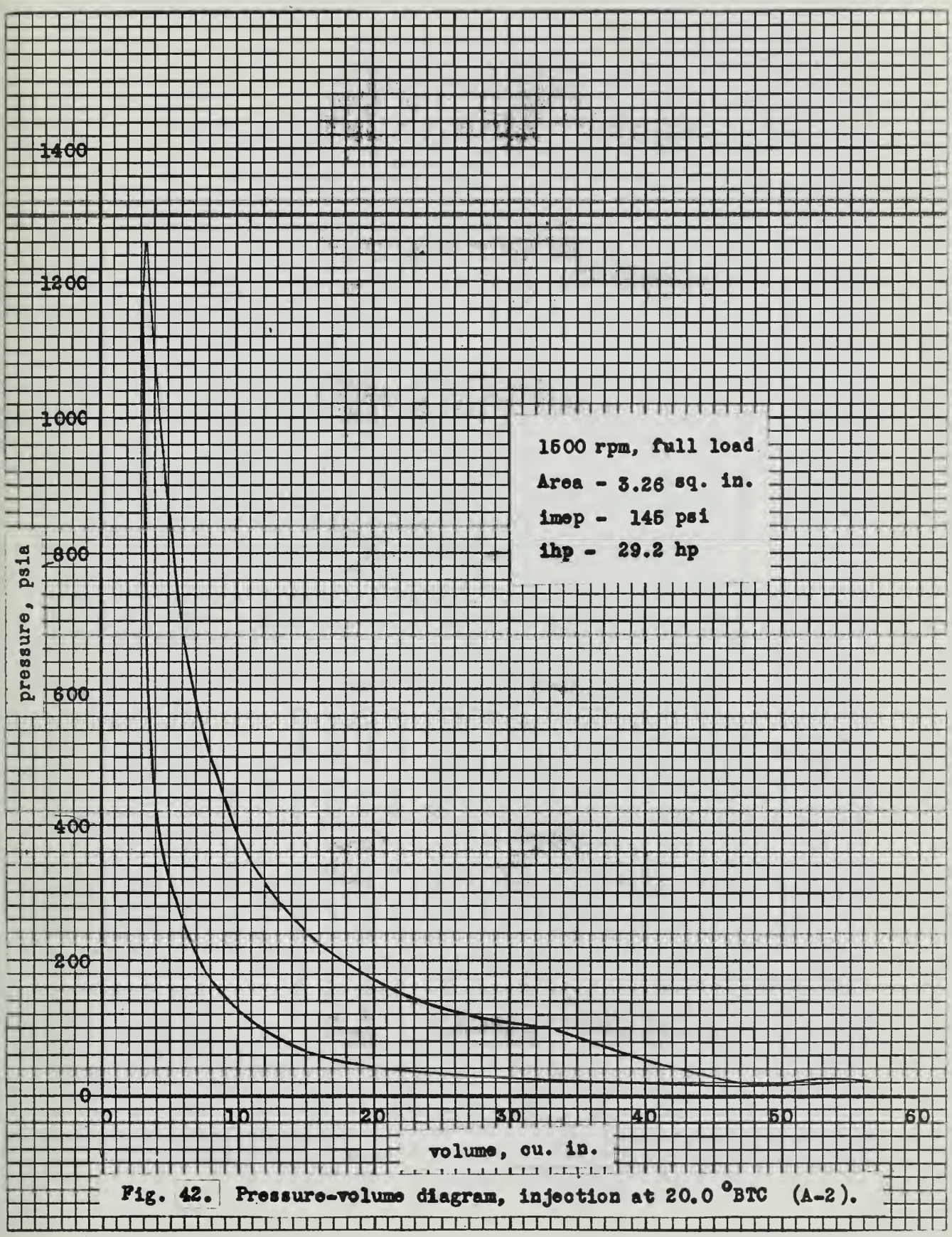

Fig. 42. Pressure-volume diagram, injection at 20.0 °BTC (A-2).

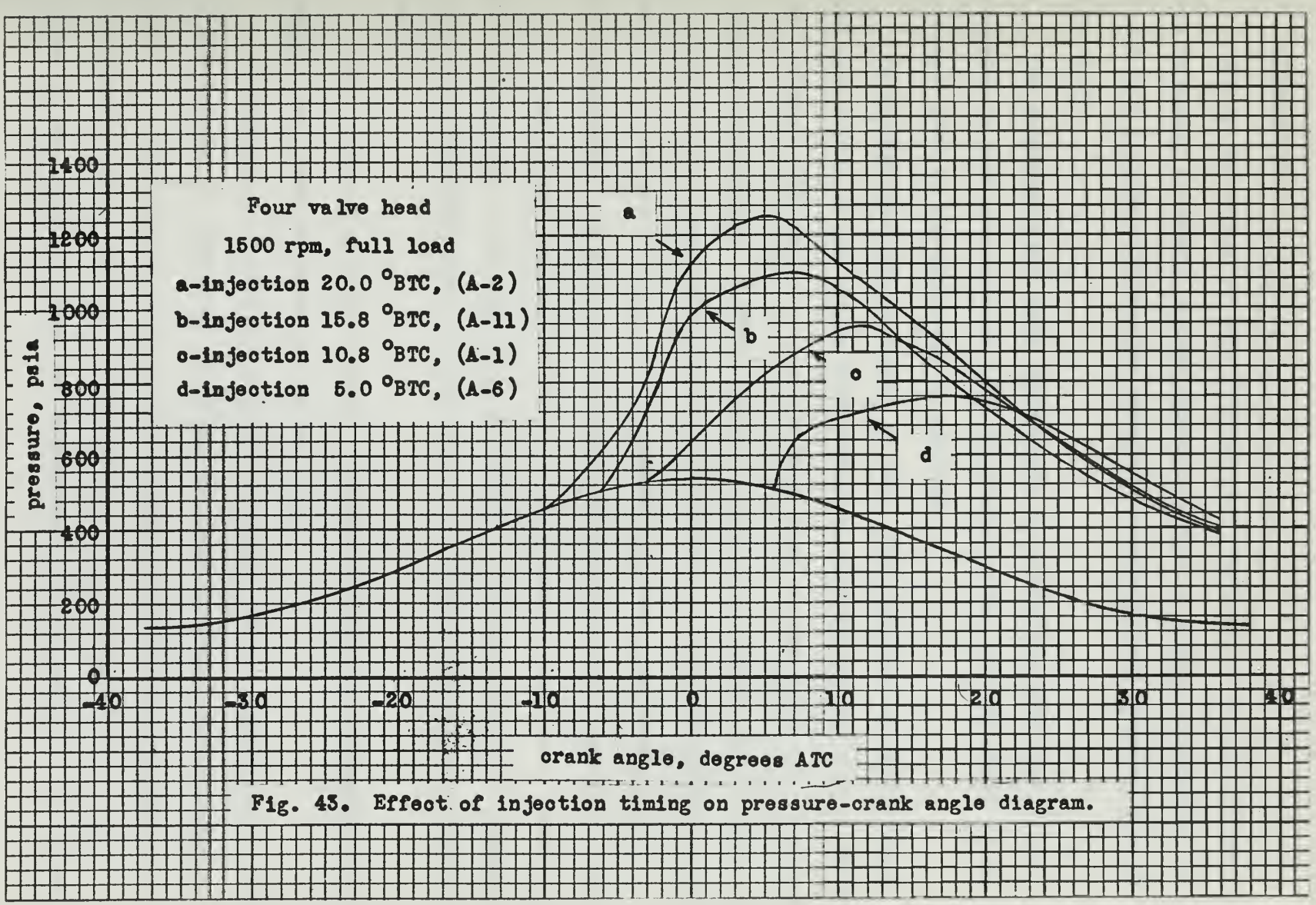

Fig. 43. Effect of injection timing on pressure-crank angle diagram.

5. Discussion.

Due to the volume of data obtained and displayed in tabular format it was necessary to select certain characteristics to present graphically which would most clearly indicate the variation in performance obtained with the two heads.

The pressure-crank angle photographs in themselves show clearly the decrease in peak pressure and rate of pressure rise, and the shift of the pressure peak as the injection is retarded.

An attempt was made to inject at TDC. This resulted in intermittent and late firing of the engine with combusion starting between 30° to 35° ATC. The pressure peaks due to combustion were normally less than the compression peak for this timing. However, engine vibration and knock were excessive and no further tests were conducted with this setting. The intermittent firing was due to the piston being on the downstroke thereby decreasing pressure and temperature. No attempt was made to advance injection beyond 20 °BTC since several runs resulted in peak pressures greater than those reported by the manufacturer. The range from 20 °BTC to 5 °BTC for injection bracketed the best performance point in each case so no further advance or retard was warranted.

Fig. 28 is of interest in that it depicts clearly the difference in the exhaust and inlet processes of the two heads.

Retarding fuel injection resulted in higher exhaust temperatures. This is due in part to combustion occurring at higher pressure and temperature and also to less work obtained from the energy available before opening of the exhaust valves. In every case ignition delay was greatest at the extremes of the injection range and decreased at the mid-points. The values

of ignition delay obtained compare closely with those cited by Taylor /2/ for a slightly larger engine and the variation is in the same manner as reported here.

The variation of exhaust timing produced pronounced effects also. There is a decrease in brake horsepower and brake thermal efficiency when departure from normal timing is made, with the exhaust timing advanced condition the poorest. Likewise the brake specific fuel consumption was lowest for normal timing and highest with advanced timing. Exhaust temperatures were highest for the advanced exhaust and lowest when the exhaust timing was retarded due to the greater expansion which had occurred. Scavenging ratios increased as the exhaust timing was retarded and is confirmed by Taylor /2/ for a similiar size engine. The two valve head ran hotter overall due in part to poorer scavenging. The normal exhaust produced the higher peak pressures with the retarded position showing the lowest peaks. This is partly due to some loss of the small supercharging effect of the scavenging blower.

As was to be expected the air flow was greater for the four valve head with its larger exhaust area.

The comparison of the engine operation in modes A-1 to A-3 with B-1 to B-3 indicates that on the basis of brake thermal efficiency the two valve head is the better performer up to about 2500 rpm after which it falls off rapidly. On the basis of brake thermal efficiency McCord /1/ found the four valve to be best at A-3 (injection advanced and exhaust retarded slightly), while the two valve head was best when operated at B-1 (normal timing).

Fig. 29, normal timing, shows that the two valve develops more horsepower than the four valve up to about 2700 rpm, but then falls off sharply. It was difficult to control engine load and speed at the high end of the speed range with the two valve head, and for this reason it was not tested at speeds as

high as those used with the four valve head. Figs. 30 and 31 show that advancing the fuel injection improves power output at high speeds for both heads. The four valve head now becomes best on the basis of brake horsepower. Note in Fig. 33 that at 1500 rpm there is an optimum point of fuel injection, which is different for the two heads, and that injection at 20 °BTC, as used in Figs. 30 and 31, causes a decrease in brake horsepower.

On the basis of brake thermal efficiency and brake specific fuel consumption the two valve head is better than the four valve over the full speed range. This refers only to timing modes depicted in Figs. 29 to 31.

It is concluded that the four valve head is best suited to continuous operation at speeds around 2000 rpm, and the two valve at speeds around 1500 rpm. The normal configuration appears best for the two valve head at this speed, and the four valve could best be used with normal exhaust timing and advanced injection timing. Fig. 33 suggests that injection at about 17 °BTC might be best for the four valve head.

The comparison of friction horsepower from motoring tests and from the difference in indicated and brake horsepower resulted in rather conclusive support of the fact that it is dependent upon the mean gas pressure in the cylinder. Most texts on engine testing present the theory that there should be little difference between the two results. However, Taylor /2/ presents data obtained from motoring tests in which the ports and valves were secured, and the mean cylinder pressures were varied over a wide range. The result of these tests was that increased pressure caused sharp increases in the measured friction horsepower. Thus, the difference in friction horsepower of the two methods reported here is supported. It is noted that at the 5 °BTC injection point where the lowest peak pressure and lowest mean effective pressures occurred that the discrepancy is smallest.

It will be noted that the indicated horsepowers given with Figs. 39 through 42 are not the same as tabulated in the tables for these runs. The discrepancy is due to transcribing from the pressure-crank angle photographs to the pressure-volume diagrams. These diagrams are given to point out the large effect that varied fuel injection made.

Fig. 43 is for the same timings as shown in the pressure-volume diagrams referred to above. The sector around top dead center has been expanded to illustrate more clearly the decrease and shift in the peak pressure and the decrease in rate of pressure rise as fuel injection is retarded.

6. Conclusions.

The variables that affect the amount of useful power obtainable from an internal combustion engine are many. This investigation indicates some of the control available to the operator.

The use of the pressure transducer and its associated electronic equipment is not adaptable to short laboratory periods unless sufficient time is provided for student familiarization. However, as now instrumented the engine is adaptable to qualitative demonstrations to emphasize class room material, and this latter usage may well be the more rewarding.

The data presented herein will provide a useful reference for future laboratory exercises and student projects.

7. Bibliography.

1. S. R. McCord, Lcdr., U. S. Navy, General Motors Single Cylinder Diesel Engine Model 1-53X3 Installation and Tests, Thesis U. S. Naval Postgraduate School, 1960.

2. C. F. and E. S. Taylor, The Internal-Combustion Engine, 2nd. Edition, International Textbook Co., 1961.

3. T. G. Beckwith and N. L. Buck, Mechanical Measurements, Addison-Wesley Publishing Company, Inc., 1961.

4. Kistler Model 601 Pickup and Model 651 Piezo-calibrator, Kistler Instrument Corporation.

5. R. J. Sweeney, Measurement Techniques in Mechanical Engineering, John Wiley and Sons, 1953.

6. L. C. Lichty, Internal Combustion Engines, McGraw Hill Book Company, Inc., 1939.

7. ASME Power Test Codes, Internal Combustion Engines, 1957.

8. Supplement to ASME Power Test Codes, Chapter 4, Flow Measurement, ASME, 1959.

9. J. H. Keenan and J. Kaye, Gas Tables, John Wiley and Sons, Inc., 1948.

10. T. Baumeister, Marks Mechanical Engineers Handbook, McGraw Hill Book Company, Inc., 6th. Edition, 1958.

11. S. J. Kline and F. A. McClintock, Describing Uncertainties in Single-Sample Experiments, Mechanical Engineering, 75, pp. 3-8, January 1953.

APPENDIX A

Fixed Parameters.

A more complete list of engine dimensions are given by McCord /1/. The following are required herein.

cylinder bore	3.875 in.
piston stroke	4.50 in.
displacement volume	53.1 cu. in.
piston area	11.8 sq. in.
connecting rod	9.0 in.
crank arm	2.25 in.
compression ratio	17:1
air ports uncover	123 °ATC
air ports cover	237 °ATC
exhaust valves, four valve head	
diameter	1.09 in.
Total exhaust area	3.73 sq. in.
exhaust valves, two valve head	
diameter	1.400 in.
total exhaust area	3.08 sq. in.
air intake nozzles, ASME long radius	
diameter, number one	1.375 in.
diameter, number two	2.00 in.

APPENDIX B

EQUIPMENT

1. Cylinder heads.

Both heads had been bored and tapped by General Motors to receive pressure transducers. This had been done in different manners and required further modification for this project.

The four valve head did not have sufficient room to bore without penetrating the water side so a sleeve was pressed in to close the water side. This was dependent upon a plug or a pressure transducer to seat its lower end against a machined shoulder and copper gasket. The opening into the cylinder had 14mm. threads. When the plug was removed the seal was broken. The water cooled adaptor did not provide sufficient force to reseat the sleeve, and leakage occurred between the cylinder and the water side.

Inspection revealed that the gasket had deteriorated and that there was localized pitting of the sleeve base. Subsequent attempts to machine and lap the surfaces failed to provide a satisfactory repair. Several combinations of sealants and gaskets were then made,and the problem was eventually solved using an epoxy. The cooling effect afforded by the water side and the water cooled adaptor were sufficient to protect the epoxy. Epoxy was also used to repair the threads in the pressure cavity. This process is recommended if future repairs are necessary.

Fig. 5 shows the opening in the base of the four valve head for the adaptor. Fig. 3 shows the adaptor and pickup installed and also the upper portion of the sleeve. The sleeve acts also to prevent oil from entering the pressure cavity and is sealed at its upper end by the head cover and an O-ring. The pressure transducer's upper surface must be open to atmospheric

pressure at all times.

The two valve head was drilled without penetration of the water side and tapped with 18mm. threads. An 18mm. thread die was not available locally so the existing plug was drilled and tapped to 14mm. threads to receive the transducer adaptor. It is recommended that a set of 14mm. and 18mm. thread dies and taps be obtained and that plugs be made for the pressure cavities.

It was also necessary to fabricate a sleeve which would seal off all oil as previously described for the four valve head. This addition required a further modification to the injector rack linkage. The sleeve seats on a machined surface and gasket and is held in place by a bridge arrangement installed on the head cover which is shown in Fig. 2.

It was also necessary to install a Type 5 Synchro to permit control of engine speed from a remote position, and to modify the cooling water outlet piping. A comparison of Figs. 2 and 3 shows the variations in these external connections.

2. Characteristics of the pressure sensing equipment.

Selected characteristics are given. For complete details refer to the manufacturer's instruction book /4/.

Model 601 Pressure Pickup

pressure range	0.5 - 5000 psi
overload capacity	50 percent
linearity	$\pm$ 1 percent
natural frequency	150,000 cycles/sec
maximum continuous temperature	500 °F
maximum intermittent temperature	3000 °F
length	0.591 in.
diameter	0.249 in.
weight	0.08 ounces

Model 651 Piezo-Calibrator

input signal, maximum	0.6 volts
output signal	0.3 volts
gain	0.5
input impedance	10^{14} ohms
output impedance	10^{5} ohms
response	0 - 10,000 cycles/sec
linearity	$\pm$ 1 percent
dimensions	7 x 10 x 6 in.
weight	4.7 lb.

3. Pressure transducer calibration.

Prior to using the Kistler Model 601 piezoelectric pressure pickup it was statically calibrated. This calibration was made with the equipment assembled as in Fig. 7, and the water cooled adaptor mounted in an Aschroft dead weight tester. A high pressure fitting was made for this purpose.

The calibrations were performed on each range scale and up to 1500 psi which exceeded any pressure later encountered. The tests indicated that the crystal is linear throughout the range tested.

Since the electromotive force developed by the crystal will decrease with time the static tests were conducted in two ways; loading in increments and loading in one full step. The results indicated that the leakage is small for this crystal. During repeated tests to 1000 psi the maximum discrepancy did not exceed 10 psi and to 1500 psi did not exceed 30 psi. When loaded in one step repeatable results were obtainable, and the discrepancy was practically eliminated. This ability to accurately retain a charge is due to the piezo-calibrator. The electrostatic charge generated by the crystal forms a voltage on a high insulating capacitor. An electrometer tube measures this charge without providing a leakage path. The charge is removed by grounding the circuit.

The manufacturer /4/ recommends a check calibration only in the upper one-third of each range to be used. In addition, he states that shock tube tests have proved that static sensitivity and dynamic sensitivity are identical over a large frequency range.

The method of calibration is outlined by the manufacturer /4/. The

following steps which are not set forth are given.

a. Insure that all cable connectors are wiped clean with industrial wiping paper only, and that connections are tight.

b. Make alignment checks of the oscilloscope in use. Zeroing the vertical amplifier is of special importance.

c. Allow a full five minute warm-up period of the piezo-calibrator and oscilloscope.

d. After this warm-up period insure that the piezo-calibrator voltage dial reads one millivolt, and that the output voltage is zero when the circuit is grounded. Use the meter adjust and output adjust potentiometers to correct discrepancies.

e. Insure that the oscilloscope vertical amplifier is set on DC coupled at all times.

f. Check for electrical interference on the most sensitive scale of the oscilloscope. Unwanted signals as little as one millivolt can create sizeable errors and must be eliminated.

After observing the oscilloscope deflection that a given input produces the values are recorded. These are then used as calibration signals for determining the magnitude of pressure signals observed with the oscilloscope.

The following calibration signals were determined. After equipment alignment the settings in the first three columns should produce the value given in the last column. If this value is not obtained, and a check of equipment and procedures does not indicate an operator error, use the calibrate adjust setting on the piezo-calibrator.

APPENDIX B

Range Switch psi/div	Calibrator Dial div.	Oscilloscope Vert. Sens. mv/cm	Calibrate Signal, Oscilloscope deflection, cm
100	15	5	8.0
100	15	10	4.0
10	100	20	10.0
10	50	10	10.0
1	100	10	6.0
0.1	100	10	0.8
0.1	100	5	1.6

For future tests requiring a good degree of accuracy it is recommended that check calibrations be performed.

It was observed that stability of the equipment was satisfactory and that frequent adjustments were unnecessary.

Beckwith /3/ and Sweeney /5/ give good discussion of dead weight testers and their usage. Of particular importance to the operator is the rotation of the load piston to eliminate vertical components of friction. This effect was noticeable at the low pressures.

4. Special tools.

Several tools that are required in the installation of the pressure pickup and in engine timing were fabricated locally and are described. See Fig. 11.

The torque wrench, made from flame hardened drill rod, is used to seat the pickup in the water cooled adaptor. Twenty-five inch-pounds torque is recommended to prevent leakage of cylinder gas.

The timing gear wrench is used to turn the desired cam shaft when the variable timing gear lock nuts are loosened. It permits timing changes while the engine is hot.

The injector timing gauges are used for accurately setting the distance from the injector base to the plunger follower. They are used in conjunction with the injector cam curves and pumping characteristics curve if timing changes are made at the injector.

Two wrenches for seating the water cooled adaptor in the head cavity are required. These differ since the diameter of the passages are not the same in the two heads. They are essentially deep sockets.

A high pressure fitting, not shown in Fig. 11, is available for mounting the water cooled adaptor in a dead weight tester.

5. Miscellaneous notes on equipment operation.

a. Electrical interference.

On several occasions it was necessary to eliminate 60 cycle interference from the oscilloscope display. The source of such interference was usually traced to neon lights, or ground circuits on 60 cycle, 120 volt power sockets. It was necessary at times to locate and eliminate signals of one-half millivolt peak voltage. If these cannot be eliminated by securing equipment, additional shielding and grounding of the piezo-calibrator is necessary. On repeated occasions a high frequency square wave of small magnitude appeared. Its source could not be located.

b. Piezo-calibrator power supply.

There is a problem with procurement of the 6.7 volt mercury cell battery for the piezo-calibrator. It was found that an external D. C. source using dry cells and a slide wire voltage divider will provide a reliable supply. The current drain is extremely small.

c. Vertical drift of piezo-calibrator signal.

The drift of the calibrator signal or its collapse into a rate signal is discussed in detail in the operating instructions /4/. However, a source of trouble not indicated was discovered. The frame that the piezo-calibrator batteries mount in is part of the same frame that mounts to the case. If the holding screws are drawn down too tightly the four volt battery will make poor contact, and the result is drift or even collapse of the output signal. An analysis of the symptom using the circuit diagram would cause one to determine erroneously that the electrometer tube was bad.

d. Oscilloscope selection.

APPENDIX B

The output of the piezo-calibrator must go to an impedance of 100,000 ohms. The Hewlett Packard 120, 122 and 130 series have this input impedance. The Model 130 was selected for this project since it has a larger range of sensitivity. The Model 130 does not have a sweep expand, but the same effect can be produced.

e. Pickup cooling.

Adequate cooling of the pickup is necessary if good low frequency response is to be assured. Cooling water was turned on prior to engine start and left on until the engine had cooled to nearly ambient after running.

Date: 2-15-63

Data sheet - GM 1-53X3 One Cylinder Diesel Engine - Bldg. 500 USNPGS

Bore: 3-7/8 in. Stroke: 4-1/2 in. Sheet No. 5

Compression ratio: 17/1. Fuel Heat Value: 18,860 BTU/lb$_f$

Exhaust Opens: 109 °ATC Fuel type: lab diesel

Exhaust Shuts: 234 °ATC Fuel sp. gr.: 0.818

Injection Starts: see remarks Fuel temp., °F: 67

Head installed: 4 Timing Configuration:

		A-5	A-8	Motor	A-10	A-13
		1	2	3	4	5
1.	Hours to date 974 Run:					
2.	Average RPM:	1505	1505	1500	1509	1502
3.	Duration of run, secs:	342	294	---	329	330
4.	Torque, ft-lb.:	57.1	55.5	27.0	56.5	57.0
5.	Burette temp., °F.	68	72	---	70	74
6.	Corr. sp. gr. fuel.	0.820	0.820	0.820	0.820	0.820
7.	Fuel column start, in.	61.0	57.5	---	59.0	60.5
8.	Fuel column stop, in.	36.0	36.0	---	35.0	36.5
9.	Fuel pressure, psi.	60	57	60	58	57
10.	Water temp. in, °F.	174	175	170	171	173
11.	Water temp. out, °F.	192	196	170	190	193
12.	Flowmeter, % flow	100	100	100	100	100
13.	Oil pressure, psi.	57	56	57	57.5	55.5
14.	Oil temperature, °F.	162	168	172	172	175
15.	Air intake nozzles	#2	#2	#2	#2	#2
16.	Air ambient temp., °F.	69	71	71.5	72	74
17.	Air box temp., °F.	252	256	---	235	245
18.	Intake air temp., °F.	69	71	71.5	72	74
19.	Atmosphere press, in-hg.	30.31	30.31	30.32	30.31	30.29
20.	Intake air den., in. H_2O corr: -0.005	0.590	0.575	0.550	0.575	0.565
21.	Air box press., in.-hg.	4.0	4.0	4.5	4.05	3.9
22.	Exh. back press., in. H_2O	4.2	4.45	4.7	4.7	5.0
23.	Exhaust temp. °F.	728	764	---	662	672
24.	Piezo Cal. Range Scale	V A R I O U S				
25.	Cal. dial setting	(Seperate photograph log maintained)				
26.	Oscilliscope sens. mv/cm.		"		"	
27.	Sweep time, msec/cm		"		"	
28.	Numbers of photos	37-39	40-42	43,44	45-47	48-50

29.	Started engine:	A-5	0930	Secured engine:	A-5	1025
		A-8	1040		A-8	1110
30.	Remarks:	Motor	1112		Motor	1130
		A-10	1245		A-10	1330
		A-13	1345		A-13	1515

12ND NPS 95 (11-59)

Injection: (°BTC), A-5, 10.8; A-8, 5.0; A-10, 20.0; A-13, 15.8 .

APPENDIX D

Sample Calculations.

The data used in the calculations presented herein are taken from Run 1, Timing configuration A-5 given in Appendix C.

1. Fuel specific gravity

$$\text{sp. gr. burette} = \text{sp. gr.}_{60^\circ} - \left[\frac{t - 60}{3600}\right]$$

$$\text{sp. gr. burette} = 0.820 - \left[\frac{68 - 60}{3600}\right] = 0.818$$

2. Fuel lower heating value

$$LHV = 16{,}380 + 60 \times API^\circ_{60}$$

where: $$API^\circ_{60} = \frac{141.5}{\text{sp.gr.}_{60^\circ}} - 131.5$$

and, $$\text{sp.gr.}_{60^\circ} = \text{sp.gr.}_t + \frac{t - 60}{3600}$$

$$LHV = 16{,}380 + 60\left[\frac{141.5}{0.820}\right] - 131.5 = 18{,}860 \text{ BTU/lb}_f$$

This checks closely with values given for $C_{12}H_{26}$ given by Taylor /2/.

3. Brake horsepower

In order to have a reference on which to compare horsepowers the observed values were corrected to a standard of 60°F and one atmosphere in accordance with Lichty /6/. This is also recommended by ASME /7/.

$$bhp = \frac{2 \times \pi \times N \times T}{33{,}000}$$

where 33,000 is the conversion factor from ft-lb/min to hp.

$$bhp = \frac{2 \times \pi \times 1505 \times 57.1}{33{,}000} = 16.35 \text{ hp}$$

$$bhp_{(corr)} = bhp \times \frac{29.92}{p_o} \left(\frac{T_o}{520} \right)^{1/2}$$

$$bhp_{(corr)} = 16.35 \times \frac{29.92}{30.31} \left(\frac{529}{520} \right)^{1/2} = 16.3 \text{ hp}$$

4. Brake mean effective pressure

$$bmep = \eta_m \times imep$$

$$\text{but, } imep = \frac{33{,}000 \times ihp}{LAN}$$

$$\text{and, } \eta_m = \frac{bhp}{ihp}$$

and bhp is as previously defined.

therefore,

$$bmep = \frac{2 \times \pi}{LA} \times T = \frac{2 \times \pi}{0.375 \times 11.8} T = 1.42\ T$$

$$bmep = 1.42 \times 57.1 = 81 \text{ psi}$$

5. Fuel consumption

Cross sectional area of the fuel burette is 1.08 sq. in.

$$\text{cu. in. of fuel} = (h_1 - h_2)\ 1.08$$

$$\dot{m}_f = \frac{1.08\ (h_1 - h_2)\ (\text{sp. gr. burette})}{t} \times \frac{(62.4)(3600)}{1728}$$

where: 1728 is the conversion from cu. in. to cu. ft.

62.4 is the density of water, lb/cu. ft.

3600 is the conversion from seconds to hours

$$\dot{m}_f = \frac{140.4\ (h_1 - h_2)(\text{sp. gr. burette})}{t}$$

$$\dot{m}_f = \frac{140.4(61 - 36)(0.818)}{342} = 8.4\ lb_f/\ hr$$

6. Air consumption

Two ASME long radius nozzles are used to admit air to the inlet surge tank. Either or both may be used. The pressure drop across the nozzles is measured by an inclined manometer in inches of water. The equations were developed by McCord /1/ and assume incompressible flow. Values of the coefficient of discharge, C_D, are from ASME Code /8/.

nozzle one	nozzle two
$V = 66.1\ C_D\ (R)^{1/2}$	$V = 66.1\ C_D\ (R)^{1/2}$
$\dot{m}_a = 187\ C_D\ (R)^{1/2}$	$\dot{m}_a = 396\ C_D\ (R)^{1/2}$

These equations are based on an ambient atmosphere of 70°F and one atmosphere. The following equations are used to correct to the conditions actually existing at the time of test.

$$V_{(corr)} = V \left(\frac{T_o \times p_{std}}{T_{std} \times p_o} \right)^{1/2}$$

$$\dot{m}_{a(corr)} = \dot{m}_a \left(\frac{T_{std} \times p_o}{T_o \times p_{std}} \right)^{1/2}$$

For Run A-5 nozzle two was used. Estimate that $C_D = 0.98$.

$$V_{(corr)} = 66.1\ (0.98)(0.585)^{1/2} \left(\frac{529 \times 29.92}{530 \times 30.31} \right)^{1/2} = 49.1 \text{ fps}$$

To obtain C_D from the chart in the Code /8/ compute the Reynold's Number.

$$Re = \frac{V\ d}{\nu} = \frac{(49.1)(2/12)}{1.69 \times 10^{-4}} = 4.84 \times 10^4$$

where: ν is kinematic viscosity of air at 69 °F.

For this value of the Reynold's Number read $C_D = 0.979$, and no further iteration is required.

$$\dot{m}_a = 396(0.979)(0.585)^{1/2} \left(\frac{530 \times 30.31}{529 \times 29.92} \right)^{1/2} = 298 \text{ lb}_a / \text{ hr}$$

7. Air - fuel ratio

$$A/F = \dot{m}_a / \dot{m}_f = \frac{298}{8.4} = 35.5 \ / \ 1$$

8. Horsepower loss to exhaust

This loss is computed using the First Law of Thermodynamics. The specific heat is taken at the mean temperature of exhaust and inlet to the cylinder. The fuel is considered to $(CH_2)_n$. Tables 5, 8 and 9 of Keenan and Kayes /9/ are used to interpolate for $\bar{C}_p$ and M_p based on the A/F ratio and the mean temperature. This is a first approximation of the loss.

$$hp = \frac{(\dot{m}_a + \dot{m}_f) \ \bar{C}_p \ (T_e - T_i)}{2545 \ M_p}$$

where: 2545 is the conversion from BTU/hr to hp.

$$hp = \frac{(306.4)(7.436)(476)}{(2545)(28.73)} = 14.8 \text{ hp}$$

9. Horsepower loss to cooling water

The flow of cooling water is measured by a flowmeter whose calibration curve appears in McCord's thesis /1/.

$$hp = \frac{\dot{m}_w \ C_p \ (T_{w,out} - T_{w,in})}{42.4}$$

where: 42.4 is the conversion from BTU/min to hp.

$$hp = \frac{21 \times 1\ (192 - 174)}{42.4} = 8.9\ hp$$

10. Friction horsepower from motoring

$$fhp = \frac{2 \times \pi \times N \times T}{33{,}000} = \frac{2 \times 3.14 \times 1500 \times 27}{33{,}000} = 7.71\ hp$$

$$fhp_{(corr)} = 7.71 \times \frac{29.92}{30.32} \left(\frac{531.5}{520} \right)^{1/2} = 7.7\ hp$$

11. Fuel horsepower

$$\text{fuel hp} = \frac{\dot{m}_f \times LHV}{2545} = \frac{(3.4)(18{,}860)}{2545} = 62.3\ hp$$

12. Horsepower loss, unaccounted

hp, unaccounted = fuel hp - (bhp + fhp + losses)

hp, unaccounted = 62.3 - (18.3 + 7.7 + 14.8 + 8.9) = 14.6 hp

13. Indicated mean effective pressure

$$imep = \frac{Area \times Y \times Z}{X}$$

where: Area, is area under the pressure-crank angle photograph curve measured with a planimeter, sq. in.

X is the length of the photograph base,

Y is the scale of the ordinate, psi/div

Z is the number of divisions per inch of ordinate on the photograph

$$imep = \frac{0.856 \times 200 \times 2.78}{3.58} = 133\ psi$$

14. Indicated horsepower

$$ihp = \frac{(imep)\ LAN}{33{,}000}$$

$$ihp = \frac{(133)(0.375)(11.8)(1505)}{33{,}000} = 26.8 \text{ hp}$$

15. Friction horsepower from pressure-crank angle photograph

$$fhp = (ihp - bhp) = 26.8 - 16.3 = 10.5 \text{ hp}$$

16. Brake specific fuel consumption

$$bsfc = \frac{\dot{m}_f}{bhp} = \frac{8.4}{16.3} = 0.515 \text{ lb}_f / \text{bhp-hr}$$

17. Indicated specific fuel consumption

$$isfc = \frac{\dot{m}_f}{ihp} = \frac{8.4}{24.0} = 0.350 \text{ lb}_f / \text{ihp - hr}$$

18. Brake specific air consumption

$$bsac = \frac{\dot{m}_a}{bhp} = \frac{298}{16.3} = 18.3 \text{ lb}_a / \text{bhp - hr}$$

19. Indicated specific air consumption

$$isac = \frac{\dot{m}_a}{ihp} = \frac{298}{24} = 12.4 \text{ lb}_a / \text{ihp - hr}$$

20. Brake thermal efficiency

$$\eta_{tb} = \frac{bhp}{\text{fuel hp}} = \frac{16.3}{62.3} = 26.2 \text{ percent}$$

21. Indicated thermal efficiency

$$\eta_{ti} = \frac{ihp}{\text{fuel hp}} = \frac{24.0}{62.3} = 38.6 \text{ percent}$$

22. Mechanical efficiency

$$\eta_m = \frac{bhp}{ihp} = \frac{16.3}{24.0} = 67.9 \text{ percent}$$

23. Scavenging ratio

$$R_s = \frac{\dot{m}_a}{60 \text{ N } V_c \rho}$$

where: $V_c = V_d \left[\frac{r_k}{r_k - 1}\right] = 53.1 \left[\frac{17}{17-1}\right] = 56.32$ cu. in.

$$V_c = 0.0326 \text{ cu. ft.}$$

$$\rho = \frac{p_e \times 144}{53.3 \times T_i} = \frac{15.07 \times 144}{53.3 \times 529} = 0.077 \text{ lb}_m / \text{cu. ft.}$$

$$R_s = \frac{298}{(60)(1505)(0.0326)(0.077)} = 1.32$$

24. Theoretical compression pressure

This is an empirical relationship from Marks /10/, and was used primarily as a check on engine and pressure transducer performance.

$$p = r_a^{1.33} \times P_{manifold}$$

where: $r_a = (r_k - 1)(\text{relative effective stroke}) + 1$

$$\text{relative effective stroke} = \frac{\text{stroke when ports close}}{L}$$

then, $r_a = (17 - 1)\left(\frac{3.56}{4.50}\right) + 1 = 13.68$

$$p = (13.68)^{1.33} P_{manifold} = 32.4 P_{manifold}$$

$$p = 32.4(17.04) = 552 \text{ psia}$$

The compression pressure as measured with the transducer was 545 psia.

25. Ignition delay

The delay angle is the crank angle between the start of fuel

injection and the first pressure rise due to fuel combustion. The delay period is the time corresponding to this angle.

$$\text{delay period} = \frac{(\text{delay angle})\ (60)}{360\ N}$$

where: 360 is the number of degrees of crank angle per revolution, and

60 is the conversion from minutes to seconds

$$\text{delay period} = \frac{8.3 \times 60}{360 \times 1505} = 0.92 \text{ ms}$$

26. The remainder of the tabulated results are measured directly from the pressure-crank angle photographs.

APPENDIX E

Effect of the Pressure Transducer on Compression Ratio.

The geometry of the cylinder heads prevented the drilling of the pressure transducer cavity normal to the machined face of the heads. The angle is eight degrees from the vertical for the four valve and nine degrees for the two valve. This prohibits completely flush mounting of the water cooled adaptor, but the effect on the overall compression is small as is shown below.

1. Original compression ratio.

$$r_k = \frac{V_d + V_c}{V_c} = \frac{53.1 + 3.32}{3.32} = 17.0$$

2. Compression ratio with adaptor installed.

   a. Two valve head

$$r_k = \frac{53.1 + (3.32 + 0.010)}{(3.32 + 0.010)} = 16.94$$

   b. Four valve head

$$r_k = \frac{53.1 + (3.32 + 0.009)}{(3.32 + 0.009)} = 16.95$$

The difference is of the order of 0.35 percent and has been neglected in calculations.

APPENDIX F

Uncertainty Analysis.

The uncertainty in the tabulated results is given using run A-5 which was presented in Appendix D. The method of analysis is that proposed by Kline and McClintock /11/ for single sample data and is based on 20 to one odds. Since the magnitude of the variables differs between runs these values are to be considered only as representative. They are rounded off to the nearest tenth of one percent.

Result	Percent Uncertainty Interval, 20 to 1 odds
rpm	$\pm$ 0.3
sp. gr. (burette)	$\pm$ 0.2
torque	$\pm$ 0.4
bhp	$\pm$ 0.6
bhp (corrected)	$\pm$ 0.9
bmep	$\pm$ 0.4
$\dot{m}_f$	$\pm$ 2.6
$\dot{m}_a$	$\pm$ 2.0
air-fuel ratio	$\pm$ 3.3
hp loss to exhaust	$\pm$ 3.0
hp loss to cooling water	$\pm$ 19.3
fhp - motoring test	$\pm$ 1.2
fuel hp	$\pm$ 2.6
hp loss unaccounted	$\pm$ 41.6
imep - from pressure-crank angle diagram	$\pm$ 6.6

APPENDIX F

Result	Percent Uncertainty Interval, 20 to 1 odds
ihp - based on imep	± 6.6
fhp = (ihp - bhp)	± 18.2
ihp = (bhp + fhp)	± 1.0
bsfc	± 2.8
isfc	± 2.8
bsac	± 2.2
isac	± 2.2
η_{tb}	± 2.8
η_{ti}	± 2.8
η_{m}	± 1.4
exhaust temperature	± 0.7
scavenging ratio	± 2.5
compression pressure from photograph	± 3.7
theoretical compression pressure	± 1.1
exhaust starts	± 0.1
exhaust stops	± 0.1
injection theoretically starts	± 0.1
delay angle	± 24.0
delay period	± 24.0
peak pressure	± 2.4
peak pressure location	± 0.6